

TRANSCRIPTIONAL REGULATION OF IL-7R ALPHA GENE IN T
LYMPHOCYTES

by

İZZET MEHMET AKÇAY

Submitted to the Graduate School of Engineering and Natural Sciences
in partial fulfillment of
the requirements for the degree of
Master of Science

Sabancı University
August 2010

TRANSCRIPTIONAL REGULATION OF IL-7R ALPHA GENE IN T
LYMPHOCYTES

APPROVED BY:

Assoc. Prof. Dr. Batu Erman
(Thesis supervisor)


.....

Assist. Prof. Deniz Sezer


.....

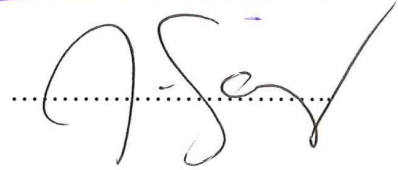
Assist. Prof. Elif Damla Arısan


.....

Prof. Dr. Selim Çetiner


.....

Prof. Dr. Zehra Sayers


.....

DATE OF APPROVAL:10.08.2010.....

© İzzet Mehmet Akçay 2010

All Rights Reserved

ABSTRACT

TRANSCRIPTIONAL REGULATION OF IL-7R ALPHA GENE IN T LYMPHOCYTES

İzzet Mehmet Akçay

Biological Sciences and Bioengineering, M.Sc. Thesis, 2010

Thesis advisor: Assoc. Prof. Batu Erman

Keywords: T lymphocyte, IL-7R alpha, Gfi1, regulation of transcription, real-time RT-PCR

Interleukin-7 signaling is vital for the proper functioning of the immune system. It is required for the development and homeostasis of lymphocytes. This signaling is greatly controlled by the regulation of IL-7 Receptor alpha expression, whereas IL-7 production is thought to be constant. As the dramatic changes during the development of T lymphocytes illustrate, IL-7R alpha expression is strictly regulated. IL-7R alpha expression also varies with the activation stage of mature T cells. Therefore, the molecular events underlying the regulation of IL-7R alpha in T lymphocytes has been an intensive research area since its discovery.

The glucocorticoid receptor has been known to induce transcription of IL-7R alpha, whereas Gfi1 transcription factor represses its expression. Here, we investigated if glucocorticoid stimulation induced IL-7R alpha in T cells due to the post-transcriptional silencing of Gfi1. We performed real time reverse transcriptase polymerase chain reaction (RT-PCR) analyses of several miRNAs predicted to target

Gfi1 mRNA upon dexamethasone (a glucocorticoid) stimulation. Our data suggested that Gfi1 was not silenced by RNA interference.

We also investigated the roles of different Gfi1 domains in the repression of IL-7R alpha expression. By retroviral overexpression studies in T lymphocytes, we demonstrated that none of this transcription factor's domains was capable of exerting the function of Gfi1 on the IL-7R alpha gene by itself. Moreover, the SNAG domain and the Zinc Fingers were specifically required for this function. Finally, we showed that overexpression of the transcription factors Gfi1b and Foxp3 also repressed dexamethasone-induced IL-7R alpha gene in T cells.

ÖZET

IL-7R ALFA GENİNİN T LENFOSİTLERDE TRANSKRİPSİYONEL DÜZENLENMESİ

İzzet Mehmet Akçay

Biyolojik Bilimler ve Biyomühendislik, Master Tezi, 2010

Tez danışmanı: Doç. Dr. Batu Erman

Anahtar kelimeler: T lenfosit, IL-7R alfa, Gfi1, transkripsiyon düzenlenmesi,
gerçek zamanlı RT-PCR

İnterlökin-7 (IL-7) sinyal iletimi bağışıklık sisteminin çalışması için hayati önem taşımaktadır. Bu sitokin reseptöründen gelen sinyaller lenfositlerin gelişimi ve homeostazı için gereklidir. Bu sinyal iletimi büyük oranda İnterlökin-7 Reseptör alfa'nın (IL-7R alfa) ifadesinin düzenlenmesiyle kontrol edilir; IL-7'nin üretiminin ise sabit olduğu düşünülmektedir. T lenfosit gelişimi sırasında IL-7R alfa ifadesindeki dramatik değişiklikler bu proteini ifade eden IL-7R alfa geninin sıkıca kontrol edildiğini belirtmektedir. IL-7R alfa ifadesi aynı zamanda olgun T hücrelerinin aktivasyon durumlarına göre de değişiklik göstermektedir. Bu nedenle IL-7R alfa'nın düzenlenmesine neden olan moleküler olguların aydınlatılması reseptörün keşfinden beri yoğun araştırma konusu olmuştur.

Transkripsiyon faktörlerinden glukokortikoid reseptörünün IL-7R alfa'yı indüklediği, Gfi1'in ise baskıladığı bilinmektedir. Bu çalışmada, T lenfositlerinin glukokortikoid ile uyarılması sonucunda, Gfi1'in transkripsiyon sonrası susturulmasına

bađlı olarak IL-7R alfa ifadesinin indüklenmesini arařtırdık. Gerçek zamanlı ters-transkriptaz polimeraz zincir tepkimesi (RT-PCR) metodu ile Gfi1 mRNA'sını hedeflediđini düřündüğümüz mikroRNA'ların (miRNA) deksametazon (bir glukokortikoid) uyarılmasına bađlı olarak ifadelerini analiz ettik. Sonuçlarımız T hücrelerinde deksametazon uyarılması sırasında Gfi1'in RNA interferans yoluyla susturulmadığını belirtmektedir.

Ayrıca, bu tezde Gfi1 proteininin farklı bölgelerinin IL-7R alfa'nın baskılanmasındaki rolünü arařtırdık. T lenfositlerinde retroviral gen ifadesi deneyleriyle bu transkripsiyon faktörünün hiçbir bölgesinin kendi başına Gfi1'in IL-7R alfa'yı baskılama fonksiyonunu yerine getiremediğini gözlemledik. Ayrıca, Gfi1'in SNAG ve çinko parmak bölgelerinin bu fonksiyonda gerekli olduğunu gösterdik. Son olarak Gfi1b ve Foxp3 proteinlerinin de T hücrelerinde deksametazon uyarılması sonucu indüklenen IL-7R alfa'yı baskılayabildiğini belirledik. Bu sonuçlar, IL-7R alfa geninin kontrol mekanizmalarının belirlenmesine katkı sağlamıştır.

ACKNOWLEDGEMENTS

Firstly, I would like to thank to my dear supervisor Assoc. Prof. Batu Erman, whose belief and encouragement have no doubt enabled me to accomplish the task of completing my master's degree. In his laboratory, I experienced a peaceful and motivating atmosphere for making science. I am so grateful to him for giving me the opportunity to learn new experimental techniques and new scientific thinking ways.

I would like to thank to my tutors, Prof. Selim Çetiner, Prof. Zehra Sayers, Prof. Hüveyda Başağa, and Assist. Prof. Alpay Taralp, who always supported and encouraged me. Besides, I would like to thank to jury members Prof. Selim Çetiner, Prof. Zehra Sayers, Assist. Prof. Elif Damla Arısan and Assist. Prof. Deniz Sezer for evaluating my thesis.

I am also very grateful to Dr. Ceren Tuncer, Dr. Özgür Gül, Emel Durmaz and Tuğsan Tezil. They helped me a lot in learning many of the techniques that I used throughout the project.

Last, but never least, I am very thankful to my friends Nazlı Keskin, Jitka Eryılmaz, Manolya Ün, Ceren Tuncer, Belkıs Atasever, Emel Durmaz, Özgür Gül, Tuğsan Tezil, Derin Demiroğlu, Yekta Yamaner, and to my supervisor, Assoc. Prof. Batu Erman, for sharing many enjoyable moments during my study.

TABLE OF CONTENTS

ABSTRACT	IV
ÖZET	VI
ACKNOWLEDGEMENTS	VIII
TABLE OF CONTENTS	IX
LIST OF FIGURES	XII
LIST OF TABLES	XIV
LIST OF ABBREVIATIONS	XV
1. INTRODUCTION	1
1.1. IMPORTANCE OF IL-7R FOR THE IMMUNE SYSTEM	1
1.2. IL-7R SIGNAL TRANSDUCTION	2
1.3. REGULATION OF IL-7R SIGNALING	3
1.3.1. <i>Altruistic Utilization of IL-7</i>	4
1.3.2. <i>IL-7Rα Expression during T Cell Development</i>	5
1.3.3. <i>IL-7Rα Expression in Peripheral T Cells</i>	7
1.3.3.1. Homeostasis of naive T cells.....	7
1.3.3.2. Homeostasis of memory T cells.....	7
1.3.4. <i>IL-7Rα Expression during B Cell Development</i>	8
1.4. TRANSCRIPTION FACTORS THAT ACT ON IL-7R α GENE	9
1.4.1. <i>The Ets Family Transcription Factors</i>	10
1.4.2. <i>Runx1</i>	11
1.4.3. <i>The Glucocorticoid Receptor</i>	11
1.4.4. <i>Gfi1</i>	11

1.4.5.	<i>Gfi1b</i>	13
1.4.6.	<i>Foxp3</i>	14
1.4.7.	<i>Other Transcription Factors</i>	14
2.	AIM OF THE STUDY	15
3.	MATERIALS & METHODS	16
3.1.	MATERIALS	16
3.1.1.	<i>Chemicals</i>	16
3.1.2.	<i>Equipments</i>	19
3.1.3.	<i>Solutions and Buffers</i>	21
3.1.4.	<i>Growth Media</i>	22
3.1.5.	<i>Molecular Biology Kits</i>	22
3.1.6.	<i>Cell Types</i>	23
3.1.7.	<i>Vectors and Primers</i>	23
3.1.8.	<i>Software and Computer-based Programs</i>	26
3.2.	METHODS	26
3.2.1.	<i>Vector Construction</i>	26
3.2.2.	<i>Bacterial Cell Culture</i>	28
3.2.3.	<i>Mammalian Cell Culture</i>	29
3.2.4.	<i>Flow Cytometry</i>	31
3.2.5.	<i>Immunoblotting</i>	32
3.2.6.	<i>Quantitative miRNA Analysis</i>	34
4.	RESULTS	36
4.1.	INVESTIGATING THE ROLE OF RNA INTERFERENCE IN THE REGULATION OF GF11 UPON DEXAMETHASONE STIMULATION IN T CELLS	36
4.1.1.	<i>Target miRNA Prediction against Mouse Gfi1</i>	36
4.1.2.	<i>Flow Cytometric Analysis of IL-7Ra Induction upon Dexamethasone Treatment</i>	37
4.1.3.	<i>Quantitation of miRNA Levels Using Real Time RT-PCR</i>	38
4.2.	UNDERSTANDING THE ROLES OF GF11 DOMAINS IN REPRESSION OF IL-7RA EXPRESSION	48
4.2.1.	<i>Cloning of Gfi1 Truncations</i>	48

4.2.2. Infection Experiments	50
4.2.2.1. IL-7R α expression on cells infected with control retroviruses	51
4.2.2.2. IL-7R α expression on cells infected with full length mouse Gfi1 expressing retroviruses	52
4.2.2.3. IL-7R α expression on cells infected with mGfi1-SNAG expressing retroviruses.....	53
4.2.2.4. IL-7R α expression on cells infected with mGfi1- Δ SNAG expressing retroviruses.....	54
4.2.2.5. IL-7R α expression on cells infected with mGfi1-ZFs expressing retroviruses.....	55
4.2.2.6. IL-7R α expression on cells infected with mGfi1- Δ ZFs expressing retroviruses.....	56
4.2.2.7. IL-7R α expression on cells infected with mGfi1- Δ SNAG, Δ ZFs expressing retroviruses	56
4.2.3. Immunodetection of Gfi1 Truncations in 3B4.15 Cells	57
4.3. REPRESSION OF IL-7RA EXPRESSION BY FOXP3 AND GFI1B IN 3B4.15 CELLS.....	58
5. DISCUSSION.....	62
REFERENCES.....	68
APPENDICES.....	76
APPENDIX A – PCL-ECO MAP.....	76
APPENDIX B – CONFIRMATION OF THE CLONING OF GFI1 TRUNCATIONS BY SEQUENCING	77
APPENDIX C – AMINO ACID SEQUENCE OF THE GFI1 TRUNCATIONS	80

LIST OF FIGURES

Figure 1. 1. IL-7 signaling pathway in the context of cell survival.....	3
Figure 1. 2. Altruistic downregulation of IL-7R by signaled T cells.....	4
Figure 1. 3. Regulation of IL-7R expression during T cell development.....	5
Figure 1. 4. Regulation of IL-7R expression during B cell development.....	8
Figure 1. 5. Transcription factors that act directly on IL-7R α gene locus.....	10
Figure 1. 6. Functions of Gfi1 in T cells.....	12
Figure 1. 7. Domains of Gfi1	12
Figure 3. 1. Map of the LZRS vector.....	24
Figure 3. 2. Schematic representation of flow cytometry data analysis	32
Figure 4. 1. Induction of IL-7R α upon Dex treatment.....	37
Figure 4. 2. RNA quality after isolation	38
Figure 4. 3. Schematic representation of stem-loop RT-PCR for quantification of miRNAs	39
Figure 4. 4. PCR amplification vs. cycle graphs for the standard samples.	42
Figure 4. 5. Standard curve analyses	43
Figure 4. 6. Melting curve analyses.....	45

Figure 4. 7. PCR amplification vs. cycle graphs for the experimental samples (control and Dex treatment).....	47
Figure 4. 8. Gfi1 truncations used in the project	48
Figure 4. 9. Strategy for cloning of Gfi1 truncations into LZRS vector.....	49
Figure 4. 10. Confirmation of the recombinant LZRS vectors by restriction enzyme digestion.....	50
Figure 4. 11. Retroviral insertion of LZRS alone did not alter IL-7R expression levels in 3B4.15 cells	51
Figure 4. 12. Full length Gfi1 repressed IL-7R α induction upon Dex treatment.	52
Figure 4. 13. Gfi1-SNAG domain did not suppress IL-7R α induction upon Dex stimulation.	53
Figure 4. 14. Overexpression of Gfi1- Δ SNAG did not repress IL-7R α induction upon Dex stimulation.....	54
Figure 4. 15. Gfi1-ZFs domain was not sufficient by itself to repress IL-7R α expression	55
Figure 4. 16. Overexpression of Gfi1- Δ ZFs did not result in repression of IL-7R α induction	56
Figure 4. 17. Gfi1- Δ SNAG, Δ ZFs had no effect in IL-7R α repression by itself.....	57
Figure 4. 18. Immunoblotting of infected cell lysates against α -Flag antibody	58
Figure 4. 19. Repression of IL-7R α expression by Foxp3 in 3B4.15 cells.....	60
Figure 4. 20. Repression of IL-7R α expression by Gfi1b in 3B4.15 cells	61
Figure 5. 1. Alternative means of Gfi1 downregulation upon Dex stimulation in 3B4.15 cells.	63

LIST OF TABLES

Table 3. 1. List of chemicals.....	19
Table 3. 2. List of equipments	20
Table 3. 3. List of primers used in cloning of Gfi1 truncations.....	24
Table 3. 4. List of primers used in cDNA synthesis and real-time PCR..	25
Table 3. 5. Optimized PCR conditions.	27
Table 3. 6. Ingredients of polyacrylamide gels.....	33
Table 3. 7. The thermal cycling program for real time PCR..	35
Table 4. 1. The threshold cycle values for the standard and experimental samples.....	46

LIST OF ABBREVIATIONS

α	Alpha
β	Beta
γ	Gamma
γ_c	Common gamma chain
δ	Delta
7-AAD	7-aminoactinomycin D
BAC	Bacterial artificial chromosome
Bad	Bcl-2-associated agonist of cell death
Bcl-2	B cell lymphoma 2
BCR	B cell receptor
CD	Cluster of differentiation
Cdc25A	Cell division cycle 25 homolog A
Cdk	Cyclin-dependent kinase
cDNA	Complementary DNA
CLP	Common lymphoid progenitor
C_T	Threshold cycle
Dex	Dexamethasone
DMEM	Dulbecco's Modified Eagle Medium
DN	Double negative
dNTPs	Deoxynucleotid triphosphates
DP	Double positive

<i>E. coli</i>	<i>Escherichia coli</i>
EBF	Early B cell factor
Eto	Eight twenty one protein
Ets	E-twenty six
FACS	Fluorescence-activated cell sorting
FBS	Fetal bovine serum
FITC	Fluorescein isothiocyanate
FKHRL1	Forkhead homolog (rhabdomyosarcoma) like 1
FLT3	FMS-like tyrosine kinase 3
Foxp3	Forkhead box 3
GABP	GA binding protein
Gfi	Growth factor independent
GFP	Green fluorescent protein
GR	Glucocorticoid receptor
HBS	HEPES-buffered saline
HDAC	Histone deacetylase
HEK293T	Human embryonic kidney 293 T
HSC	Hematopoietic stem cell
IgH	Immunoglobulin heavy chain
IL	Interleukin
IL-7R	Interleukin-7 Receptor
IPEX	Immunodysregulation polyendocrinopathy enteropathy X-linked syndrome
IRES	Internal ribosome entry site
IRF	Interferon regulatory factor
ISP	Immature single positive

JAK	Janus kinase
LB	Luria broth
LEF-1	Lymphoid enhancer-binding factor 1
LTR	Long terminal repeat
MCF	Median channel fluorescence
Mcl-1	Myeloid cell leukemia 1
MFI	Mean fluorescence intensity
mGfi1-SNAG	Mouse Gfi1 SNAG domain
mGfi1- Δ SNAG	Mouse Gfi1 SNAG deleted
mGfi1- Δ SNAG, Δ ZFs	Mouse Gfi1 intermediate domain (SNAG and zinc fingers deleted)
mGfi1-ZFs	Mouse Gfi1 zinc fingers domain
mGfi1- Δ ZFs	Mouse Gfi1 zinc fingers deleted
miRNA	Micro RNA
Mo-MLV	Moloney murine leukemia virus
mRNA	Messenger RNA
NF- κ B	Nuclear factor - kappa light chain enhancer of activated B cells
NIH3T3	National Institute of Health 3T3
NK	Natural killer
OD	Optical density
Pax-5	Paired box protein 5
PBS	Phosphate-buffered saline
PE	Phycoerythrin
Pfu	<i>Pyrococcus furiosus</i>
PI-3K	Phosphatidylinositol-3 kinase
PIAS3	Protein inhibitor of activated STAT3

PU.1	PU-box (purine-rich) binding protein 1
RAG	Recombination activating gene
RIPA	Radioimmunoprecipitation assay
ROR γ t	RAR-related orphan receptor gamma t
Rpm	Revolution per minute
RPMI	Rosewell Park Memorial Institute
RT-PCR	Reverse-transcriptase polymerase chain reaction
Runx1	Runt-related transcription factor 1
SCID	Severe combined immunodeficiency
SDS-PAGE	Sodium dodecyl sulfate – polyacrylamide gel electrophoresis
SH2	Src homology 2
SNAG	Snail/Gfi1 domain
SnoRNA	Small nucleolar RNA
SOCS1	Suppressor of cytokine signaling 1
SP	Single positive
STAT	Signal transducer and activator of transcription
TAE	Tris-acetate-EDTA
Taq	<i>Thermus aquaticus</i>
Tbr	<i>Trypanosoma brucei</i>
TCF-1	T cell-specific factor 1
TCR	T cell receptor
Tg	Transgenic
TNF	Tumor necrosis factor
UTR	Untranslated region

1. INTRODUCTION

1.1. IMPORTANCE OF IL-7R FOR THE IMMUNE SYSTEM

The interleukin-7 receptor (IL-7R) consists of the IL-7R α chain (CD127) and the common γ chain (CD132, γ_c). Although expression of IL-7R α is restricted to the lymphoid lineage, the γ_c chain is shared by several cytokine receptors expressed in most hematopoietic lineage cells. IL-7R α is not instructive for the differentiation of hematopoietic progenitors into cells of the lymphoid lineage, but it is indispensable for the development and maintenance of lymphocytes^{1,2,3,4}.

At early stages, IL-7R signaling is responsible for the survival and development of T cell precursors in mice and humans. IL-7R signaling also controls the accessibility of the T cell receptor (TCR) γ locus to the recombination machinery⁵ and the commitment to the CD8 single positive thymocyte lineage⁶. At later stages, IL-7R signaling supports the survival and homeostatic proliferation of naive and memory T cells⁷. IL-7R is critical for the development of B lymphocytes in mice, but not in humans⁸. In mice, IL-7R controls the rearrangement of the immunoglobulin heavy chain (IgH) gene locus and the proliferation of B cell precursors at early stages. In contrast to T cells, mature B cells are not dependent on the IL-7 cytokine⁹. Similar to B lymphocytes, natural killer cells are not dependent on the IL-7 cytokine¹⁰.

Because IL-7R signaling is crucial for the lymphoid lineage, mice and humans deficient in the IL-7 pathway suffer from severe lymphopenia, whereas other hematopoietic cell lineages are mostly not affected. In particular, in IL-7, IL-7R α and γ_c knockout mice, both T and B lymphopoiesis is inhibited^{11,12,13}. This phenotype is also observed in mice that are injected with monoclonal anti-IL-7 antibodies^{14,15}. Naive T

cells are not able to survive or proliferate in host mice that are IL-7 null. Induction of memory T cells is also partly impaired in these mutant hosts^{16, 17}. Similarly, in human thymic organ cultures treated with anti-IL-7 antibody, T cell production is also inhibited^{18, 19, 20}. Moreover, severe combined immunodeficiency disease (SCID) patients that have mutations in their IL-7R α and γ_c genes profoundly lack T cells, but have normal numbers of B and NK cells^{8, 18}.

1.2. IL-7R SIGNAL TRANSDUCTION

IL-7 signaling starts with binding of IL-7 to its receptor. As IL-7 crosslinks the α and γ_c chains of the IL-7 receptor, two tyrosine kinases JAK1 and JAK3, which are bound to the intracellular domains of the chains, are brought together and activate each other⁷. This results in the phosphorylation of IL-7R α , to which several signaling molecules, including STAT5, are recruited. After phosphorylation and dimerization, STAT5 translocates into the nucleus to initiate the transcription of many genes including Bcl-2 and Mcl-1 that are responsible for exerting the survival function of IL-7. Increase in the expression of these anti-apoptotic proteins renders the cell resistant to apoptosis and maintains its survival²¹. Moreover, upon signal initiation, PI3K is recruited to the phosphorylated IL-7R α ; this initiates the Akt survival pathway. Activation of the Akt pathway results in many anti-apoptotic activities, such as the inhibition of pro-apoptotic proteins Bad and FKHRL1 as a result of sequestration by 14-3-3, inhibition of caspase-9 by phosphorylation, and upregulation of the glucose metabolism⁷ (See Figure 1.1). The proliferation pathway initiated by IL-7 is different from those of conventional growth factors, and is mainly mediated by the post-translational regulation of p27, a Cdk inhibitor, and Cdc25a, a Cdk-activating phosphatase^{22, 23, 24}.

IL-7 is constitutively produced by stromal cells of the lymphoid organs and by epithelial cells²⁵. The amount of IL-7 supply is not influenced by external factors such as the fluctuations in the lymphocyte population or feedback from IL-7 itself¹. IL-7 supply also appears to be limiting as it is produced to support the survival of only a

finite number of lymphocytes²⁶. In line with this finding, mice transgenic for the IL-7 gene develop lymphomas due to increased survival and proliferation capacity of B and T lymphocytes^{27, 28}. This is interesting because even though mature B cells do not express the receptor for IL-7, aberrant signaling during B cell development may be the cause of these B lymphomas.

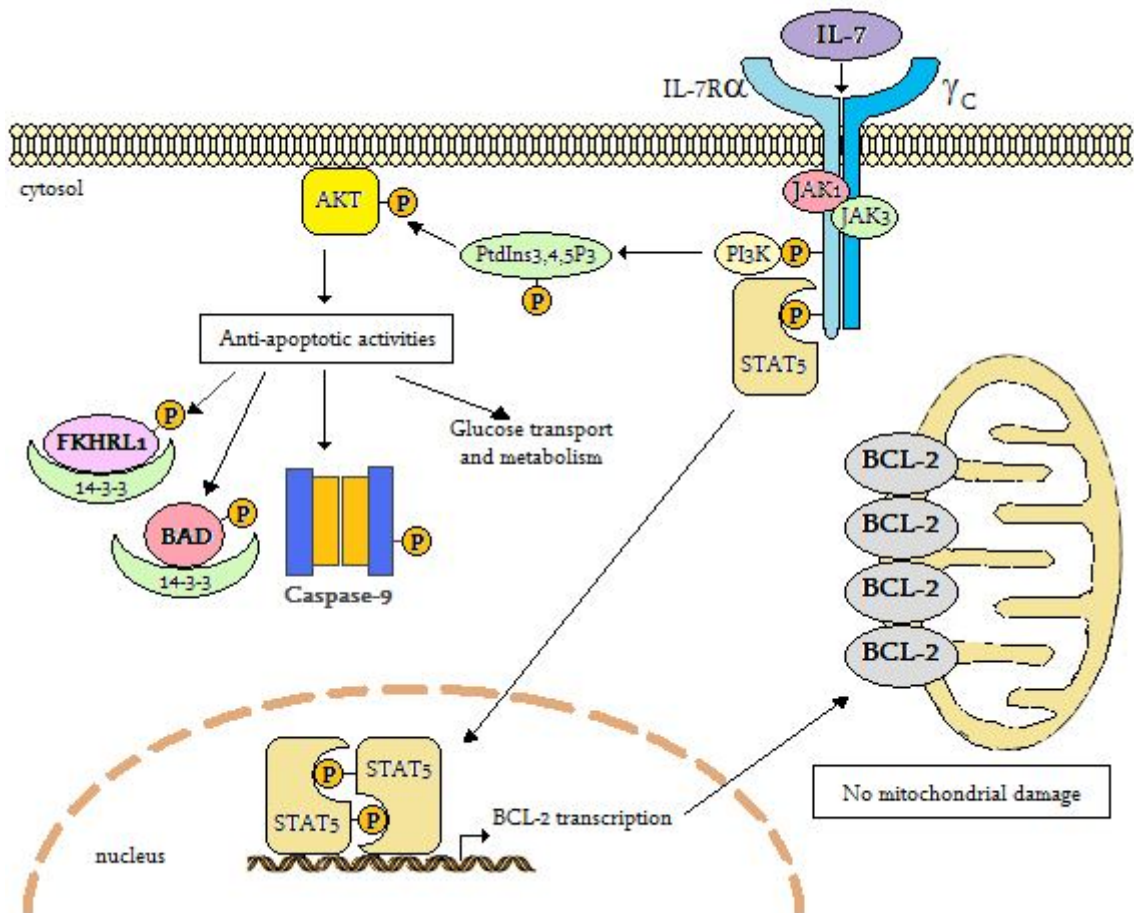


Figure 1. IL-7 signaling pathway in the context of cell survival. (Adapted from ref 7).

1.3. REGULATION OF IL-7R SIGNALING

Regulation of IL-7 signaling is governed by the control of consumption of IL-7 by its receptor rather than its production. Because, unlike IL-7, IL-7Rα expression is strictly upregulated and downregulated in lymphocytes according to their developmental and activation stage. The developmental and activation status-dependent expression patterns of IL-7R will be detailed in the oncoming sections.

1.3.1. Altruistic Utilization of IL-7

IL-7 should be consumed wisely and altruistically because it is not present in abundance *in vivo*. T lymphocytes that encounter IL-7 or other prosurvival cytokines, such as IL-2, IL-4, IL-6 and IL-15, transiently downregulate IL-7R α expression. Consequently, these signaled cells stop competing with un signaled T cells for the remaining IL-7^{29, 30}. TCR triggering also results in IL-7R α downregulation³¹ (see Figure 1.2). Consistent with these observations, transgenic expression of IL-7R α in mice, unlike that of IL-7, does not cause increased numbers of lymphomas. Instead, T cell numbers are reduced markedly in IL-7R α transgenic mice due to over-consumption of the non-abundant IL-7 survival signal^{1, 32}.

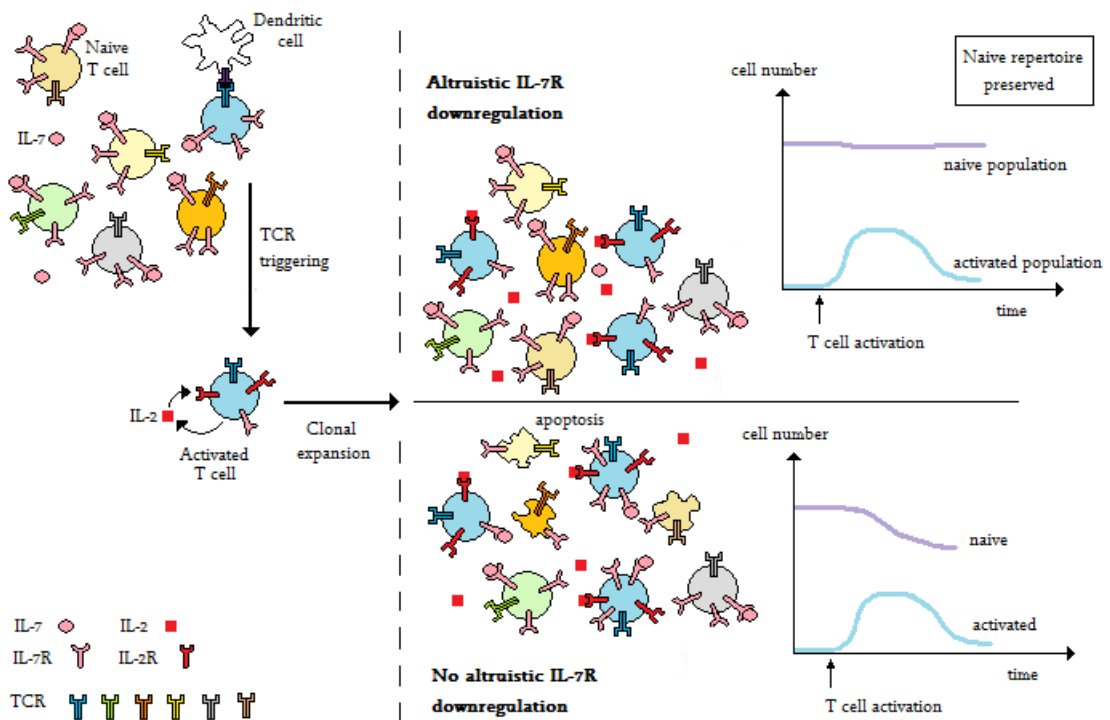


Figure 1. 2. Altruistic downregulation of IL-7R by signaled T cells. (Adapted from ref. 33). This altruistic mechanism aims to preserve the survival of naive T cell pool. Activated T cells rely on other signals, such as IL-2 cytokines for survival. Therefore, they downregulate IL-7R in order to stop needlessly consuming IL-7, which is required by naive T cells. The consequence of this altruistic downregulation is the preservation of the naive T cell population. Thus IL-7 may be thought of as a naive T lymphocyte cytokine.

1.3.2. IL-7R α Expression during T Cell Development

The progenitors of the T lymphocyte lineage proceed through well-defined stages in the thymus to become mature T cells, showing dramatic changes in the expression of IL-7R α . As depicted in Figure 1.3.A, CD4⁻CD8⁻ double negative (DN) thymocytes, which express IL-7R, progress through the immature single positive (ISP) stage to become CD4⁺CD8⁺ double positive (DP) thymocytes, which lack IL-7R. Then as they mature into CD4⁺ or CD8⁺ single positive (SP) T cells, they restart IL-7R expression¹.

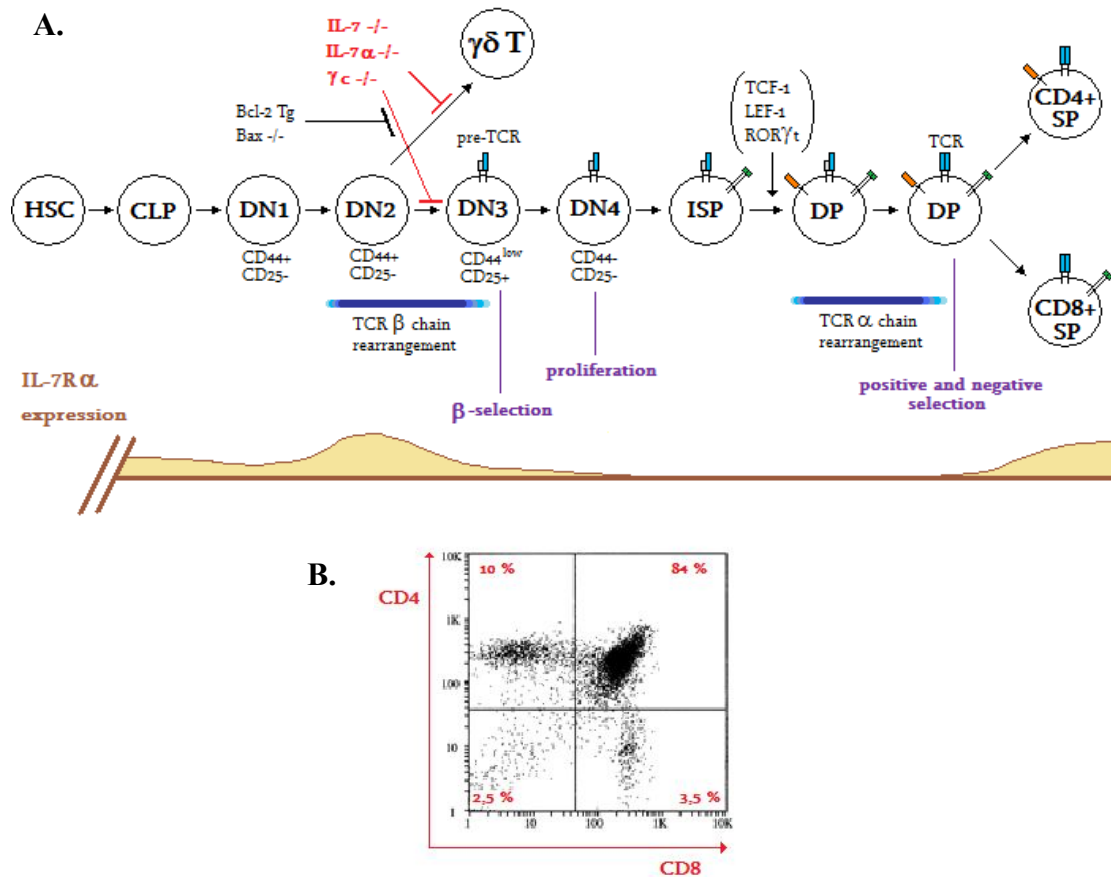


Figure 1. 3. Regulation of IL-7R expression during T cell development. A) IL-7R α expression pattern throughout T cell development. HSC: hematopoietic stem cell, CLP: common lymphoid progenitor, DN: double negative, ISP: immature single positive, DP: double positive, SP: single positive. B) Flow cytometric analysis of thymocyte populations depicting the expression of CD4 and CD8 co-receptors (Adapted from ref. 34).

IL-7R signaling at the DN2 stage is essential and indispensable for T cell development. IL-7R knockout mice are lymphopenic and the few mature T cells that remain functionally impaired. Bcl-2 overexpression and Bax deficiency completely rescue $\alpha\beta$ T cell development in these IL-7R^{-/-} mice implying that IL-7R protects DN2 cells from apoptosis and provides signals for their survival^{35, 36, 37}. IL-7R knockout mice completely lack the $\gamma\delta$ T cell lineage, as IL-7R is also essential for the rearrangement of the TCR γ gene locus. This effect of IL-7R deficiency cannot be rescued by protecting the cells from apoptosis^{1, 38}. IL-7R α expression declines beyond the DN2 stage². As a result, proliferation of DN4 cells, which have completed the rearrangement of the TCR β gene locus and have started to express pre-T cell receptor (pre-TCR) on their surface, does not greatly rely on IL-7R signaling.

Once DP thymocytes successfully complete the rearrangement of their TCR α chain locus, they start to express the full T cell receptor on their surface. Afterwards, they pass through positive and negative selection. Although the survival factor IL-7R is not expressed at the DP stage, this does not play a role in the apoptotic clearance of inappropriate clones during selection events at this stage. Recent experiments have shown that even if IL-7R were expressed in DP thymocytes, it would not be able to initiate signal transduction cascades because these cells highly express the signaling inhibitor SOCS1, which effectively blocks IL-7R signaling³⁹. This view is further supported by the observation that overexpression of IL-7R α in DP cells fails to perturb the selection process and to protect them from cell death^{2, 40}.

Suppression of IL-7R α at the DP stage has at least two different functions. The first one is to govern the efficient utilization of the IL-7 cytokine, which is not abundantly expressed in the thymic niche. DP cells constitute the vast majority of the thymocyte population (see Figure 1.3.B), and consumption of IL-7 by DP cells would deprive the minor DN and SP thymocyte populations of IL-7^{1, 41, 42}. The second function of IL-7R α suppression is to achieve the transition of immature single positive (ISP) cells into DP cells. IL-7R normally inhibits the expression of TCF-1, LEF-1, and ROR γ t, which are required by ISP cells to become DP cells. Hence, IL-7R signaling should be terminated at the ISP stage². IL-7 transgenic mice show a marked reduction in the number of DP thymocytes probably due to a perturbation of this transition step²⁷.

As DP cells mature into CD4⁺ SP or CD8⁺ SP cells, they reexpress IL-7R α . At these later stages, IL-7R is required by SP thymocytes and naive T cells for survival and homeostatic proliferation²⁹.

1.3.3. IL-7R α Expression in Peripheral T Cells

1.3.3.1. Homeostasis of naive T cells

Most naive T cells have a long lifespan. They require exogenous signals to maintain their long-term survival and homeostatic proliferation. Among many cytokines including IL-4 and IL-15, only IL-7 seems to be critical in this context⁴³. When signaling from IL-7R is abolished, naive T cells have a shortened lifespan of around 2-3 weeks. In contrast, overexpression of IL-7 results in T cell expansion in the periphery. Therefore, the basal level of IL-7 appears to govern the overall size of the naive T cell pool^{16, 44}.

1.3.3.2. Homeostasis of memory T cells

When a naive T cell encounters its antigen, it initiates a new differentiation program and clonally expands. IL-7R α is downregulated by the majority of these activated T cells, although the decrease in IL-7R α is not as marked as it is in DP thymocytes^{16, 45}. These IL-7R α ^{low} T cells are the effector T cells and after antigen clearance they die by apoptosis. A small subset of these activated cells retains high levels of IL-7R expression. These IL-7R α ^{high} cells are the precursors of memory T cells. They survive after antigen clearance and develop into long-lived memory T cells^{46, 47, 48}.

Because the survival and proliferation of short-lived effector T cells are already supported by other cytokines and TCR signaling, downregulation of IL-7R α in these cells probably aims to prevent the unnecessary consumption of IL-7. If this mechanism were absent, elevated numbers of effector T cells would compete with naive and

memory T cells for the limiting supply of IL-7¹ (see Figure 1.2). IL-7R is generally considered to be critical for the long-term survival and maintenance of CD4⁺ and CD8⁺ memory T cells^{16, 17, 49}, although some studies showed that IL-15 can substitute for some IL-7 functions^{50, 51}.

That IL-7R signaling is instructive for memory precursors to become memory T cells is controversial and has been questioned in many studies. Some studies report that IL-7 is required for the generation of CD4⁺ and CD8⁺ memory T cells^{45, 48, 49, 52, 53, 54} while others reach the opposite conclusion^{17, 55}. Therefore studying the regulation of IL-7R gene control is critical for understanding T cell function in the peripheral immune system.

1.3.4. IL-7R α Expression during B Cell Development

The requirement for IL-7R during B cell development is different in mice and humans. IL-7R plays an essential, non-redundant role in B cell development in adult mice. In IL-7^{-/-} or IL-7R α ^{-/-} mice, B cell development is inhibited at the transition from CLP cells to pro-B cells in adulthood, but not in fetal and neonatal periods^{11, 12, 56, 57}. In humans, on the other hand, IL-7R is not critical for B-cell development as IL-7R-deficient SCID patients produce normal numbers of B cells^{18, 58}.

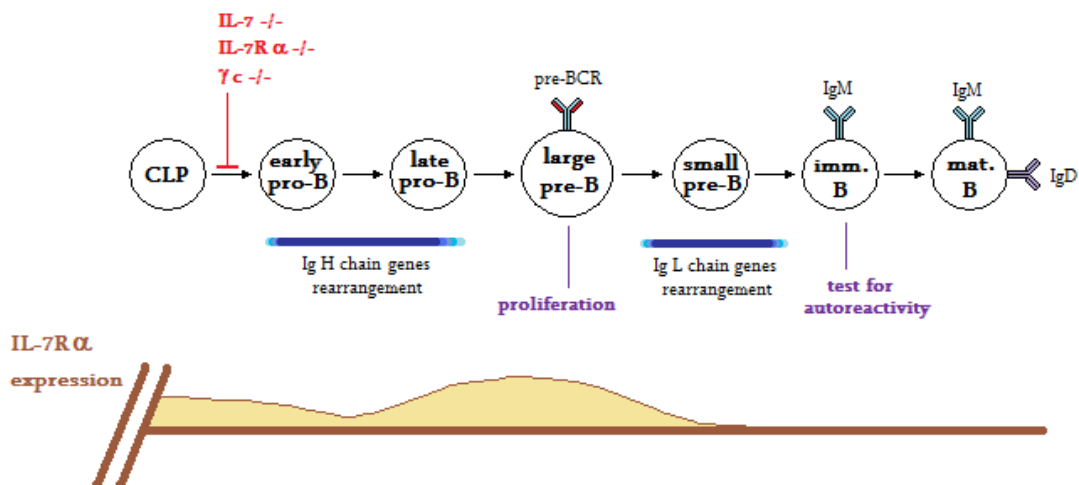


Figure 1. 4. Regulation of IL-7R expression during B cell development.

As shown in Figure 1.4, IL-7R was also required during B cell development for proliferation of pro-B and large pre-B cells^{60, 61}. A successful VDJ_H rearrangement at the late pro-B cell stage leads to the expression of the complete Ig heavy chain as part of the pre-B cell receptor. Large pre-B cells that express pre-BCR on their surface start to proliferate and become small pre-B cells, at which point they start to undergo rearrangements in their Ig light chain genes. Proliferation at the large pre-B stage therefore aims to enhance the overall BCR diversity because a single heavy chain can match with many different light chains. The signal through IL-7R that induces proliferation is distinct from those that induce IgH gene rearrangements and includes association with PI-3 kinase via its SH2 domain⁶². IL-7R expression is lost after the small pre-B cell stage. Unlike mature single positive T cells, immature and mature B cells do not need IL-7R for survival⁶³.

To sum up, IL-7R α is dynamically regulated throughout B and T cell development. Moreover, it is strictly regulated depending on the activation stage of mature T cells. This strict regulation of IL-7R α is greatly dependent on the functions of the transcription factors that directly bind to the IL-7R α promoter.

1.4. TRANSCRIPTION FACTORS THAT ACT ON IL-7R α GENE

The transcription factors that are known to act on IL-7R α promoter are shown in Figure 1.5. These include the Ets family proteins PU.1 and GABP, Runx1, glucocorticoid receptor (GR), Gfi1 and Gfi1b, interferon regulatory factors IRF-1 and IRF-2, Foxp3, and NF- κ B.

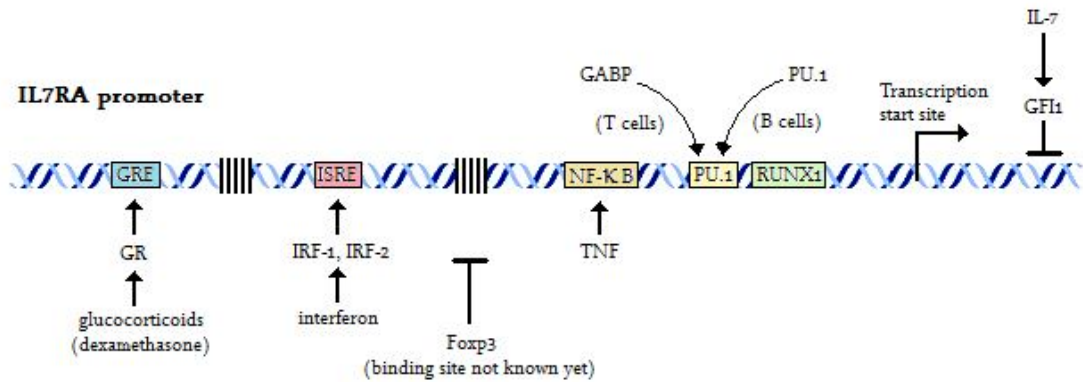


Figure 1. 5. Transcription factors that act directly on IL-7R α gene locus. (Adapted from ref 1).

1.4.1. The Ets Family Transcription Factors

The promoter region of the IL-7R α gene is highly conserved among human, mouse and rat; the region spanning 197 base pairs from the translation initiation site is 75 % homologous between mouse and human. This region has conserved consensus binding motifs for the transcription factors PU.1 and Runx1, which are indispensable for the development of hematopoietic stem cells and lymphocyte progenitors^{64, 65}.

Mice mutant for functional PU.1 showed defects in the generation of B and T lymphocytes, monocytes and granulocytes^{66, 67}. It was demonstrated that PU.1^{-/-} hematopoietic progenitors failed to express IL-7R α . Retroviral transduction of IL-7R α into these progenitors partly restored the generation of pro-B cells, which underwent normal development. This indicates that PU.1 induces early B cell development partly by inducing IL-7R expression. PU.1 acts in concert with FLT3 signaling to induce IL-7R expression in CLP cells^{68, 69}.

PU.1 is not expressed after the pro-T cell stage in the T-cell lineage. But another Ets family transcription factor, GABP, binds to the same PU.1 motif and drives the expression of IL-7R α in thymocytes and peripheral T cell⁷⁰.

1.4.2. Runx1

Runx1 also induces the expression from the IL-7R α promoter. Runx1 is a critical transcription factor for the maintenance of CD4 single positive T cells as conditional knockout of Runx1 in the CD4⁺ lineage resulted in a reduction of CD4⁺ thymocytes and T cells. This effect is partly due to regulation of IL-7R α expression by Runx1 because in the absence of Runx1, this lineage exhibited shorter survival rates and a profound reduction in IL-7R expression ⁷¹.

1.4.3. The Glucocorticoid Receptor

The IL-7R α gene locus contains a highly conserved region 3 kilobases upstream of the transcription initiation site. The homology between mouse and human is 86 % for 300 bp in this region. A glucocorticoid response element (GRE) is localized here and required for induction of IL-7R α by glucocorticoids ⁷². Glucocorticoids have been shown to induce IL-7R α expression *in vitro*. This induction is mediated through binding of the activated glucocorticoid receptor (GR) to the GRE ^{73, 74}.

Thymocytes express high levels of GR, and thymic epithelial cells produce high levels of glucocorticoids. These observations initially led to the assumption that glucocorticoids played some vital role in T cell development ^{75, 76}. But it was later shown that GR signaling was not essential for T cell development and selection because T cell development was normal in GR^{-/-} mice ⁷⁷.

1.4.4. Gfi1

The transcription factor Gfi1 represses transcription of its target genes. As depicted in Figure 1.6, it acts by recruiting histone deacetylases (HDACs) to the target promoters in cooperation with the cofactor Eto ⁷⁸. Deacetylated histones cause the chromatin to package more firmly ultimately silencing transcription. An alternative

function of Gfi1 is the upregulation of the STAT3 transcription factor by interacting with the STAT3 inhibitor PIAS3⁷⁹.

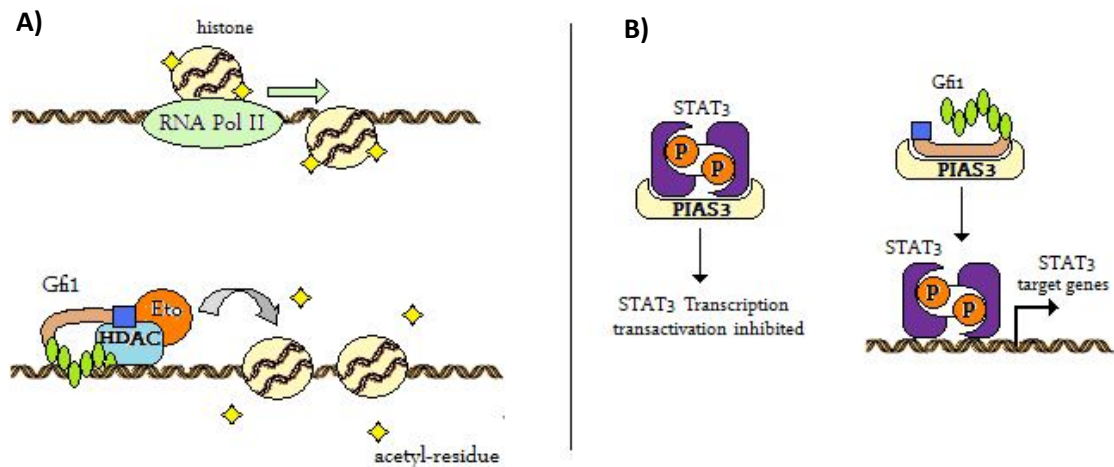


Figure 1. 6. Functions of Gfi1 in T cells. A) Transcription repression. B) STAT3 activation. (Adapted from ref 80).

Gfi1 is a nuclear protein with an N-terminal SNAG domain of 20 amino acids and six C-terminal C₂H₂-type zinc fingers (see Figure 1.7). The SNAG domain has been shown to be indispensable for Gfi1's function. Although 3 of the 6 zinc fingers are responsible for DNA binding, none of them is required for Gfi1 to bind and sequester PIAS3^{79, 81}. The intermediate region is less characterized with no function and structure assigned yet, and it is also the least conserved part of the protein. Yet, it harbors an alanine and glycine-rich region, which could also possibly contribute to Gfi1's repression function⁸⁰.

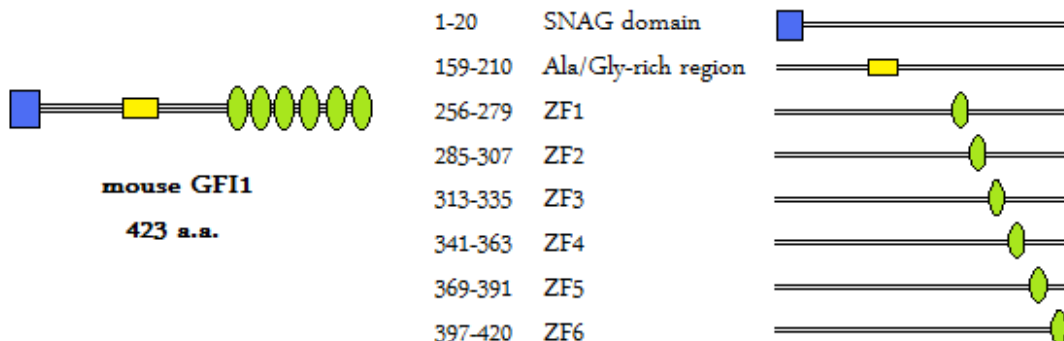


Figure 1. 7. Domains of Gfi1. The N-terminal SNAG domain is shown as a blue box, the Alanine/Glycine-rich region as a yellow box and the 6 zinc finger domains as green circles.

Gfi1 has functional conserved binding sites in introns 2 and 4 of IL-7R α gene. It has been shown that repression of IL-7R α gene upon stimulation by IL-7 involves the induction and function of Gfi1 in mature CD8⁺ T cells, but not in CD4⁺ T cells. In Gfi1 knockout mice, this negative feedback is inhibited in CD8⁺ cells, but unaffected in CD4⁺ cells²⁹. Furthermore, Gfi1's role of inhibiting the IL-7R gene has been shown to be effective only in the DN and CD8 SP stages of T cell development using BAC transgenic IL-7R reporter mice. In these mice, a GFP reporter was inserted into the IL-7R gene locus. When these IL-7R α :GFP transgenic (Tg) mice were crossed with Gfi1 knockout mice, GFP levels were much higher in IL-7R α :GFP Tg, Gfi1^{-/-} knockout thymocytes, compared to their IL-7R α :GFP Tg, Gfi1^{+/+} littermates. On the other hand, GFP levels did not differ significantly in the DP and CD4⁺ SP stages (Park, H. & Erman, B., unpublished). Gfi1 has also been shown to suppress IL-7R α expression in the B cell lineage⁸².

Expression of Gfi1 in the T cell lineage peaks at the DN2 and DP stages. It is found at low levels in resting mature T cells. Antigenic TCR stimulation, however, transiently induces Gfi1, which, in turn, represses IL-7R^{83,84}.

1.4.5. Gfi1b

The 330 amino acids-long transcription factor Gfi1b is highly homologous to the 423 amino acids-long Gfi1. They share 97 % sequence identity in their zinc fingers and 90 % sequence identity in their SNAG domains. On the other hand, the intermediary region, which is much smaller in Gfi1b than in Gfi1, does not bear any homology^{80,85}.

Gfi1 and Gfi1b bind to the same DNA consensus sequence and repress the same target genes. However, their expression shows tissue-specific variety⁸⁶. Furthermore, as illustrated by the loss of and defects in different cell types in Gfi1 and Gfi1b knockout mice, these paralog proteins appear to function in different types of cells⁸⁷. Because of the high similarity between the N- and C-termini of these two proteins, it is likely that the intermediate domains of Gfi1 and Gfi1b are involved in different protein-protein interactions resulting in their different functions.

Transgenic overexpression of Gfi1b in mice demonstrated that it can repress IL-7R α , like its paralog Gfi1⁸⁶. It also appears that Gfi1 and Gfi1b function almost equivalently in T lymphocytes as Gfi1:Gfi1b (Gfi1^{Gfi1b/Gfi1b}) mice show normal T cell development⁸⁷.

1.4.6. Foxp3

The Foxp3 transcription factor is known as a repressor of its targets. Its expression in T cells is generally inversely correlated with IL-7R expression. Foxp3^{high} natural regulatory suppressor T cells have very low levels of IL-7R α ⁸⁸. Foxp3 expression also increases at the ISP stage of the T cell development where IL-7R α is suppressed⁸⁹. Finally, T cell activation results in IL-7R downregulation and transient Foxp3 induction⁹⁰. Although chromatin immunoprecipitation-microarray (ChIP-chip) data suggested that the IL-7R α promoter is a target for Foxp3 binding, the exact location of Foxp3 binding in this promoter is not known⁸⁸.

1.4.7. Other Transcription Factors

The promoter of mouse IL-7R α gene also contain a functional interferon-stimulated response element (ISRE) 1,1 kilobases upstream of the transcription initiation site. It was shown that type I interferon induced expression of IL-7R α *in vitro* by inducing interferon regulatory factors IRF-1 and IRF-2. This suggests that IL-7R signaling may have a role in responses to viral infection⁹¹.

It was also shown that TNF- α upregulates the expression of IL-7R α in mouse T cells. This upregulation is mediated by the NF- κ B transcription factor. Yet, NF- κ B is not sufficient by itself for induction of IL-7R α expression^{29, 92}.

2. AIM OF THE STUDY

IL-7R is an important receptor for the survival and development of T and B lymphocytes. Characterizing the features of the transcription factors that act on IL-7R α gene and understanding how these transcription factors are regulated in response to extracellular and intracellular stimuli are important for defining the roles of IL-7R in hematopoiesis, autoimmunity and leukemia development. In this project, we aimed to gain more insight about the functioning and regulation of transcription factors that repress IL-7R α in T cells, particularly those of Gfi1.

We first investigated if Gfi1 was silenced by RNA interference upon glucocorticoid stimulation in T cells. Glucocorticoids, such as dexamethasone (Dex), induce IL-7R α expression in T cells. Downregulation of Gfi1 has also been observed upon Dex treatment by northern blotting method, suggesting that Gfi1 plays a role in the induction of IL-7R α expression. In order to search if Gfi1 was suppressed by RNA interference upon glucocorticoid stimulation, we aimed to quantitate expression levels of Gfi1-targetting miRNAs with and without Dex treatment. To this end, we first determined the possible target miRNA species against Gfi1 by *in silico* target prediction. And then we performed real time RT-PCR assays for these miRNAs.

Next, we investigated the importance of the different domains of Gfi1 protein in the repression of IL-7R α . Gfi1 harbors a SNAG domain at the N-terminus, six zinc fingers at the C-terminus, and a less-characterized intermediate domain. We aimed to test which of these domains are essential and which are redundant in Gfi1's IL-7R α repression function. We generated 5 different truncations of Gfi1; these are the SNAG domain, the SNAG-deleted Gfi1, the zinc fingers, the zinc fingers-deleted Gfi1 and the intermediate domain. We retrovirally overexpressed these truncations in the 3B4.15 T hybridoma cell line and examined their capability of repressing IL-7R α . We also searched if the transcription factors Gfi1b and Foxp3 also inhibited induction of IL-7R α in 3B4.15 cells upon Dex stimulation.

3. MATERIALS & METHODS

3.1. MATERIALS

3.1.1. Chemicals

The chemicals used in this project are given in Table 3.1.

<u>CHEMICALS & MEDIA COMPONENTS</u>	<u>SUPPLIER COMPANY</u>
7-AAD	Calbiochem, 129935
Acetic acid (glacial)	Merck, 1000562500
Acrylamide/bis-acrylamide 30% solution	Sigma Aldrich, A3699
Ampicilline sodium salt	Cellgro, 61-238-RM
Ammonium persulfate	Sigma, A3678
Anti-mouse CD127 antibody, PE-conjugated	eBioscience, 12-1271-83
Anti-mouse IgG-peroxidase antibody	Sigma, A9044
Anti-Flag mouse monoclonal antibody	Sigma, F3165
Hydrochloric acid 37%	Merck, 100317.2500
Agarose	PEQLAB, 35-1010
Bacto Agar	BD Company, 214050
Bovine Albumin Fraction V	Immuno, 810034
Bradford reagent	Sigma, B6916

Bromophenol blue	Sigma, B5525
Calcium chloride	Sigma, C2661
Chloroform	Amresco, 0757
Chloroquine diphosphate	AppliChem, A2143,0100
DEPC	Aldrich, 40718
Dexamethasone	Sigma, D4902
Dextrose monohydrate	Sigma-Aldrich, 9559
DMEM	PAN, P04-3590
DMSO	PAN Biotech, P60-36720100
EDTA	BioChemica, A1103,1000
Ethanol	Sigma Aldrich, 32221
Ethidium bromide	Sigma, E1510
Fetal Bovine Serum	Thermo Sci. HyClone, SV30160.03
Fluorescein calibration dye	BIO-RAD, 170-8780
GeneRuler DNA Ladder Mix	Fermentas, SM0331
Glycine	AppliChem, A3707,9010
Glycerol	Molekula, M63186664
L-glutamine solution, 200mM	Sigma, G7513
HEPES	AppliChem, A3724,0100
Kanamycin sulfate	GIBCO, 11815-032
LB Broth	Difco Lennox, 240210
MEM NEAA solution, 100X	Sigma, M7145
MEM vitamin solution, 100X	Sigma, M6895
β -Mercaptoethanol	Sigma, M7522
Methanol	Riedel-de Haen, 24229
Nonidet P40 Substitute	Sigma BioChemika, 74385

PageRuler Prestained Protein Ladder	Fermentas, SM0671
Penicillin-streptomycin	GIBCO, 15140
pH:4.00 buffer solution	Merck, 1.09435.1000
pH:7.00 buffer solution	Merck, 1.09439.1000
Phenol red	Sigma-Aldrich, P4633
PIPES	Sigma, P6757
PMSF	Sigma, P7626
Polybrene (hexadimethrine bromide)	Sigma, H9268
Potassium chloride	Sigma-Aldrich, P9333
Potassium dihydrogen phosphate	Sigma, 9791
2-Propanol	Merck, 100995.2500
Protease Inhibitor cocktail tablets	Roche Diagnostics, 13191000
5X Protein loading dye & 20X Reducing agent	Fermentas, R0891
RPMI	PAN, P04-17500
Skim milk powder	Fluka, 70166
Sodium dodecyl sulfate	AppliChem, A1502,0500
Sodium Azide	Amresco, 0639-2506
Sodium chloride	AppliChem, A2942,1000
di-Sodium hydrogen phosphate dihydrate	AppiChem, A3905,1000
Sucrose	Sigma, 84097
TEMED	AppliChem, A1148,0250
TRI Reagent	Sigma, T3934
Tris	Amresco, 0826
Tris hydrochloride	Amresco, 0234
Triton X-100	Promega, H5142
Trypan Blue Solution	Fluka, 95395
Trypsin-EDTA, 0,05%	GIBCO, 25300

Tween 20	Sigma, P9416
Xylene Cyanol FF	Sigma, X-0377

Table 3. 1. List of chemicals.

All restriction enzymes, DNA polymerases and T4 DNA ligase used throughout the project were purchased from Fermentas.

3.1.2. Equipments

The equipments used in this project are given in Table 3.2.

<u>EQUIPMENT</u>	<u>COMPANY</u>
Autoclave	Hirayama, Hiclave HV-110
Balance	Sartorius, BP610
	Schimadzu, Libror EB-3200 HU
Centrifuge	Eppendorf, 5415D and 5415R
	Hitachi, Sorvall RC5C Plus
	Heraeus Multifuge 3 S-R
CO2 incubator	Binder
Deepfreeze	-80 C, Forma, Thermo Electron Corp.
	-20 C, Bosch
Distilled water	Millipore MilliQ Academic
Electrophoresis apparatus	Biorad Inc. Mini-Protean Tetra-Cell
	Labnet International Inc.
ELIZA Reader	Biorad Model 680 Microplate Reader
Flow cytometer	BD FACSCanto

Heating Magnetic stirrer	VELP Scientifica, ARE
Hematocytometer	Hausser Scientific, Blue Bell Pa.
Ice machine	Scotsman Inc. AF20 R134a
Incubators	Memmert, Modell 300 (bacterial incubator) Memmert, Modell 600 (oven)
Laminar Flow	Kendro Lab. Prod., Heraeus, Herasafe HS12
Liquid Nitrogen Tank	International Cryogenics, Inc. DIRECTOR D-4000
Microscopes	Olympus CK40 light microscope Olympus IX70 Inverted fluorescent microscope
Microwave oven	Bosch
pH meter	WTW, pH540 GLP MultiCal
Pipettes & Dispensers	Finnpipette, Thermo Scientific BD Falcon Express Pipetman
Power supply	Biorad, PowerPac 300
Real-time PCR machine	Biorad, iCycleriQ multicolor real time PCR detection system
Refrigerator	Bosch
Shaker Incubator	New Brunswick Sci. , Innova 4330
Spectrophotometer	Nanodrop Spectrophotometer ND-1000
Thermal cycler	Biorad, DNA Engine Gradient Cycler
UV Illuminator	BioRad, UV-Transilluminator 2000
Vacuum Pump	Integra VacuSafe
Vortex	Velp Scientifica
Waterbath	Huber, Polystat cc1

Table 3. 2. List of equipments.

3.1.3. Solutions and Buffers

CaCl₂ solution for competent cells: 60 mM CaCl₂, 10 mM PIPES pH:7,0, 15% glycerol

Lower gel buffer for SDS-PAGE: 1,5 M Tris, 0,4% SDS, pH: 8,8

Upper gel buffer for SDS-PAGE: 0,5 M Tris, 0,4% SDS, pH: 6,8

Red Solution for Primary Antibodies: 5% BSA, 0,02% Sodium azide, 0,05% Tween in PBS, pH:7,5, including phenol red

RIPA buffer: 50 mM Tris pH:7,6; 150 mM NaCl; 0,1% SDS; 1% NP40; 0,5% deoxycholic acid

2X HBS buffer: 280 mM NaCl, 10 mM KCl, 1,5 mM Na₂HPO₄, 12mM dextrose, 50 mM HEPES, pH:7,10

Running buffer: 0,1% SDS in 1X Tris-glycine

Transfer buffer: 20% methanol, 0,0375% SDS in 1X Tris-glycine

PBS: 137 mM NaCl, 2,7 mM KCl, 10 mM Na₂HPO₄, 2 mM K₂HPO₄

PBT: 0,05% Tween20 in PBS

50X TAE buffer: 2 M Tris-acetate, 50 mM EDTA

10X Tris-glycine electrophoresis buffer: 330 mM Tris base, 1,92 M Glycine, pH:8,3

FACS buffer: 1% BSA, 0,1% Sodium azide in PBS

7-AAD working solution: 50 ng/ml 7-AAD in PBS

6X DNA loading dye: 0,25% bromophenol blue, 0,25% xylene cyanol FF, 40% sucrose

3.1.4. Growth Media

Bacterial Growth Media:

Luria Broth (LB) medium was used to grow bacteria. Selective media were prepared by adding ampicilline to a final concentration of 100 µg/ml or kanamycin to a final concentration of 50 µg/ml. Selective LB agar plates were prepared by first autoclaving LB agar solution, then adding ampicilline/kanamycin after cooling it down to 50 °C. After mixing thoroughly, LB agar was poured on Petri plates to solidify. The final antibiotic concentration in LB agar was the same as that in LB liquid medium.

Mammalian Cell Culture Growth Media:

DMEM was prepared by adding fetal bovine serum (FBS), penicilline/streptomycin and L-glutamine to final concentrations of 10% (v/v), 100 unit/ml and 2mM, respectively. Aside from the same concentrations of FBS, pen/strep and L-glutamine, RPMI medium was also supplemented with 1X MEM vitamins, 1X MEM nonessential amino acids (NEAA) and 55 µM β-mercaptoethanol.

3.1.5. Molecular Biology Kits

QIAGEN QIAquick Gel Extraction Kit, cat no: 28706

QIAGEN Plasmid Midi Kit, cat no: 12145

Roche Genopure Plasmid Midi Kit, cat no: 03143414001

Finnzymes DyNAmo cDNA Synthesis Kit, cat no: F-470L

Finnzymes DyNAmo HS SYBR Green qPCR Kit, cat no: F-410L

3.1.6. Cell Types

Escherichia coli DH5 α cells (F⁻, ϕ 80dlacZ Δ M15, Δ (lacZYA-argF)U169, *deoR*, *recA1*, *endA1*, *hsdR17*(rk⁻,mk⁺), *phoA*, *supE44*, λ ⁻, *thi-1*, *gyrA96*, *relA1*) were used in all of the molecular cloning experiments.

The Phoenix and NIH3T3 adherent cells and 3B4.15 suspension cells were used in tissue culture experiments. The Phoenix cell line was derived from HEK293T cells, and is capable of producing pol-gag and envelope proteins. These cells are specialized in virus production at high titers. NIH3T3 cells are known to be easily infected by retroviruses; hence they were used as positive controls in infection experiments. The 3B4.15 cell line is a CD4 single positive T cell hybridoma. Effects of the Gfi1 truncations on IL-7R α expression in infection experiments and alterations in miRNA levels upon dexamethasone treatment were investigated in these cells.

3.1.7. Vectors and Primers

pBluescript II KS (+) and LZRS ϕ BMN-link-ires-eGFP vectors containing the mouse Gfi1 cDNA were previously constructed by Dr. Ceren Tuncer. In this study, truncations of Gfi1 were amplified by PCR from pBluescript-mGfi1 and cloned into empty LZRS vectors. The retroviral LZRS vector is based upon Mo-MLV and the region that is flanked by two LTRs is integrated into the genome of transduced cells (see Figure 3.1). It produces a bicistronic mRNA, so that both eGFP and the protein of interest are expressed in the host cell. Expression of this mRNA is driven by the promoter/enhancer in the 5'LTR, and the IRES sequence in the mRNA governs the translation of eGFP⁹³.

pCL-ECO packaging vector was also used along with LZRS vectors in infection experiments at the transfection step of Phoenix cells. Phoenix cells co-transfected with pCL-ECO produce more of the retroviral proteins, Pol, Gag and Env. Therefore virus titers are maximized⁹⁴. The map of pCL-ECO is shown in Appendix A.

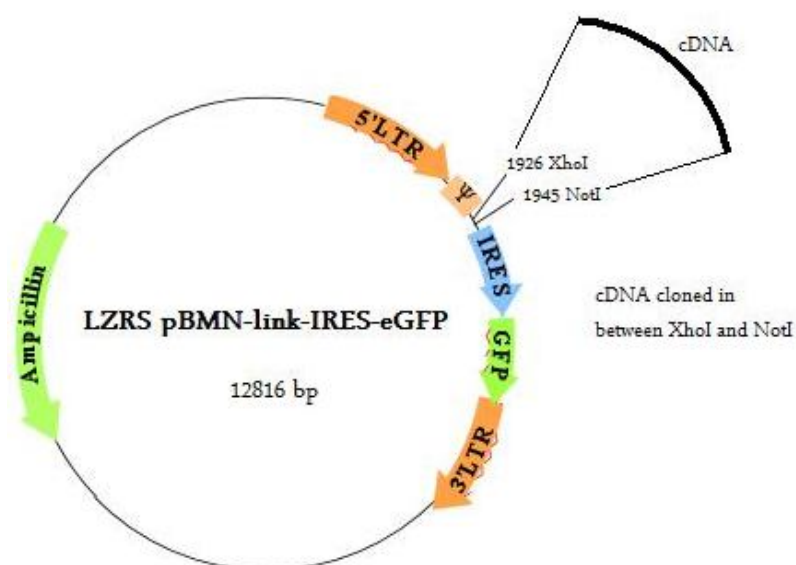


Figure 3. 1. Map of the LZRS vector. (Adapted from Nolan, G.). Cells infected with the recombinant LZRS vector-driven viruses produce both the Gfi1 truncation proteins and eGFP.

The primers used in cloning of Gfi1 truncations and in real-time RT-PCR experiments were given in Tables 3.3 and 3.4, respectively. All the primers were purchased from MCLAB, USA.

Name of the Primer	Sequence	Features in the Primer
mGfi1-dSNAG forward	AT CTCGAG <i>GCC ACC ATG</i> CCA GGG CCG GAC TAC TCC	<i>XhoI site, Kozak</i>
mGfi-ZFs forward	AT CTCGAG <i>GCC ACC ATG</i> TCC TAC AAA TGC ATC AAA TG	<i>XhoI site, Kozak</i>
mGfi1-dZFs reverse	AT <i>GCGGCCGCTA</i> ttt atc gtc atc gtc ttt gta gtc cat gga tcc TTT GTA GGA GCC GCC G	<i>Flag tag, stop codon, NotI site</i>
mGfi1-SNAG reverse	AT <i>GCGGCCGCTA</i> ttt atc gtc atc gtc ttt gta gtc cat gga tcc AGA ACG CGG CTG GTG ATA G	<i>Flag tag, stop codon, NotI site</i>
M13 primer	GTAAAACGACGGCCAGT	
T7 primer	TAATACGACTCACTATAGGG	
LZRS Sequencing Forward	GCATCGCAGCTTGGATACAC	for sequencing

Table 3. 3. List of primers used in cloning of Gfi1 truncations.

Name of the Primer	Sequence
mir142-3p stem loop RT	gtcgtatccagtg <u>caggggtccgaggtattcg</u> cactggatacgcacTCCATA
mir142-3p forward primer	cggcggcTGTAGTGTTTCCTACTT
mir378 stem loop RT	gtcgtatccagtg caggggtccgaggtattcg cactggatacgcacCCTTCT
mir378 forward primer	gccggtgACTGGACTTGGAGTC
mir155 stem loop RT	gtcgtatccagtg caggggtccgaggtattcg cactggatacgcacACCCCT
mir155 forward primer	cggcggcTAAATGCTAATTGTGAT
mir10a stem loop RT	gtcgtatccagtg caggggtccgaggtattcg cactggatacgcacCACAAA
mir10a forward primer	gcccgcTACCCTGTAGATCCGAA
mir133a stem loop RT	gtcgtatccagtg caggggtccgaggtattcg cactggatacgcacCAGCTG
mir133a forward primer	tggtcgTTTGGTCCCCTTCAAC
mir466b-3-3p stem loop RT	gtcgtatccagtg caggggtccgaggtattcg cactggatacgcacTCTTAT
mir466b-3-3p forward primer	gcctccgAATACATACACGCACAC
sno420 stem loop RT	gtcgtatccagtg caggggtccgaggtattcg cactggatacgcacTCTCAG
sno420 forward primer	gcgggcTGAAACCCATTATCAGT
mir universal reverse primer	GTGCAGGGTCCGAGGT
mGfi1 quantitative forward	GCTCCGAGTTCGAGGAC
mGfi1 quantitative reverse	CATAGGGCTTGAAAGGCAG
mGAPDH RT-PCR forward	TCCTGCACCACCAACTG
mGAPDH RT-PCR reverse	TCTGGGTGGCAGTGATG

Table 3. 4. List of primers used in cDNA synthesis and real-time PCR. Specific sequences were shown in capitals. The complementary sequences were typed in bold in one of the stem-loop RT primers. And the complementary of the underlined sequence pair with the mir universal reverse primer during real-time PCR (see also Figure 4.3).

3.1.8. Software and Computer-based Programs

BD FACSDiva (default program used in collecting flow cytometry data)

FlowJo7 (software for analyzing flow cytometry data)

FinchTV (DNA sequencing chromatogram viewer)

BIORAD iCycler (default program used in collecting and analyzing real time PCR data)

MicroCosm Targets, miRGen Targets, TargetScanMouse and PicTar were the internet-available services used to predict the target miRNAs against mouse Gfi1.

3.2. METHODS

3.2.1. Vector Construction

Polymerase Chain Reaction (PCR):

Optimized PCR reaction conditions using Taq and Pfu polymerases are given together in Table 3.5. Thermal cycling starts with initial denaturation at 95 °C for 3 minutes followed by 30 cycles of subsequent denaturation (95 °C for 30 seconds), annealing (56 °C for 60 seconds) and extension (72 °C for 1-2 min) steps. These cycles were then followed by a final extension step at 72 °C for 10 minutes.

PCR Ingredient	Volume Used for Taq PCR	Volume Used for Pfu PCR	Final Concentration
10X Taq buffer with KCl	2,5 µl	-	1X
MgCl ₂ (25 mM)	2 µl	-	2 mM
10X Pfu buffer with MgSO ₄	-	2,5 µl	1X
dNTPs (10mM each)	1 µl	1 µl	0,4 mM
Forward primer (10 µM)	0,5 µl	0,5 µl	0,2 µM
Reverse primer (10 µM)	0,5 µl	0,5 µl	0,2 µM
Template DNA (10 ng/µl)	0,5 µl	0,5 µl	0,2 ng/µl
PCR grade water	17,75 µl *	19,5 µl	-
Taq polymerase (5u/µl)	0,25 µl	-	1,25 u
Pfu polymerase (2,5u/µl)	-	0,5 µl	1,25 u
total	25 µl	25 µl	

Table 3. 5. Optimized PCR conditions. (*): For some Taq PCRs, 1,25 µl DMSO was added (5% final) in the reaction mixture.

Restriction Enzyme Digestions:

The recommended protocols of the enzymes' manufacturer were followed. All digestions were incubated at 25 °C for 1 hour (if there is a risk of star activity) or 2 hours. 100-1000 ng vector DNA was digested for diagnostic and control purposes. 0,5-10 µg DNA were digested before gel extraction for cloning purposes.

Agarose Gel Electrophoresis and Gel Extraction:

1 % agarose gels were prepared by dissolving 1 g agarose in 100 ml 0,5X TAE buffer by heating in microwave for 3-4 min. 2 µl of 10 mg/ml stock EtBr solution was added after cooling down so that the gel contained 0,2 µg/ml EtBr. 0,7% gels were used for large vectors (>10 kb) and 2-2,5% gels were used for short PCR or digestion products. Samples were run for 30-75 min at 100 or 135 Volt before observation under UV. Gel extraction was performed according to the manufacturer's protocol.

Ligation:

Ligations were performed by using 1,25 u T4 DNA ligase and 50-100 ng vector in 20-25 μ l total volume with insert-to-vector ratios of 0:1 (control), 3:1 and/or 6:1. Reaction mixtures were incubated either at 16 $^{\circ}$ C for 16 hours or at 25 $^{\circ}$ C for 3 hours. 1/4 of the mix was used in transformation.

Sequencing:

For confirmation of the constructed vectors, sequencing was provided by MCLAB, USA.

3.2.2. Bacterial Cell Culture

Bacterial Cultures:

Mini cultures (5 ml) of E.coli DH5 α cells were grown in LB medium for 7-10 hours at 37 $^{\circ}$ C constantly shaking at 270 rpm. Midi cultures (100 ml) were grown for overnight (16 hours) starting from 1 ml of mini culture. For preparation of glycerol stocks, sterilized glycerol was added to grown cultures to a final concentration of 20 % and mixed by vortexing. Mixtures were immediately taken to -80 $^{\circ}$ C for storage. Bacterial cells were also grown on LB agar plates by incubating at 37 $^{\circ}$ C for 14-16 hours.

Preparation of Competent Cells:

Cells from frozen E.coli DH5 α stocks were inoculated into 50 ml antibiotic-free cultures and grown for overnight. Next day 4ml of the culture was diluted into 400 ml and OD₅₉₀ measurements were taken. When OD₅₉₀ reaches to 0,375, cells were pelleted and resuspended in CaCl₂ solution on ice and pelleted again. This was repeated 3 times and finally the resuspended cells were aliquoted in 200 μ l and immediately frozen in liquid nitrogen. The frozen competent cells were kept at -80 $^{\circ}$ C for several months. The competency of the cells was tested by transforming with pUC19 plasmid and determined to be above 10⁷ cfu/ μ g DNA.

Transformation:

200 μ l competent cells were taken out of -80°C and thawed on ice for 5 min. Then 1 ng plasmid vector or 5-7,5 μ l ligation reaction mixture was added and mixed by tipping. After incubation on ice for 20 min, heat shock was applied at 42°C for 90 seconds, which was followed by 5 min incubation on ice. LB was added up to 1 ml and cells were incubated shaking at 37°C for 45 min to recover. Then 100 and/or 900 μ l of them were spread on agar plates and grown for overnight.

Vector DNA Isolations from Bacterial Cells:

Vector isolations from mini cultures to be sent for sequencing and from midi cultures to be used in cell culture experiments were performed by using Roche mini-prep and Qiagen midi-prep kits, respectively. For other cloning purposes, alkaline lysis protocol with ethanol precipitation was performed using home-made P1 buffer and excess P2 and P3 buffers of the kits. Concentrations of the final DNA solutions were measured by nano-drop spectrophotometer.

3.2.3. Mammalian Cell Culture

Maintenance of Mammalian Cell Culture:

Adherent cell lines (NIH3T3 and Phoenix) were grown in DMEM and in a humidified atmosphere of 5% CO_2 at 37°C . These cells were passaged every 2-3 days at 1:10 dilution. They were detached from the plate by trypsinization. On the other hand, 3B4.15 suspension cells were grown in RPMI and split for every 2-3 days with 1:6 - 1:8 dilutions. For preparation of frozen stocks of cell lines, cells were first pelleted by centrifugation at 200 g, and then resuspended in freezing medium (FBS with 10 % DMSO). After mixing by pipetting, the cells were loaded into cryo-vials and immediately taken to -80°C in Mr. Frosty. Then within 3 days they were transferred into liquid nitrogen tank for further storage. Preferably, $3 \cdot 10^6$ cells were frozen each time. Lastly, previously frozen cells were used after thawing them in hand and

immediately replacing the freezing medium with the growth medium (DMEM or RPMI).

Transfection of Phoenix Cells:

Calcium phosphate precipitation method was used for transfection of Phoenix cells. 1×10^6 cells were split 16 hours before transfection into the wells of a 6-well plate. DNA solution was prepared by first adding 10 μg LZRS vector DNA and 2,5 μg pCL-ECO vector into water to a final volume of 380 μl . Then 120 μl of 1M CaCl_2 solution was added dropwise and mixed by pipetting. 500 μl of 2X HBS solution was added into this DNA solution fast and dropwise while being vortexed. After vortexing at high speed, the mixture was incubated for 13 min at room temperature. At the 8th minute, chloroquine was added into the media to a final concentration of 25 μM . At the 13th minute the DNA-HBS mixture was added dropwise to the media and the plate was shaken gently to ensure even distribution. 24 hours after transfection, cells were observed under fluorescent microscope to check for GFP fluorescence, and hence efficiency of transfection.

Infection:

Phoenix cells were transfected with the constructed LZRS and pCL-ECO vectors on day #1, and NIH3T3 and 3B4.15 cells were split ($1 \cdot 10^6$ cells) on day #2. On day #3, media of Phoenix cells (4 ml), which contained viruses, were collected and new media were added to cells. The collections were passed through 45 μm filters, and polybrene was added to a final concentration of 6 $\mu\text{g}/\text{ml}$ and vortexed. Media of NIH3T3 and 3B4.15 cells were then discarded and replaced by these filtrates. After centrifugation at 600 g for 1 hour at 32 $^{\circ}\text{C}$, the cells were incubated at 37 $^{\circ}\text{C}$ for 2 hours and their media were replaced by new RPMI media. This virus treatment protocol was repeated on day #4. On day #5, NIH3T3 cells were detached from the plate by trypsinization and 1/5 of them were taken for FACS analysis. Likewise, 100 μl of 3B4.15 cells were taken. Their GFP expression profiles were analyzed. After a high infection efficiency was noticed for both cell line, the rest 900 μl of 3B4.15 cells were divided into two and their media were replaced by 1 ml 1 nM dexamethasone-containing RPMI and ethanol-containing RPMI. After 16 hours of incubation, on day #6, cells were analyzed on flow cytometry.

3.2.4. Flow Cytometry

Flow cytometry was performed for two purposes. First, in order to understand whether infection worked, GFP fluorescence of NIH3T3 and 3B4.15 cells were observed (LZRS vectors enforce GFP expression in their host cells). Second, IL-7R α expression profiles were analyzed in 3B4.15 cells upon Dexamethasone (Dex) stimulation.

Preparation of Cells for FACS:

In order to observe IL-7R α levels after 16 hours of Dex treatment, 200 μ l out of 1 ml 3B4.15 suspension cultures were taken for analysis. First, the cells were pelleted by centrifugation at 200 g for 5 min and washed with FACS buffer. After washing one more time, the pellets were resuspended in 100 μ l FACS buffer, 10 μ l of 10 μ g/ml anti-CD127 PE antibody was added and vortexed briefly and gently. Following 20 min incubation in dark in cold room, they were washed twice as before. After resuspending in 500 μ l FACS buffer, 1 μ l of 50 μ g/ml 7-AAD was added and vortexed briefly and gently. Incubation in dark for 10 min in the cold room was followed by FACS analysis.

On the other hand, in order to check for the infection efficiency, cells were only washed twice and then resuspended in 500 μ l FACS buffer. 7-AAD was generally not used.

Data Acquiring and Data Analysis:

Flow cytometry data were acquired and recorded using BD FACSCanto machine and FACSDiva software. GFP fluorescence was measured in the FITC channel and IL-7R α was measured in the PE-Area channel (anti-IL-7R α antibody was conjugated to PE). During acquisition of data, compensation for both signals was ensured.

We made the data analysis using FlowJo software. First we gated on the live cell population which was defined first by the cells' size and granularity data, then by 7-AAD exclusion data. On the 7-AAD-free cell population we analyzed GFP profile. After subgrouping the cells based on their GFP expression levels, i.e. GFP-negative,

GFP, positive, etc., we analyzed IL-7R α expression levels (Figure 3.2). We recorded the mean fluorescence intensity (MFI) and median channel fluorescence (MCF) in the PE-Area.

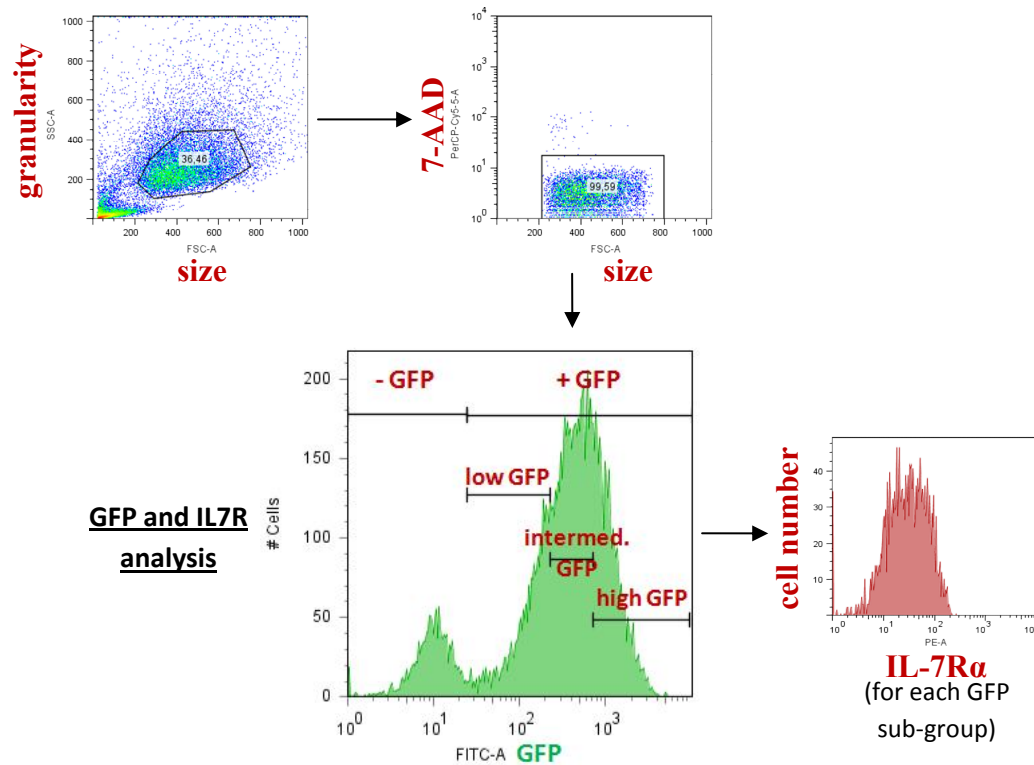


Figure 3. 2. Schematic representation of flow cytometry data analysis. Alive cells were selected first based on their granularity and size, then based on 7-AAD exclusion data (7-AAD-negative cells were taken). These live cells were analyzed for their GFP expression. Cells were grouped according to their GFP expression status and IL-7R α expression was analyzed for each group.

3.2.5. Immunoblotting

Protein Extraction:

Cells were first washed with PBS buffer twice, then pelleted again at 13000 g and resuspended in 50 μ l RIPA buffer containing 1mM PMSF and 1X Protease Inhibitor Cocktail by pipetting on ice. After centrifugation at 13000 g, the suspension was taken into a new eppendorf tube, and this was repeated twice. Protein concentration in the final cell lysate was assessed by Bradford assay.

Polyacrylamide Gel Electrophoresis (PAGE):

In order to run protein samples, 15% and 20% polyacrylamide gels were prepared according to the formulation shown in Table 3.6. Protein extracts which contain equal amounts of protein were mixed with 5X commercial protein loading solution and 20X reducing agent and then boiled at 100 °C for 5-10 min. After spin down, these protein samples were loaded on the gel and run along with Pre-stained Protein Marker for 1-1,5 hours at 200 Volts.

Western blotting and detection:

As soon as the run was completed, proteins were transferred onto nitrocellulose membranes at 250 milli Amper for 1 hour at room temperature (RT). Subsequently, the membrane was treated with the blocking solution (5% milk in PBT) for 1 hour at RT. After washing shortly with PBT buffer, the membrane was soaked in primary antibody solution (1:1000 anti-Flag antibody in red solution) and incubated for 1 hour with shaking. Then the membrane was washed with PBT for 5 min for three times, and treated with the secondary antibody (1:10000 anti-mouse IgG-peroxidase in 5 % milk PBT). Finally, it was treated with chemiluminescent substrate following three times wash in PBT for 5 min. After 2-4 min incubation in dark, films were placed on the membranes and developed in the dark room to detect the proteins of our interest, which had carboxy terminal Flag epitopes.

Ingredients	LOWER GELS – 5ml (Separating)		UPPER GEL – 2,5 ml (Stacking)
	15 %	20 %	3 %
ddH ₂ O	0,8 ml	-	1,62 ml
50 % glycerol	0,4 ml	0,4 ml	-
Lower/Upper gel buffer	1,25 ml	1,25 ml	625 µl
30 % Acry/Bis	2,5 ml	3,3 ml	250 µl
10 % APS	50 µl	50 µl	20 µl
TEMED	5 µl	5 µl	5 µl

Table 3. 6. Ingredients of polyacrylamide gels.

3.2.6. Quantitative miRNA Analysis

Total RNA Isolation:

RNA isolation was applied to 10^7 ethanol-treated (control) and dexamethasone-treated 3B4.15 cells. Pelleted cells were resuspended in 1 ml TRI and incubated for 5 min. After adding 200 μ l chloroform and vortexing, the mixture was incubated for 3 min and then centrifuged at 12.000 g for 15 min at 4 $^{\circ}$ C. The aqueous phase was transferred into a new tube and isopropanol and ethanol precipitation was applied. The final RNA pellet was dissolved in 50 μ l DEPC-treated water. RNA concentration in the sample was measured in nano-drop spectrophotometer.

Real time PCR:

Real-time PCR was also conducted using kit reagents; cDNA samples were simply mixed with primers to a final concentration of 0,5 μ M and with ready-to-use master mixes which contain hot start Tbr DNA Polymerase, SYBR Green, optimized PCR buffer, $MgCl_2$ and dNTPs. The cycling program, which is shown in Table 3.7, was started after well-factor plate reading. Well-factor plates contained 20 μ l 10 nM fluorescein dye. SYBR Green fluorescence was measured at the extension step of each amplification cycle. The program was ended with melting curve analysis to infer the nature of the amplification.

Cycle no	Repeat	Time	Temperature (°C)
1	1	2 min	50
2	1	10 min	95
3	40	10 sec	94
		30 sec	60
		30 sec	72
4	1	2 min	72
5	1	1 min	95
6	80	10 sec	55; +0,5 at each repeat
7	1	∞	4

Table 3. 7. The thermal cycling program for real time PCR. Melting curve analysis was carried out by measuring SYBR Green fluorescence at every 0,5 °C interval while heating the sample from 55 °C to 95 °C.

4. RESULTS

4.1. INVESTIGATING THE ROLE OF RNA INTERFERENCE IN THE REGULATION OF GFI1 UPON DEXAMETHASONE STIMULATION IN T CELLS

4.1.1. Target miRNA Prediction against Mouse Gfi1

MicroCosm Targets, miRGen Targets, TargetScanMouse and PicTar predicted overlapping sets of miRNA targets against mouse Gfi1, among which miR-142-3p, miR-133a, miR-466b-3-3p and miR-378 scored the highest. miR-155 and miR-10a were added to this list based on a study that reported these two miRNAs, along with miR-142-3p and miR-133a, were involved in regulation of Gfi1's expression⁹⁵.

We studied the expression of these miRNAs in a tissue culture system where Gfi1 expression is dynamically regulated. 3B4.15 T lymphocyte cell lines express high levels of Gfi1, which silences the expression of the IL-7R α gene. When 3B4.15 cell lines are treated with the glucocorticoid dexamethasone (Dex), Gfi1 levels decrease and IL-7R α gene transcription is increased (Park, H. & Erman, B., unpublished observations). The downregulation of Gfi1 expression may be mediated by the activity of various miRNAs; thus we hypothesized that Dex treatment would alter the expression levels of one or more miRNAs that target the 3'UTR of Gfi1 gene.

4.1.2. Flow Cytometric Analysis of IL-7R α Induction upon Dexamethasone Treatment

To identify miRNAs that are upregulated upon Dex treatment, we first assessed Dex responsiveness of 3B4.15 cells by measuring their surface levels of IL-7R α . As expected, control 3B4.15 cells were IL-7R α negative as they express high levels of Gfi1, and Dex treated 3B4.15 cells were IL-7R α positive as they downregulate Gfi1 expression.

Here, we treated $10 \cdot 10^6$ 3B4.15 cells with 1 nM dexamethasone. For the control group, we added the same volume (10 μ l) of ethanol to the culture medium (10 ml total), because Dex was dissolved in ethanol in the stock solution. After 16 hours of incubation, we took 200 μ l of the culture for FACS analysis and pelleted the rest for RNA isolation. In order to observe IL-7R α expression levels on cell surface, we stained the cells with PE-conjugated anti-CD127 antibody. As shown in Figure 4.1, IL-7R α expression was induced upon Dex treatment.

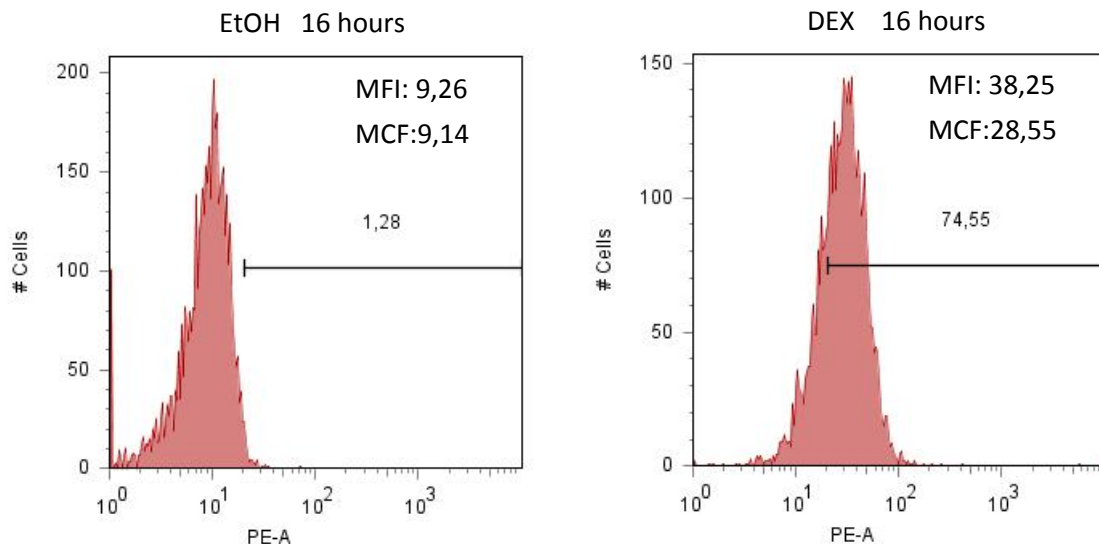


Figure 4. 1. Induction of IL-7R α upon Dex treatment. After 16 hours, PE-A (IL-7R α) mean fluorescent intensity was 9,26 for the control group and 38,25 for the treatment group. 75 % of the cells become IL-7R α positive after Dex treatment (only 1% is IL-7R α positive in the control group).

4.1.3. Quantitation of miRNA Levels Using Real Time RT-PCR

After RNA isolation, we ran total RNA samples on an agarose gel to determine RNA quality and lack of DNA contamination. We observed that final RNA product was intact and free of DNA contamination (see Figure 4.2).

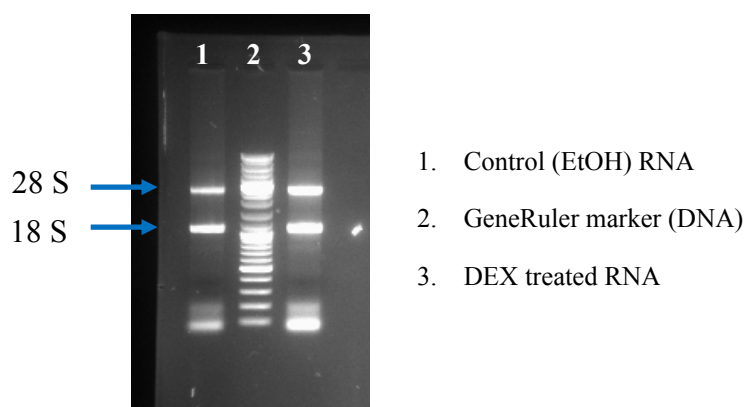


Figure 4. 2. RNA quality after isolation. RNA was intact as the bands corresponding to 28S and 18S rRNAs were sharp; absence of smear in the upper part of the gel suggested that there was no DNA contamination.

Next, we performed cDNA synthesis and real time PCR in order to quantitate miRNA expression levels in control and Dex-treated samples. In cDNA synthesis reaction, specific stem-loop RT primers were used for miRNA and snoRNA species. As shown in Table 3.4 and Figure 4.3, these stem-loop RT primers have only 6 complementary bases at their 3' ends. Besides they all contain the same backbone sequence which form a stem loop structure at the temperature of cDNA synthesis. Stem-loop structure of these primers provides efficient and specific conversion of miRNAs to cDNAs^{96,97}.

The stem loop structure unfolds at the temperatures of PCR cycles. Therefore the (universal) reverse primer is allowed anneal to its complementary site in the loop region. The forward primer is specific for each miRNA as it should anneal to the 5' miRNA part of the cDNA template to initiate specific amplification (see Figure 4.3).

Amplifications are detected by the enhanced fluorescence of SYBR Green fluorophore as it incorporates into double stranded DNA.

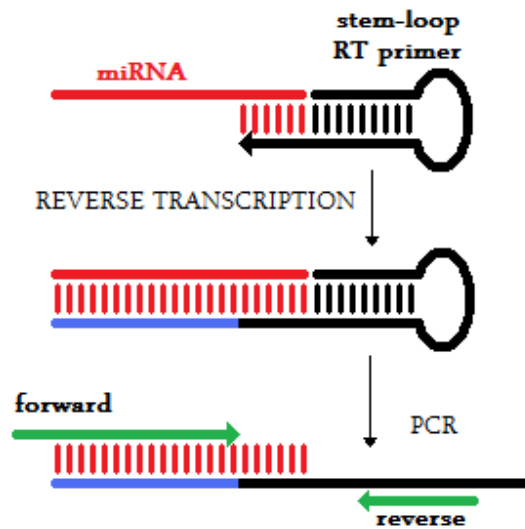


Figure 4. 3. Schematic representation of stem-loop RT-PCR for quantification of miRNAs. (Adapted from ref 96).

In order to determine the efficiency of amplification using the corresponding forward and reverse primer pair, we made standard curve analysis. To this end, we made 10 fold dilutions of the cDNA template and tracked their amplification curves (Figure 4.4) and threshold cycles (C_T) (Table 4.1) in real time PCR. The software drew the standard curve and calculated the PCR efficiency (Figure 4.5). We also analyzed their melting curves (Figure 4.6) in order to ensure the amplifications were specific. Then we analyzed the amplification curves and the C_T values for the experimental samples (Figures 4.7 and Table 4.1). Using the PCR efficiency and the average of the C_T for the triplicate samples of control and Dex treatment, we calculated the fold change in each miRNA species level due to Dex treatment. We used the below formula ⁹⁸.

$$\text{FOLD CHANGE (treatment/control)} = (\text{efficiency})^{C_{T\text{control}} - C_{T\text{treatment}}}$$

Here, efficiency is defined in the Pfaffl definition (100% PCR efficiency means that DNA amount doubles at each cycle; therefore efficiency equals 2 in the Pfaffl definition). We used small nucleolar RNA 420 (snoRNA-420) as our reference gene

because its expression has been reported to be invariable among many tissues and between treatments ⁹⁵. In order to find the actual change in a miRNA species between control and treatment, we divided the fold change in that miRNA species by the fold change in snoRNA-420. The calculation is shown in the below formula ⁹⁸.

$$\text{RATIO OF TARGET GENE EXPRESSION} = \frac{\text{Fold change in target gene (treatment/control)}}{\text{Fold change in reference gene (treatment/control)}}$$

Fold change in the reference gene snoRNA-420:

The PCR amplification vs. cycle graph for the standard dilutions and the resulting standard curve for snoRNA-420 are shown in Figure 4.4.A and Figure 4.5.A. PCR efficiency was calculated to be 108,7 %, which cannot be theoretically true, but is considered practically good (correlation coefficient was 0,996). In the Pfaffl definition, PCR efficiency was 2,087. Amplification products of the standard dilution samples gave the same pattern in the melting curve graph. It was obvious that there was only amplification of the desired product as there was only one large peak (Figure 4.6.A).

The average threshold cycles (C_T) of the triplicate control and treatment samples were 27,43 and 26,87, respectively (Figure 4.7 and Table 4.1). Using the fold change formula, we found out that the fold change in snoRNA-420 expression was 1,44 (treatment/control).

$$\text{fold change in snoRNA-420 (Dex/control)} = (2,087)^{27,43 - 26,87} = \mathbf{1,44}$$

This relatively small difference in snoRNA-420 levels between control and Dex treated samples indicated that it was a proper reference gene to use in miRNA quantitation between treatments.

Fold change in miR-142-3p:

The PCR amplification graph and the standard curve for miR-142-3p are shown in Figure 4.4.B and Figure 4.5.B. PCR efficiency was 82,8 % (1,828 in the Pfaffl definition) and the correlation coefficient was 0,993. Melting curve analysis showed that only the desired product was amplified in the PCR (Figure 4.6.B).

The amplification curves of the experimental samples were shown in Figure 4.7.B. The average C_T for control and Dex treatment samples were 23,63 and 23,2, respectively (Table 4.1). Consequently, calculation of the Dex treatment vs. control fold change for miR-142-3p gave 1,30 fold increase.

$$\text{fold change in miR-142-3p (Dex/control)} = (1,828)^{23,63 - 23,2} = \mathbf{1,30}$$

This result was solely based on miR142-3p real time PCR data. However, we had to consider the fold change in the reference gene, snoRNA-420, as well. After taking the fold change in reference gene into account, we found out that the actual ratio of miR-142-3p level for treatment vs. control was 0,90. Therefore, we concluded that miR-142-3p level did not change upon Dex treatment.

$$\text{actual miR-142-3p ratio (Dex/control)} = 1,30/1,44 = \mathbf{0,90}$$

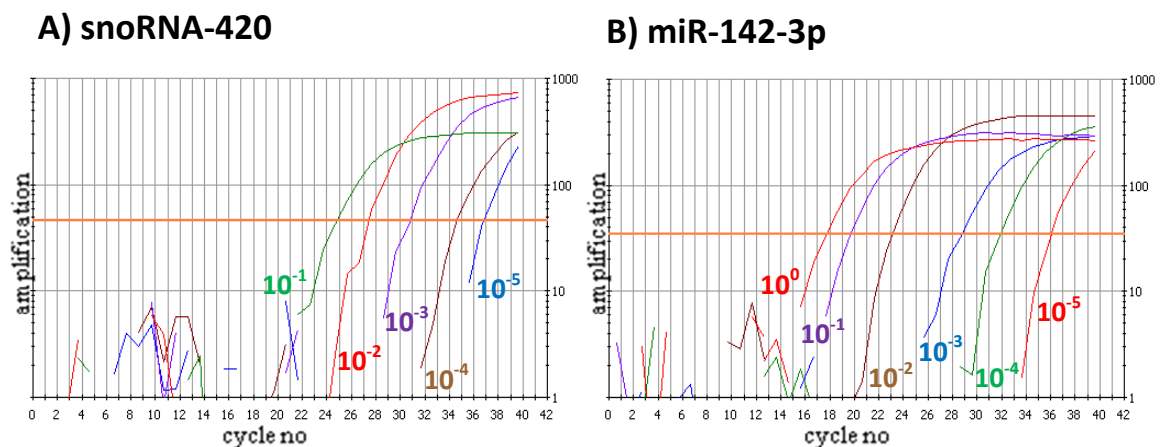
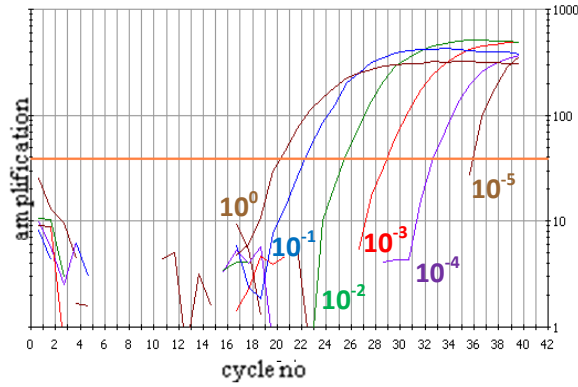
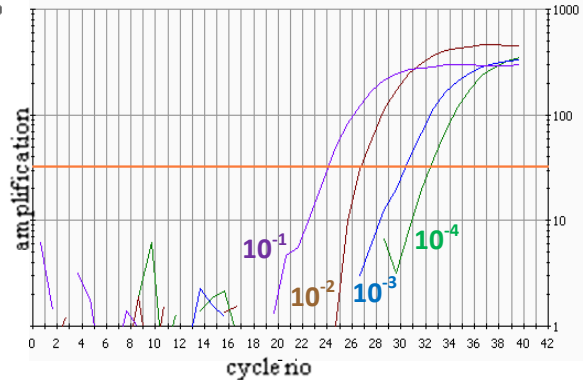


Figure 4. 4. continued.

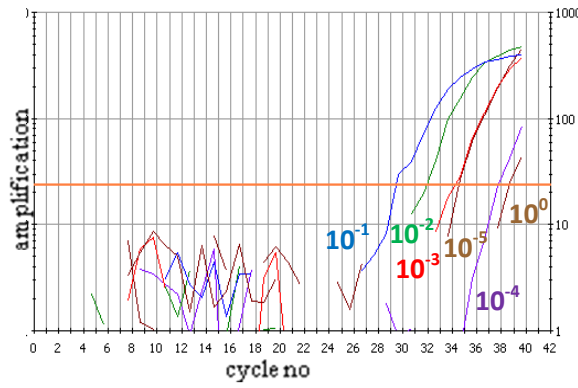
C) miR-378



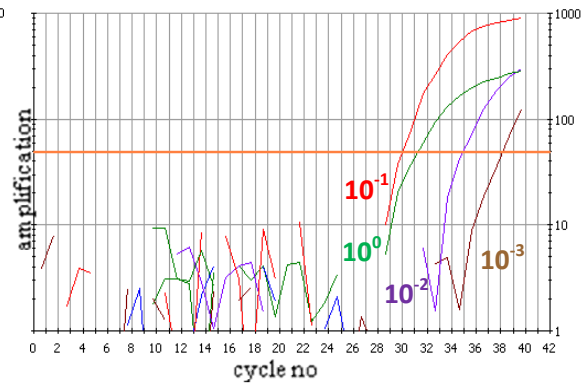
D) miR-466b-3-3p



E) miR-133a



F) miR-155



G) miR-10a

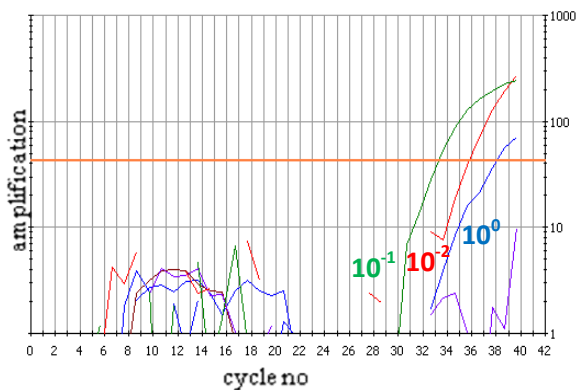
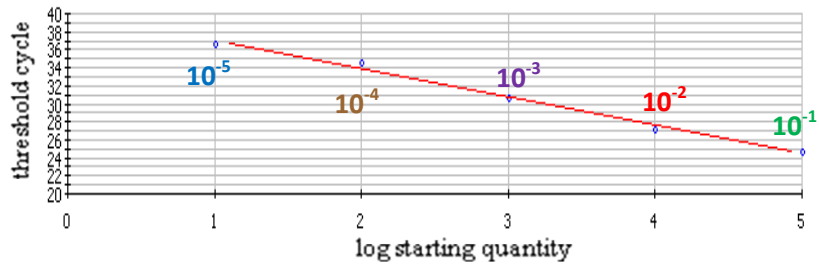


Figure 4. 4. PCR amplification vs. cycle graphs for the standard samples. Amplification scale is in arbitrary units. A) snoRNA-420, B) miR-142-3p, C) miR-378, D) miR-466b-3-3p, E) miR-133a, F) miR-155, G) miR-10a.

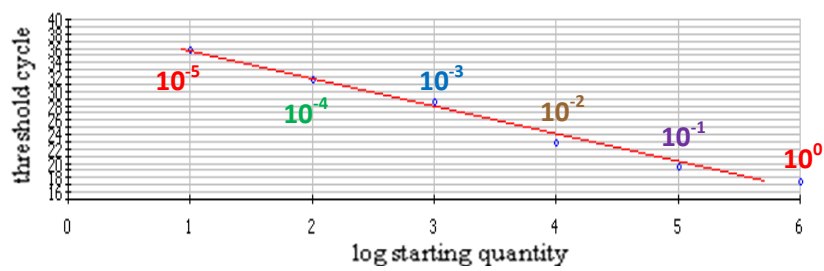
A) snoRNA-420

Correlation coefficient: 0.996
PCR efficiency: 108.7 %



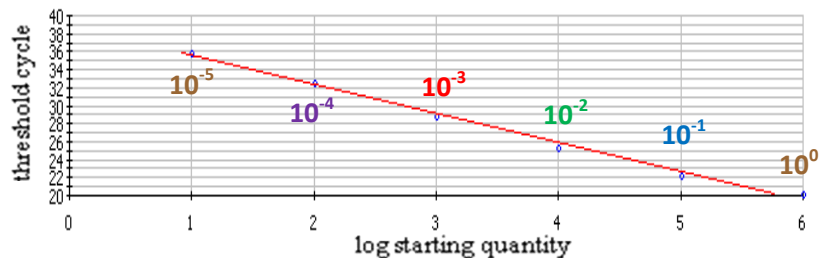
B) miR-142-3p

Correlation coefficient: 0.993
PCR efficiency: 82.8 %



C) miR-378

Correlation coefficient: 0.997
PCR efficiency: 104.3 %



D) miR-466b-3-3p

Correlation coefficient: 0.995
PCR efficiency: 123.4 %

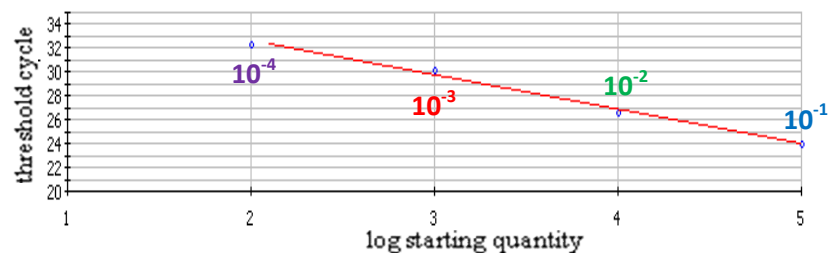


Figure 4. 5. Standard curve analyses. A) snoRNA-420, B) miR-142-3p, C) miR-378, D) miR-466b-3-3p.

Fold change in miR-378:

As shown in Figure 4.4.C, PCR of the standard samples for miR-378 achieved to give amplifications in good correlation with their dilutions. Therefore we had a PCR efficiency of 2,043 (or 104,3 %) and obtained the standard curve shown in Figure 4.5.C. We confirmed that amplification was specific in the PCR by studying the melting curve of the standard samples (Figure 4.6.C). The amplification curves and the C_T values for experimental samples were shown in Figures 4.7.C and Table 4.1, respectively. The C_T values for control and Dex treatment averaged 25,45 and 25,9, respectively. Using these, we calculated the fold change in miR-378 level between treatment and control. The fold change was 0,73. After correction based on snoRNA-420 fold change, we found that the actual fold change was 0,51. Hence we found out that miR-378 level in Dex treated samples was half of that in the control samples. Yet, this was not a significant decrease for a miRNA species.

$$\text{fold change in miR-378 (Dex/control)} = (2,043)^{25,45-25,9} = \mathbf{0,73}$$

$$\text{actual ratio of miR-378 (Dex/control)} = 0,73/1,44 = \mathbf{0,51}$$

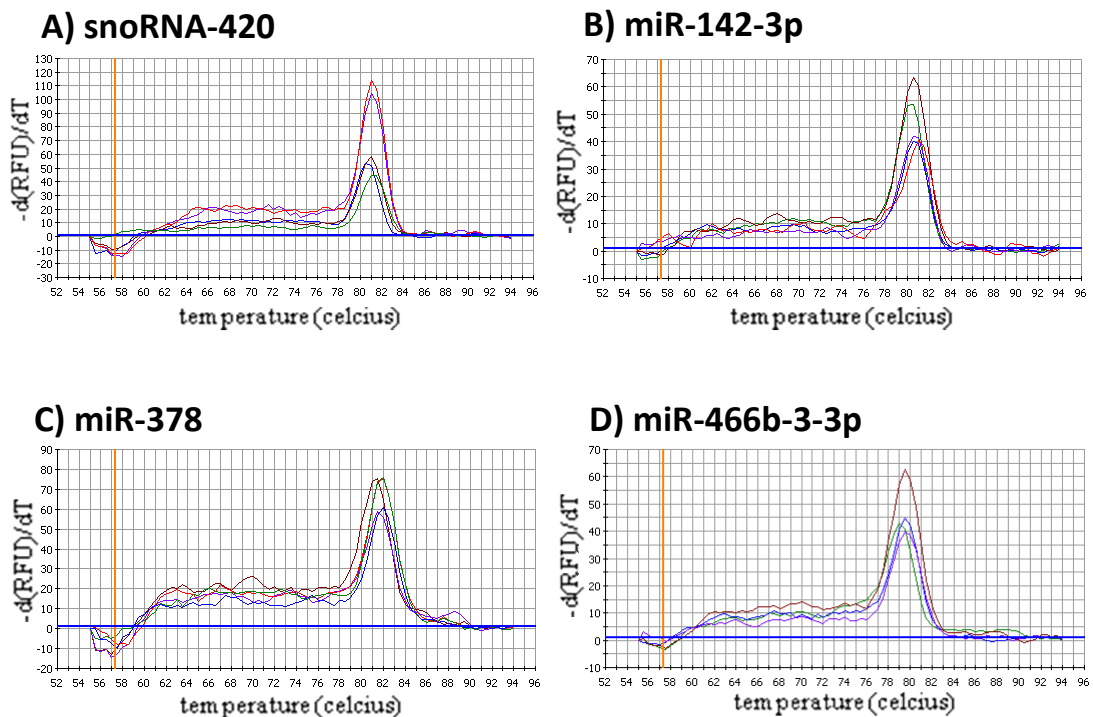


Figure 4.6. continued.

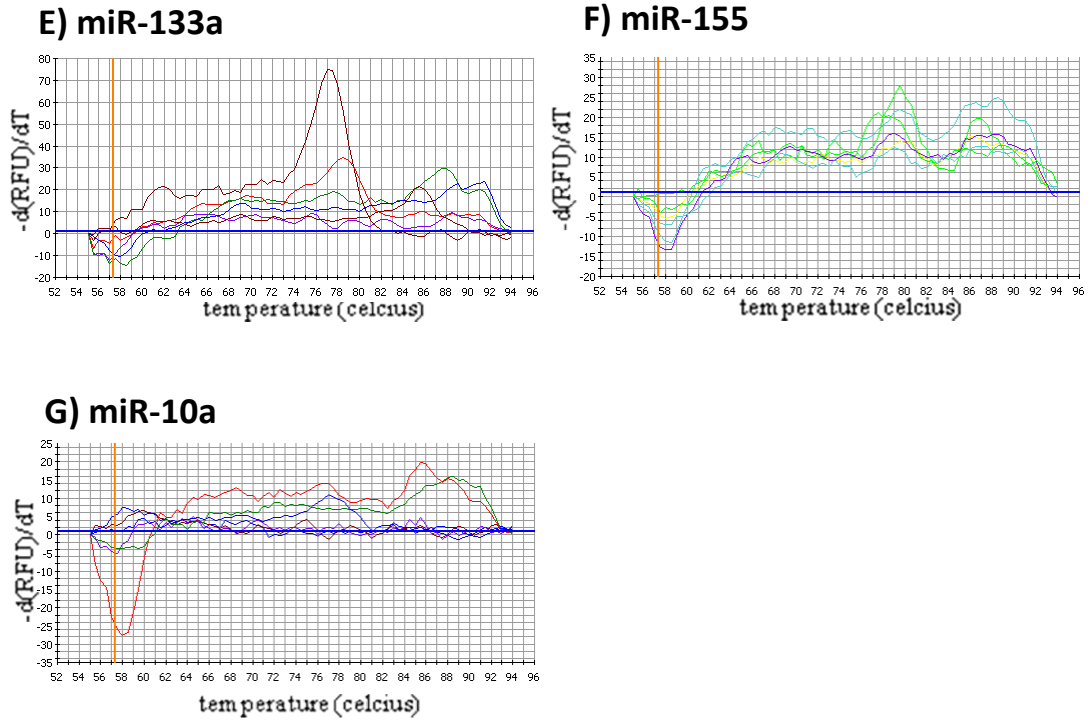


Figure 4. 6. Melting curve analyses. The graphs show the rate of change of the relative fluorescence units (RFU) with time (T) vs. temperature. The curves belong to the standard samples; experimental samples were not included.

Fold change in miR-466b-3-3p:

As shown in Figure 4.4.D, miR-466b-3-3p dilution standards gave amplification curves a bit closer to each other in the PCR amplification vs. cycle graph. This resulted in a PCR efficiency of 123,4 %, higher than 100 % (Figure 4.5.D). The correlation coefficient for the standard curve was 0,995. The melting curve analysis of the dilution standards also showed that only the desired product was amplified (Figure 4.6.D).

The threshold cycle values for the control and Dex treatment samples averaged 27,7 and 27,2, respectively (Figure 4.7.D). The calculation of the actual fold change in miR-466b-3-3p upon Dex treatment is shown below. Because the actual ratio is found to be 1,03, miR-466b-3-3p level did not change at all upon Dex treatment.

$$\text{fold change in miR-466b-3-3p (Dex/control)} = (2,234)^{27,7-27,2} = \mathbf{1,49}$$

$$\text{actual ratio of miR-466b-3-3p (Dex/control)} = 1,49/1,44 = \mathbf{1,03}$$

Real time PCR Data of miR-133a, miR-155 and miR-10a:

Analysis of miR-133a real time PCR data is given in Figure 4.4.E, Figure 4.6.E and Table 4.1. Figure 4.4.E shows the amplification vs. cycle graph of the standard dilutions. Here we noted that the order of the amplification curves was not related to the initial amount of the cDNA template. This was reflected in the C_T values, as seen in Table 4.1. When we analyzed the melting curves of the standard samples, we realized that amplifications were not specific. Because, all the curves peaked at different temperatures, and the peaks were small in height, with one exception (Figure 4.6.E). This means that contaminating DNA or RNA material or primer dimers were amplified nonspecifically during the reaction. Therefore, we were not able to determine the change in miR-133a levels upon Dex treatment.

Samples (dilution)	Threshold cycle (C_T)						
	sno420	miR142-3p	miR378	miR466b-3-3p	miR133a	mir155	miR10a
10^0		17.9	20.2		38.4	31.0	37.8
10^{-1}	24.7	19.9	22.2	24.3	29.4	29.8	33.1
10^{-2}	27.3	23.2	25.4	27.0	31.8	34.7	35.7
10^{-3}	30.7	29.0	28.9	30.7	34.2	37.9	N/A
10^{-4}	34.6	32.0	32.6	32.7	37.7	N/A	N/A
10^{-5}	36.7	36.2	35.8		34.5	N/A	N/A
Experimental samples							
Control (10^{-2})	27.3	23.2	25.4	27.8	33.0	35.6	35.7
	27.6	23.4	25.5	28.3	32.3	35.2	38.5
	27.4	24.3		27.0	31.8	34.7	36.8
DEX (10^{-2})	27.0	22.7	26.1	26.8	33.6	35.1	34.9
	27.0	23.7	25.4	26.9	32.5	34.8	36.4
	26.6	23.2	26.2	27.7	32.9	32.9	35.5

Table 4. 1. The threshold cycle values for the standard and experimental samples.

As seen in the amplification vs. cycle graph in Figure 4.4.F and in the threshold cycles given in Table 4.1, amplification of the standard dilutions for miR-155 did not have a correlation. Therefore, we could not obtain a standard curve for miR-155. Melting curve analysis, shown in Figure 4.6.F, clarified the reason for lack of

correlation. Non-specific products were amplified in the PCR, as the melting curves of the standards did not show a similar pattern and did not plot a single large peak. Hence we could not obtain information about the change in miR-155 levels resulting from Dex treatment.

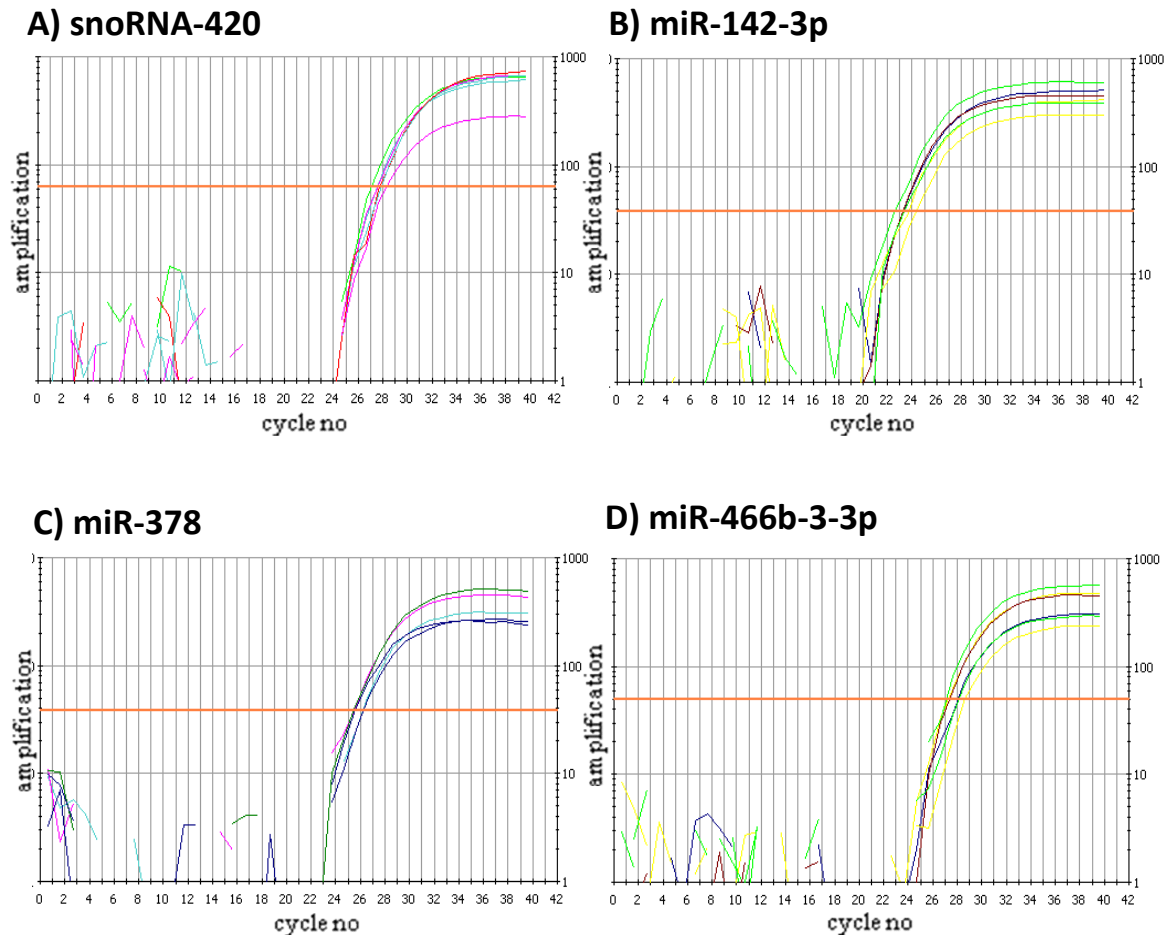


Figure 4. 7. PCR amplification vs. cycle graphs for the experimental samples (control and Dex treatment). A) snoRNA-420, B) miR-142-3p, C) miR-378, D) miR-466b-3-3p.

Lastly, real time PCR of miR-10a also did not work. Amplification curve of the standard samples in Figure 4.4.G did not show a correlation with the dilutions of the standards, and half of the samples were even not assigned with a C_T value because that amplification was very weak (Table 4.1). For each of the standard samples, PCR amplification was nonspecific as illustrated by the melting curve graph in Figure 4.6.G. Here, the melting curves did not make a large peak at a particular temperature; they rather slightly peaked at several points.

Thus, even though all cells upregulate IL-7R upon Dex treatment in this tissue culture system, presumably partly because they lose Gfi1 expression, the expression levels of the 3 miRNAs that were hypothesized to control Gfi1 expression do not change. We still do not know how expression levels of the other 3 miRNAs, for which real time RT-PCR did not work, change under this condition. In addition, miRNAs that were not predicted by the bioinformatics software may be playing a role in controlling Gfi-1 and therefore IL-7R expression.

4.2. UNDERSTANDING THE ROLES OF GFI1 DOMAINS IN REPRESSION OF IL-7R α EXPRESSION

4.2.1. Cloning of Gfi1 Truncations

We generated five different truncations of mouse Gfi1 to examine their effects in IL-7R α repression (Figure 4.8). mGfi1-SNAG was solely composed of the SNAG domain; and mGfi1- Δ SNAG (or dSNAG) contained the whole protein except the SNAG domain. mGfi1-ZFs truncation contained only the zinc fingers of the protein while mGfi1- Δ ZFs (or dZFs) excluded the zinc fingers at all. Finally, mGfi1- Δ SNAG, Δ ZFs (dSNAG,dZFs) lacked both the SNAG domain and the zinc fingers, and was comprised of the middle domain which had the Ala/Gly-rich region.

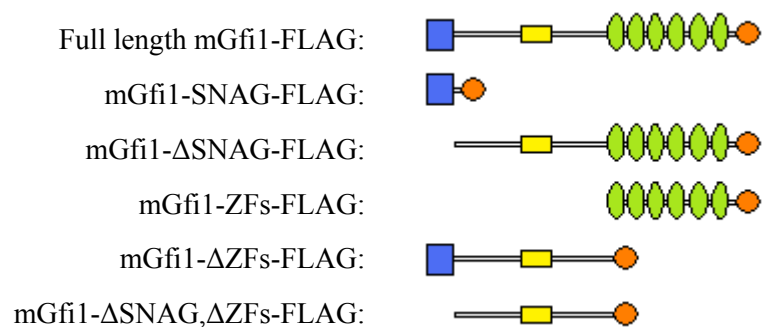


Figure 4. 8. Gfi1 truncations used in the project. Blue box: SNAG domain, yellow box: Ala/Gly-rich region, green circles: zinc finger motifs, orange circle: Flag tag.

The strategy for generating the desired Gfi1 truncations is depicted in Figure 4.9. Truncations were generated by PCR amplification from a pBluescript-mGfi1 template. For the amplification of SNAG and Δ ZFs, M13 forward primer and specific reverse primers which beared flag tag sequence, stop codon and NotI cut site were used. For the amplification of Δ SNAG and ZFs, specific forward primers which beared XhoI cut site followed by Kozak sequence and T7 reverse primers were used. Amplification of Δ SNAG, Δ ZFs required only the specific forward and reverse primers. Consequently, all of the PCR products carried the cut sites for XhoI and NotI at both ends. These PCR products were first digested with XhoI and NotI, and then ligated into the double digested LZRS vector. The resulting recombinant vectors that contain the 5 different Gfi truncations depicted in Figure 4.9 were confirmed by restriction enzyme digestion (Figure 4.10) and by sequencing (Appendix B). Diagnostic XhoI-NotI digestion of truncated cDNA-containing vectors pops out an expected size band from the LZRS plasmid backbone (Figure 3.1 and Figure 4.10).

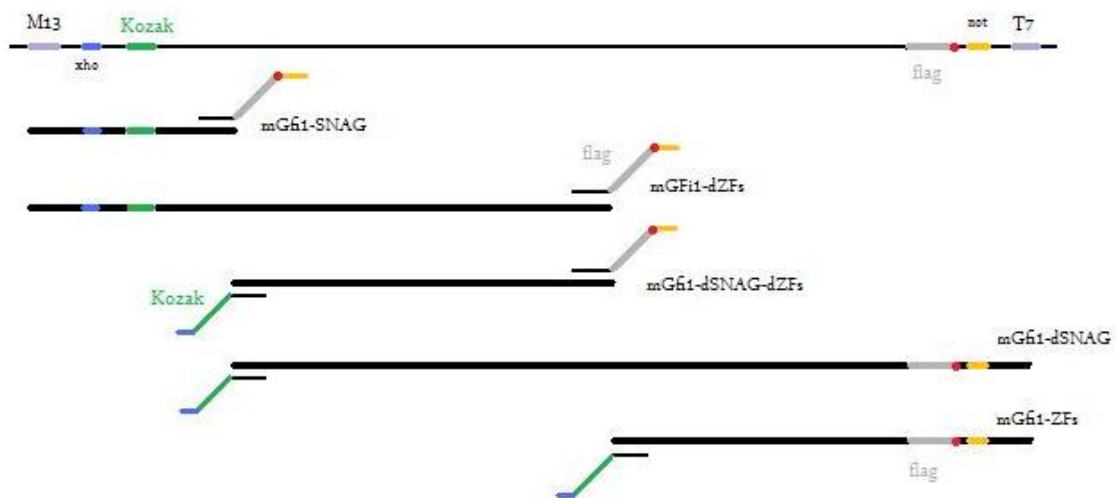


Figure 4. 9. Strategy for cloning of Gfi1 truncations into LZRS vector. Note: Amplification of mGfi1- Δ SNAG, mGfi1- Δ ZFs and mGfi1- Δ SNAG, Δ ZFs was achieved by using 5 % DMSO in the PCR reaction. Blue: XhoI cut site, green: Kozak sequence, orange: NotI cut site, red: Stop codon, gray: Flag epitope sequence, thick black bars: amplicons.

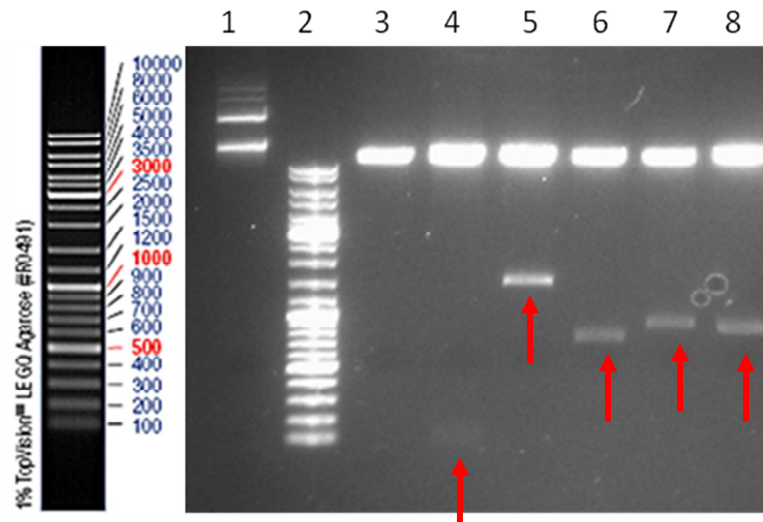


Figure 4. 10. Confirmation of the recombinant LZRS vectors by restriction enzyme digestion. Lane 1: uncut lzrs, lane 2: GeneRuler DNA Master Mix, xhoI-notI double digestions: lane 3: lzrs, lane 4: SNAG-lzrs, lane 5: Δ SNAG-lzrs, lane 6: ZFs-lzrs, lane 7: Δ ZFs-lzrs, lane 8: Δ SNAG, Δ ZFs-lzrs.

4.2.2. Infection Experiments

In order to ectopically express the full length Gfi1 and its truncations in the 3B4.15 T cell line, we generated retroviruses encoding the relevant cDNA and infected 3B4.15 T cells. To generate retroviruses, we transfected Phoenix packaging cells with the corresponding LRZS vectors. We applied supernatants of transfected Phoenix cells containing viral particles to 3B4.15 cells in culture and assessed the infection efficiency by GFP positivity (encoded by the LZRS virus backbone). As seen in Figure 3.1, the LZRS retroviral vector uses the 5'LTR to transcribe the inserted cDNA fused to and IRES element and an eGFP gene in a bicistronic mRNA. Thus, GFP can be used as a marker for cDNA expression because infected cells expressing GFP also express the cDNA.

4.2.2.1. IL-7R α expression on cells infected with control retroviruses

In these experiments, we used empty LZRS vector as a control. Phoenix cells transfected with empty vector produced viruses that transferred the coding sequence of only enhanced Green Fluorescent Protein (eGFP) into the host's genome. As GFP overexpression does not interfere with IL-7R α expression, we did not observe any difference in the IL-7R α level between GFP-negative (uninfected) and GFP-positive (infected) 3B4.15 cells. As shown in Figure 4.11, PE-A mean fluorescence intensity (MFI) and PE-A median channel fluorescence (MCF) values were approximately the same between uninfected and infected population under both control and Dex treatment conditions.

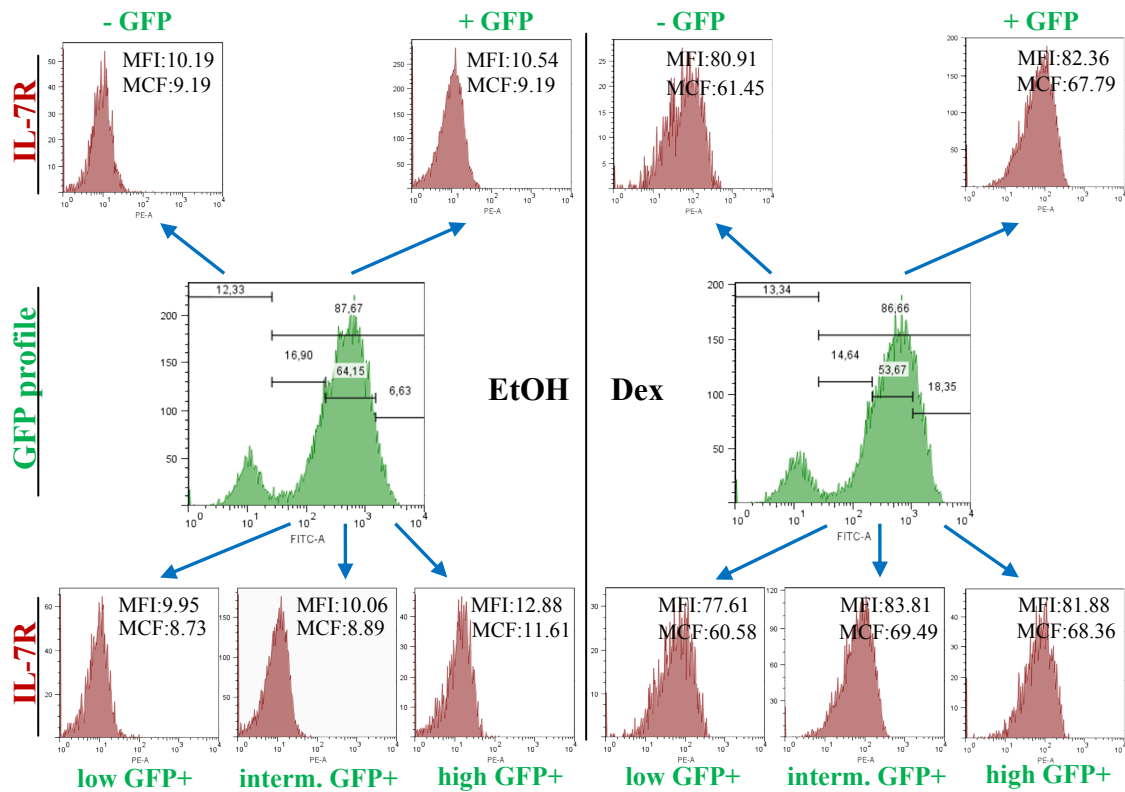


Figure 4. 11. Retroviral insertion of LZRS alone did not alter IL-7R expression levels in 3B4.15 cells. GFP fluorescence was detected in the FITC channel, and IL-7R α was detected in the PE-A channel.

4.2.2.2. IL-7R α expression on cells infected with full length mouse Gfi1 expressing retroviruses

As shown in Figure 4.12, retroviral overexpression of full length Gfi1 in 3B4.15 cells showed that Gfi1 did not suppress IL-7R α further under control conditions. This implied that 3B4.15 cells normally did not have any IL-7R on their surface. Dex treatment led to increase in IL-7R levels in uninfected cells as PE-A MFI increased from 11,63 to 71,08. Ectopic expression of Gfi1 partially suppressed this induction. PE-A MFI of GFP-positive cells only scored 50,67 for Dex treatment while it was 12,03 for control. Moreover, as the level of GFP expression increased, the decrease in PE-A MFI, and therefore repression of IL-7R α , became more marked.

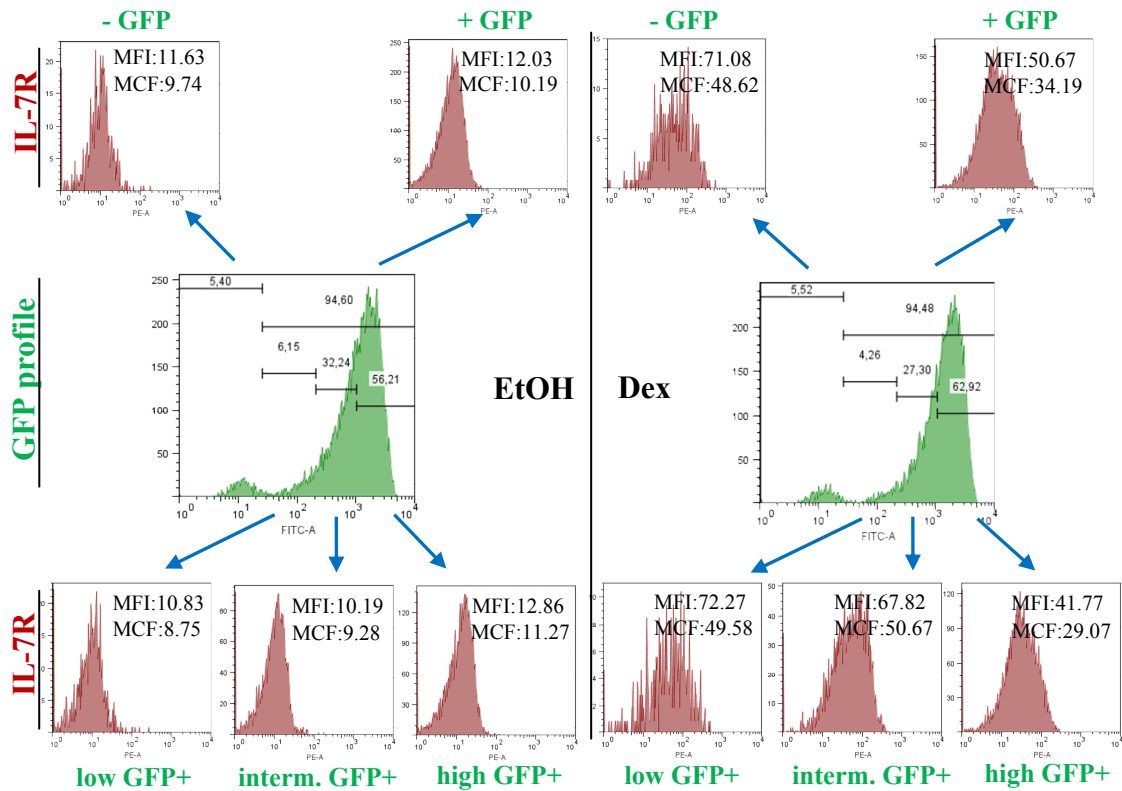


Figure 4. 12. Full length Gfi1 repressed IL-7R α induction upon Dex treatment.

4.2.2.3. IL-7R α expression on cells infected with mGfi1-SNAG expressing retroviruses

The IL-7R α expression profiles of cells after retroviral overexpression of mGfi1-SNAG and upon Dex stimulation are shown in Figure 4.13. Dex stimulation increased IL-7R α expression in infected and uninfected 3B4.15 cells to the same extent; PE-A MFI peaked to 72,57 and 73,26, respectively, from 12,07 and 11,13. Therefore, overexpression of Gfi1 SNAG domain did not suppress IL-7R α induction by itself.

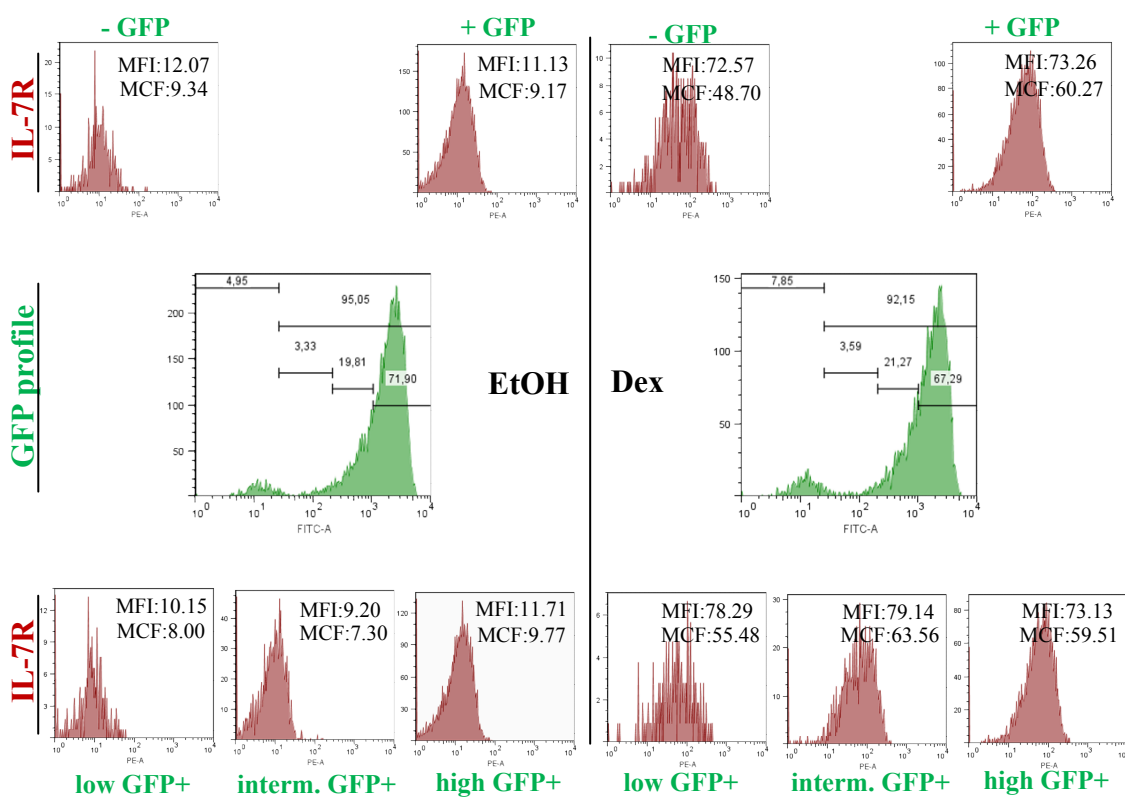


Figure 4. 13. Gfi1-SNAG domain did not suppress IL-7R α induction upon Dex stimulation.

4.2.2.4. IL-7R α expression on cells infected with mGfi1- Δ SNAG expressing retroviruses

The effect of Gfi1- Δ SNAG truncation on IL-7R α expression was also analyzed upon Dex stimulation (Figure 4.14). PE-A MFI exhibited an increase from 12,56 to 77,57 in GFP-negative cells upon Dex treatment. The increase in PE-A MFI for GFP-positive cells was also similar; from 10,96 to 79,65. Therefore, Δ SNAG truncation was not able to suppress IL-7R α expression.

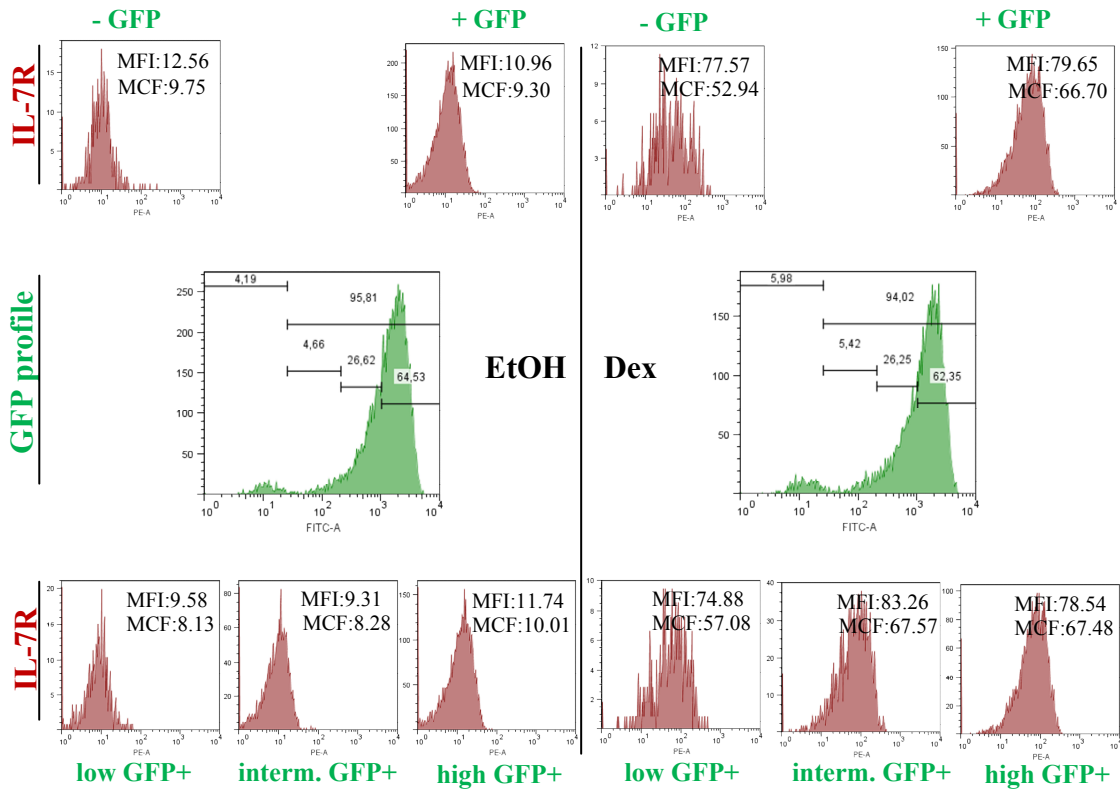


Figure 4. 14. Overexpression of Gfi1- Δ SNAG did not repress IL-7R α induction upon Dex stimulation.

4.2.2.5. IL-7R α expression on cells infected with mGfi1-ZFs expressing retroviruses

As seen in Figure 4.15, overexpression of Gfi1's zinc fingers domain in 3B4.15 cells did not alter IL-7R α levels in control and Dex treatment conditions. PE-A MFI values for infected and uninfected cells were 13,34 and 11,06, respectively, when there was no treatment. PE-A MFI values were still very close (73,21 and 78,92) for infected and uninfected cells after Dex stimulation, demonstrating that the zinc fingers of Gfi1 alone did not have an effect on the IL-7R α promoter in 3B4.15 cells upon Dex stimulation.

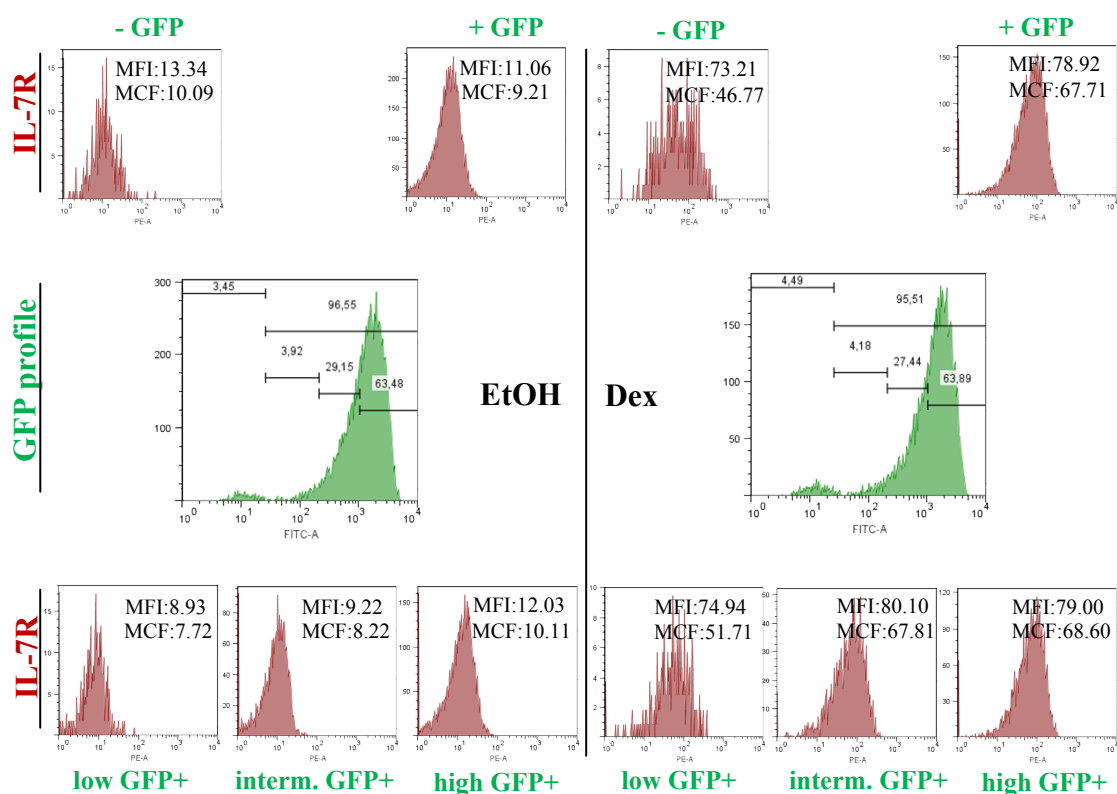


Figure 4. 15. Gfi1-ZFs domain was not sufficient by itself to repress IL-7R α expression.

4.2.2.6. IL-7R α expression on cells infected with mGfi1- Δ ZFs expressing retroviruses

Another Gfi1 truncation to be tested for its capability of repressing IL-7R α was mGfi1- Δ ZFs. Figure 4.16 shows that Dex treatment resulted in similar increases in PE-A MFI for uninfected cells (from 9,55 to 67,54) and for infected cells (from 12,54 to 72,25). This indicated that overexpression of mGfi1- Δ ZFs did not downregulate IL-7R α expression induction in 3B4.15 cells.

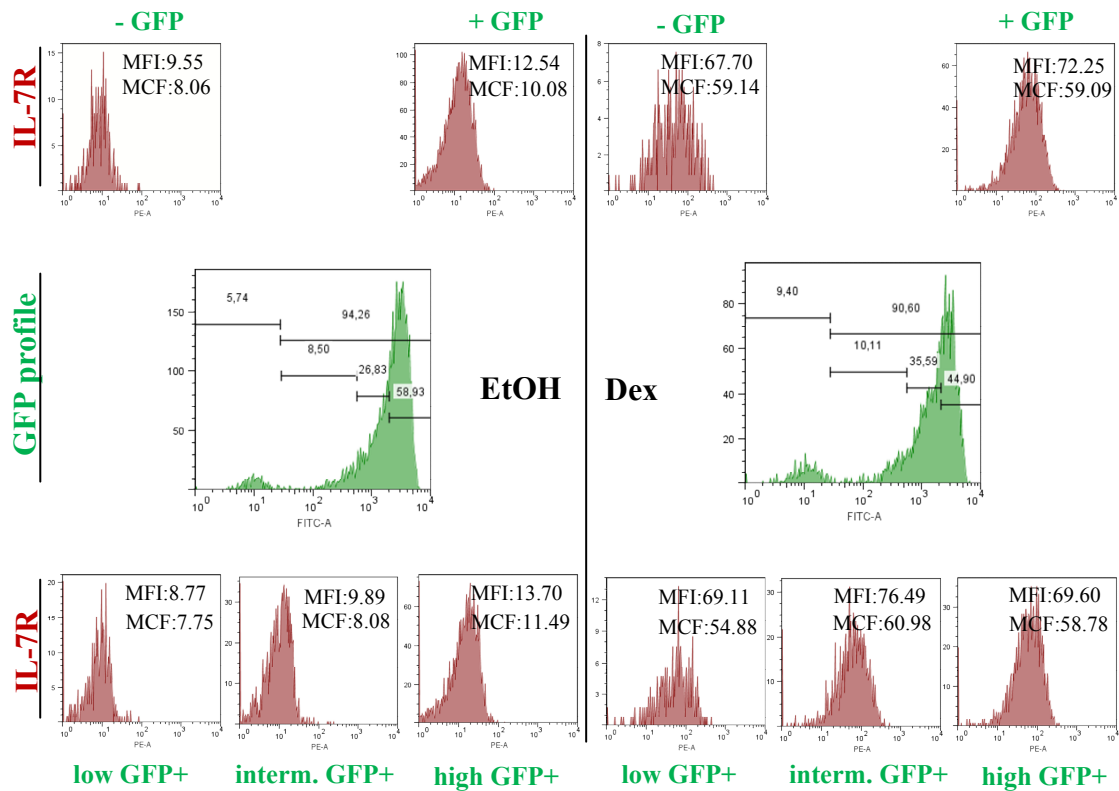


Figure 4. 16. Overexpression of Gfi1- Δ ZFs did not result in repression of IL-7R α induction.

4.2.2.7. IL-7R α expression on cells infected with mGfi1- Δ SNAG, Δ ZFs expressing retroviruses

Retroviral overexpression of mGfi1- Δ SNAG, Δ ZFs also gave results similar to other truncations (Figure 4.17). GFP-positive cells induced IL-7R α as much as GFP-negative cells upon Dex stimulation; PE-A increased from 12,06 to 71,29 for GFP-

positive cells, and from 11,97 to 66,23 for GFP-negative cells. Therefore, mGfi1- Δ SNAG, Δ ZFs did not alter IL-7R α levels.

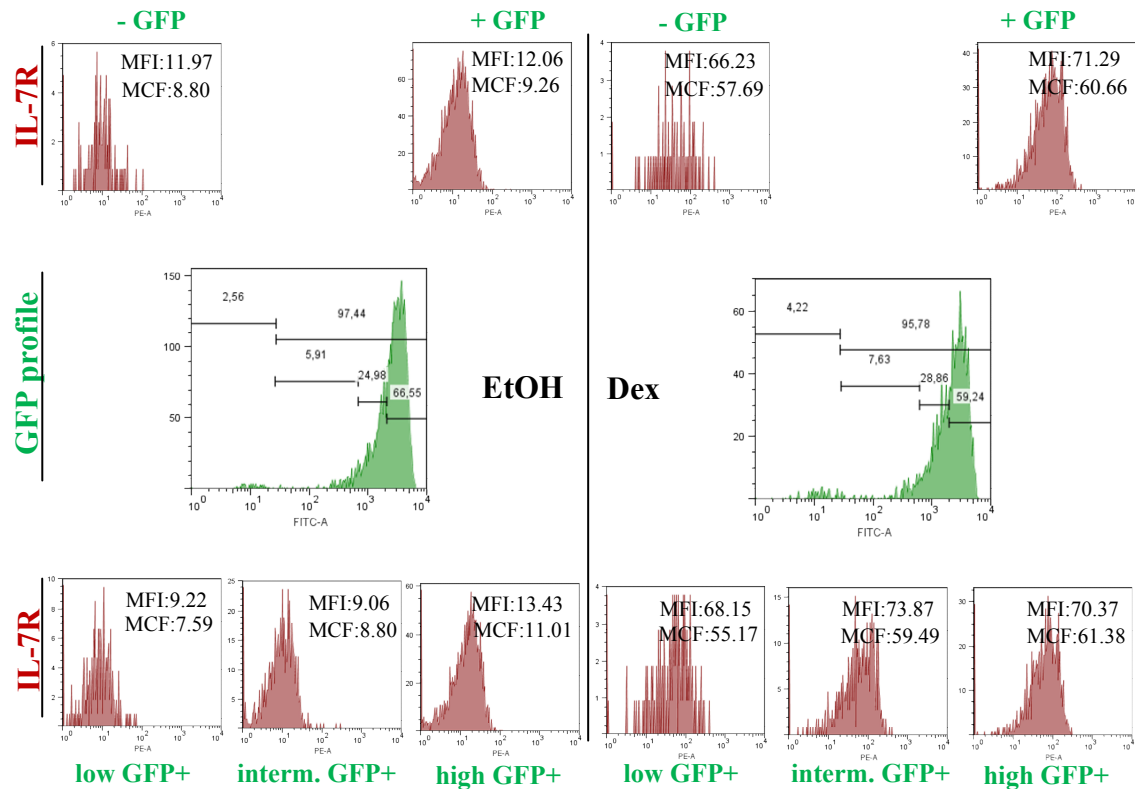


Figure 4. 17. Gfi1- Δ SNAG, Δ ZFs had no effect in IL-7R α repression by itself.

We performed the retroviral overexpression of Gfi1 truncations in 3B4.15 cells at least 2 times. The overall conclusion of these experiments is that full length Gfi1 repressed Dex-induced IL-7R α , while the truncations and individual domains of Gfi1 did not display this function.

4.2.3. Immunodetection of Gfi1 Truncations in 3B4.15 Cells

In order to ensure that the infected cells really expressed the exogenous Gfi1 truncations, we prepared protein lysates and immunoblotted these lysates against anti-Flag antibodies. Figure 4.8 shows that the full length Gfi1 and its truncations were all

epitope tagged with a Flag epitope. As seen in Figure 4.18, anti-Flag western blotting demonstrated that except for the Gfi1-SNAG truncation, all of the Gfi1 truncations were expressed in 3B4.15 cells. The calculated molecular weights of the Gfi1 truncations are given in Appendix C.

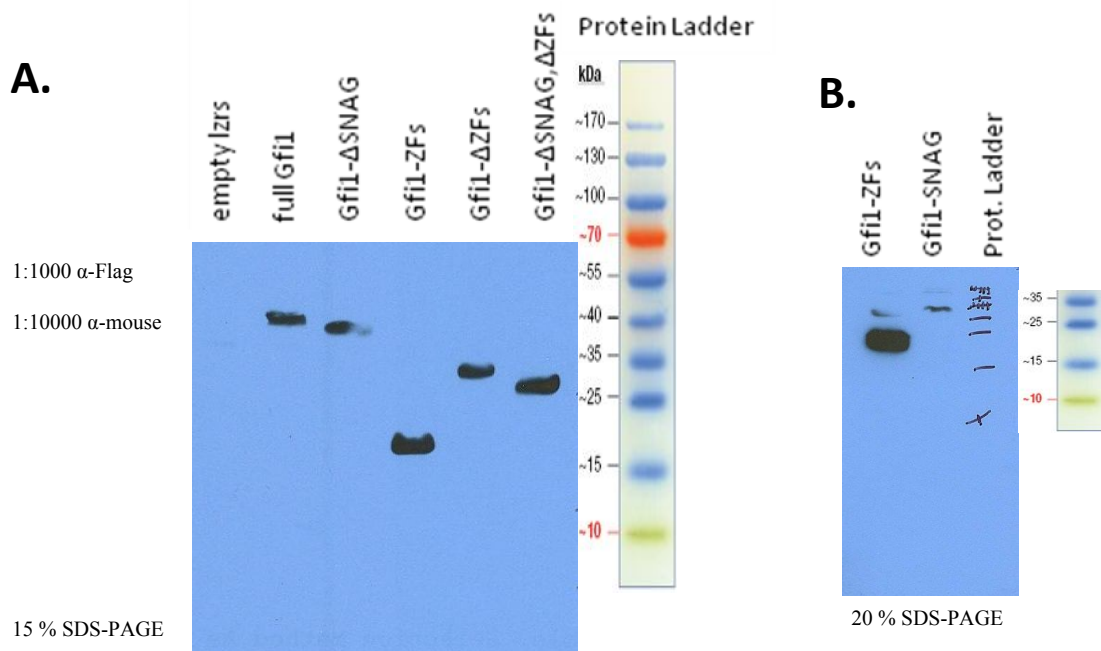


Figure 4. 18. Immunoblotting of infected cell lysates against α -Flag antibody. All of the Gfi1 truncations were detected in 3B4.15 lysates (A), with the exception of Gfi1-SNAG, which could not be detected despite increased gel concentration and overnight film exposure (B).

4.3. REPRESSION OF IL-7R α EXPRESSION BY FOXP3 AND GFI1B IN 3B4.15 CELLS

We also overexpressed Foxp3 in 3B4.15 cells by retroviral transduction. Figure 4.19 shows that Foxp3 significantly repressed IL-7R α induction upon Dex treatment. The MFI for PE-A channel increased from 6,04 to 35,38 and from 6,53 to 39,80 after Dex stimulation in uninfected cells. This increase was also observed in cells infected

with empty LZRS retroviruses (from 5,70 to 34,54), implying that LZRS had no effect on IL-7R α expression by itself. In contrast, cells infected with Foxp3-LZRS did not exert the same increase as PE-A MFI increased from 7,91 to 15,54. The repression of IL-7R α induction by Foxp3 becomes more marked in cells that express highest levels of GFP. These cells express more Foxp3, and consequently the PE-A MFI value is only 12,14 for them after Dex treatment. Therefore, overexpression of Foxp3 in 3B4.15 cells greatly, but not completely, blocked the expression of IL-7R α .

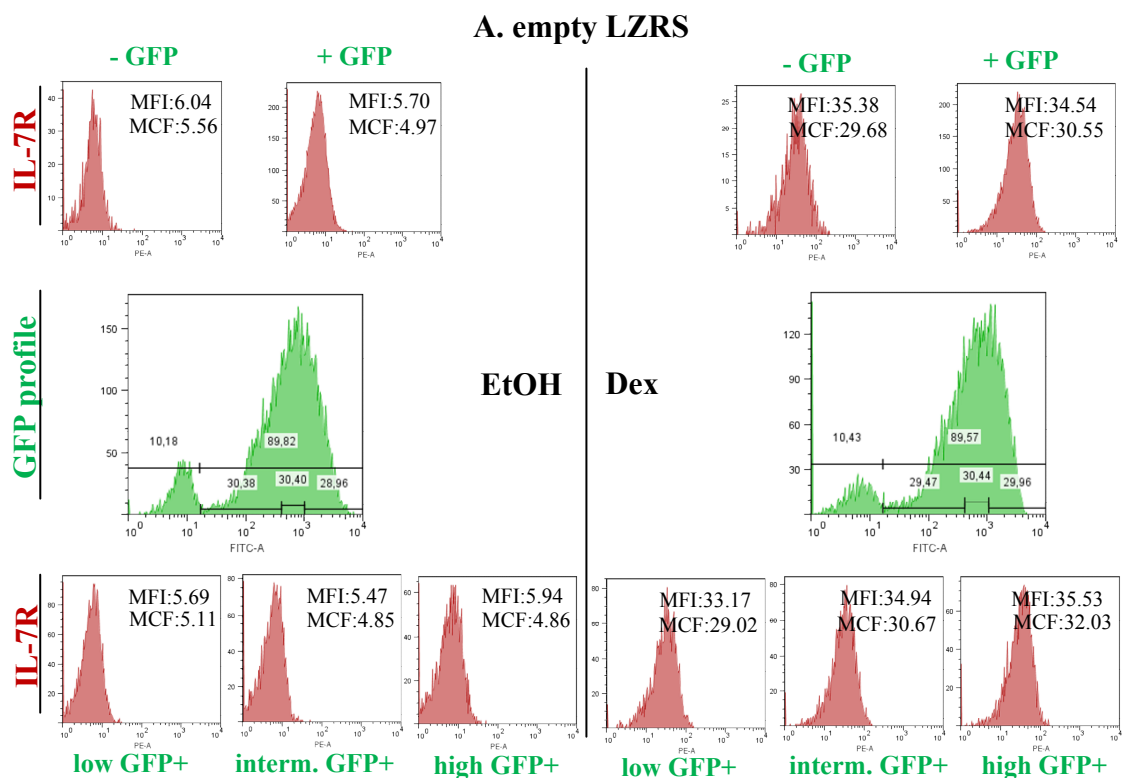


Figure 4.19. continued.

B. Foxp3-LZRS

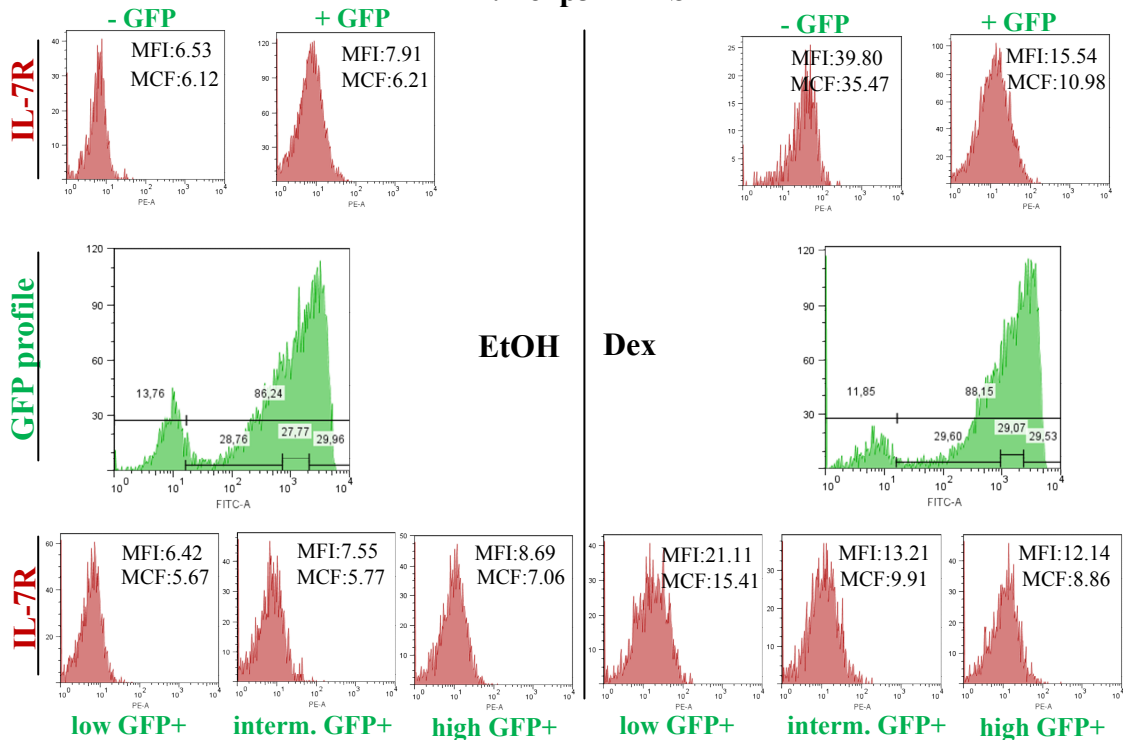


Figure 4. 19. Repression of IL-7R α expression by Foxp3 in 3B4.15 cells. A) Overexpression of empty LZRS vector had no effect on IL-7R α expression. B) Overexpression of Foxp3 in 3B4.15 greatly reduced IL-7R α induction upon Dex treatment, as PE-A MFI was 15,54 for GFP-positive population whereas it was 39,80 for GFP-negative population in the same sample.

Finally, we retrovirally overexpressed Gfi1b in 3B4.15 cells. The flow cytometry results after Dex treatment are shown in Figure 4.20. Dex treatment resulted in increase in IL-7R α levels as PE-A MFI elevated from 20,05 to 115,25 in the GFP-negative cell population of Gfi1b overexpression sample. On the other hand, the GFP-positive cells in the same sample display a much smaller increase of IL7R expression (from 16,38 to 62,10). Furthermore, PE-A MFI for cells that express the highest GFP, and therefore the highest Gfi1b, was only 32,67. This result demonstrated that the repression of IL-7R α was clearly modulated by Gfi1b in a dose dependent manner, like it was modulated by full length Gfi1 and Foxp3. On the contrary, cells infected with empty LZRS retroviruses did not differ in IL-7R α expression, when compared to uninfected cells. These results clearly demonstrated that Gfi1b greatly repressed IL-7R α expression that was induced in 3B4.15 cells upon Dex stimulation.

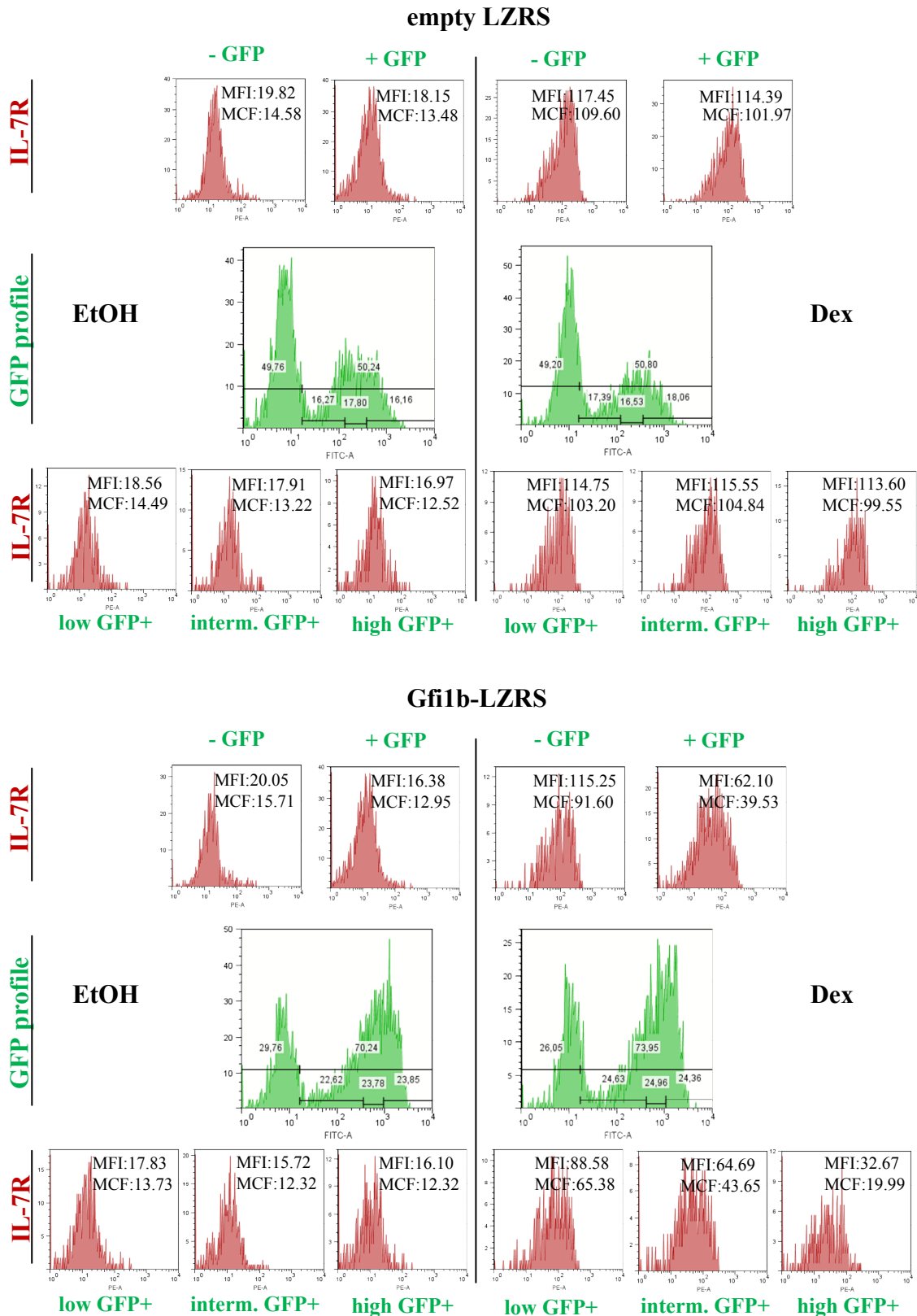


Figure 4. 20. Repression of IL-7R α expression by Gfi1b in 3B4.15 cells. Overexpression of Gfi1b in 3B4.15 greatly reduced IL-7R α levels.

5. DISCUSSION

Interleukin-7 (IL-7) signaling is vital for the development and homeostasis of lymphocytes. The IL-7 ligand is produced at a constant rate by the stromal cells of lymphoid organs and by epithelial cells. On the other hand, IL-7 Receptor (IL-7R) expression is upregulated or downregulated according to the cell's need. Therefore, IL-7 signaling is regulated at the level of IL-7R expression. This regulation of IL-7R expression should be very strict, because IL-7 is produced at a limiting amount that is just sufficient for a finite number of lymphocytes¹. It is also important as many important cellular processes highly depend on the expression status of IL-7R, such as the determination of T versus B cell fate at the CLP stage⁹⁹.

IL-7R is composed of the common γ chain and the IL-7R α chain. Because the common γ chain is shared by many other cytokine receptors, IL-7 signaling capacity of a cell is determined by its IL-7R α expression level⁷. Many transcription factors have been shown to directly act on the promoter of the IL-7R α gene to control its expression. Growth factor independent 1 (Gfi1) is one of these important transcription factors which has a repressive role on IL-7R α ²⁹. Glucocorticoids, such as dexamethasone (Dex), on the other hand, induce its expression. This induction is dependent on the action of glucocorticoid receptor (GR) which glucocorticoids bind and activate^{72, 73}. It has been shown that Dex treatment induces IL-7R α in the 3B4.15 T cell line. 3B4.15 cells have been derived from mature CD4⁺ T cells, but they have somehow lost their IL-7R α expression. After Dex stimulation it was also shown by northern blotting that Gfi1 mRNA level significantly decreased (Park, H. & Erman, B., unpublished). This observation implied a role for Gfi1 downregulation in IL-7R α induction apart from GR

activation. Downregulation of Gfi1 mRNA might be controlled either at the transcription level or at the post-transcriptional level. Figure 5.1 shows the possible means of this downregulation. One alternative is that Dex treatment activates GR which may, in turn, directly or indirectly repress transcription of the Gfi1 gene. In the indirect repression scenario, GR activates an inhibitory Factor X, which acts on the Gfi1 promoter to repress its expression. Alternatively, activated GR may directly upregulate expression of miRNAs against Gfi1 to silence its expression. Finally, it is also possible that GR may be indirectly inducing the expression of miRNAs by activating a Factor Y, which in turn induces the expression of these target miRNAs.

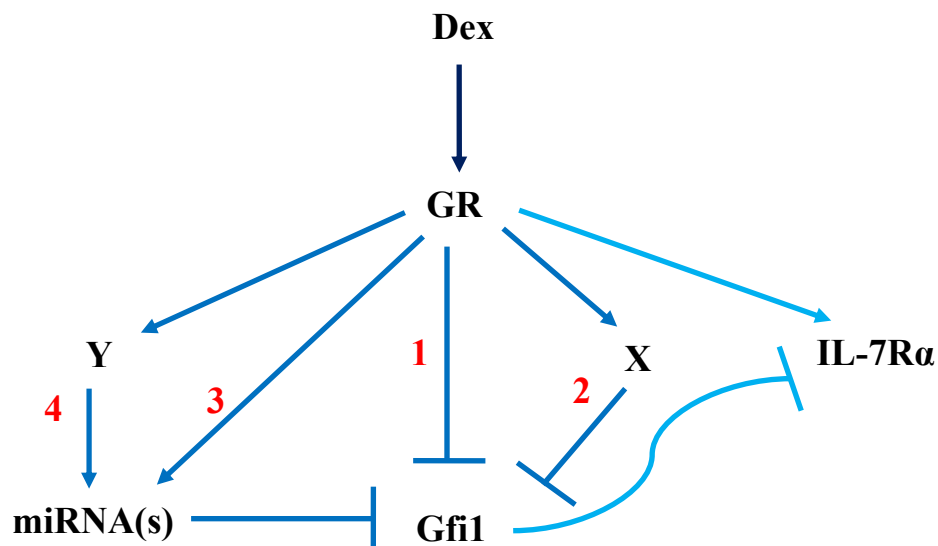


Figure 5. 1. Alternative means of Gfi1 downregulation upon Dex stimulation in 3B4.15 cells. Activated GR may directly (1) or indirectly (2), through activating another transcription factor, Factor X, induce the transcription of Gfi1 gene. Activated GR may alternatively upregulate expression of miRNA(s) which in turn silences Gfi1. This upregulation might be direct (3) or indirect via activation of a transcription factor Y (4).

Having determined the possible scenarios for Gfi1 downregulation upon Dex treatment, we decided to search whether Gfi1 is downregulated by RNA interference. It was previously shown by several studies that Gfi1 expression was frequently controlled at the level of mRNA. Some studies reported that the SL3-3 murine leukemia virus induced T-cell lymphoma by overexpression of oncogenic Gfi1 due to the loss of its miRNA binding sites by retroviral insertion⁹⁵. To this end, we aimed to use a real time

RT-PCR approach in order to observe potential increases in expression levels of Gfi1-targeting miRNAs. Therefore, we first decided on the set of miRNAs to study by searching several mouse miRNA target prediction databases. We found out that miR-142-3p, miR-133a, miR-466b-3-3p and miR-378 were the most promising Gfi1-targeting miRNAs as they scored highly in the target prediction databases. We also decided to study the expression levels of miR-155 and miR-10a since these miRNAs were also found to regulate Gfi1 levels⁹⁵. miR-378 and miR-466b-3-3p satisfied the 8nt seed match requirement, whereas miR-142-3p, miR-10a and miR-155 satisfied the 7nt seed match requirement.

Combination of stem-loop reverse transcription with real time PCR is a powerful method to relatively quantitate the expression levels of miRNAs. miRNAs are small, ~22 nucleotides long, RNA molecules, therefore it is impossible to selectively convert them to cDNAs and to amplify them in PCR using linear primers. Stem-loop primers, on the other hand, provide specificity and sensitivity of the RT reaction due to base stacking and spatial constraints of the stem loop structure^{96, 97}. The cDNA products of stem-loop reverse transcription is longer due to incorporation of the primers and can form a proper template to be amplified by linear primers in real time PCR.

The real time RT-PCR results showed that snoRNA-420 was a proper reference gene to be used in quantitative analysis of miRNAs in mouse, as its level did not change between control and Dex treatment. We found out that miR-142-3p, miR-378 and miR-466b-3-3p levels were also unaltered upon Dex treatment. The melting curve analyses of all miRNA species, as well as snoRNA-420, proved that the amplifications in real time PCR were specific. This was further confirmed by running the PCR products on agarose gels (data not shown). Therefore, we concluded that these miRNA species remained almost at the same level between control and Dex treatment in contrast to our initial hypothesis.

PCR for miR-133a, miR-155 and miR-10a, on the other hand, did not work, so that we were not able to quantitate their expression levels in control and Dex treatment

conditions. Melting curve analyses, retarded C_T values and lack of correlation between the C_T values and the dilutions implied that amplifications were not specific. The lack of specific binding might have resulted from either a lack of these miRNA species in the samples or an inability of the primers to bind to the complementary sites on their template. Consequently, amplification products observed in these PCRs originated from non-specific amplification of other contaminating DNA or RNA species, or of primer dimers.

We initially hypothesized that Gfi1 might be silenced by RNA interference upon Dex stimulation in 3B4.15 T cell line. But real time RT-PCR data eliminated the possibility that the most promising miRNA species, which scored highly in target prediction software, were upregulated upon Dex stimulation. This indicates that these 3 miRNAs do not play a role in the downregulation of Gfi1 by RNA interference. Yet, there is still a possibility that the remaining 3 miRNA species, whose PCR did not work, play a role in Gfi1 downregulation. In this context, we also cloned the 3'UTR of the mouse Gfi1 gene in order to generate a reporter vector that can be used to test the transcription regulation function of the Gfi1 3'UTR. Studies with this reporter may in the future yield important clues about the significance of miRNAs in Gfi1 transcription.

In order to characterize the nature of the repression of IL-7R α by the Gfi1 transcription factor, we aimed to determine which domains of Gfi1 were important in this function. We generated 5 different truncations of the mouse Gfi1 protein. 3 of these truncations were solely composed of one of the three domains of the Gfi1 protein, namely, Gfi1-SNAG, Gfi1-ZFs, which was formed by six zinc fingers, and Gfi1- Δ SNAG, Δ ZFs, which was the intermediate domain. The other two truncations were Gfi1- Δ SNAG and Gfi1- Δ ZFs, which lacked the SNAG and the zinc fingers domains, respectively. Gfi1 has two nuclear localization signals that direct the protein to the nucleus. One them is in the N-terminal SNAG domain, the other is localized in the zinc fingers domain¹⁰⁰. Therefore, all the truncations that we generated except Gfi1- Δ SNAG, Δ ZFs were supposed to be transported into the nucleus. The exact subcellular locations of these truncated proteins can be identified by confocal microscopy.

We used the 3B4.15 cell line in order to test the capability of Gfi1 truncations to repress IL-7R α . After infecting the cells with LZRS vectors that bear the Gfi1 truncations, we treated the cells with and without Dex. As noted before, these cells normally induced IL-7R α expression after Dex stimulation. We observed that the full length Gfi1 was able to partially repress IL-7R α induction. On the other hand, we did not notice any decrease in IL-7R α when the truncations were overexpressed. Therefore, neither of them was able to repress IL-7R α . We confirmed expression of these truncations except Gfi1-SNAG in 3B4.15 cells by immunoblotting against the Flag epitope tag which all of these truncations contained in their C-terminus. Although we loaded 100 μ g of protein extract, used 20% polyacrylamide gel and stopped running at an early time point, we were not able to detect the expression of the smallest truncation, Gfi1-SNAG. The difficulty in detecting this protein may arise from the fact that it was only 31 amino acids long including the Flag tag. Another reason that we could not detect Gfi1-SNAG might be that it was not stable in the cell because it was a very small protein and it was rapidly degraded.

The SNAG domain was also found to be crucial for Gfi1's function in previous studies^{80, 81}. Our data that Gfi1- Δ SNAG or Gfi1-ZFs overexpression did not repress IL-7R α also confirmed this observation. The zinc fingers domain was also found to be essential for Gfi1's repression function in this retroviral overexpression study, as Gfi1- Δ ZFs was not able to repress IL-7R α . It was shown that the zinc fingers are not required for Gfi1's STAT3 activation function; because zinc fingers-deleted Gfi1 was also able to bind and sequester PIAS3¹⁰¹. Therefore, we demonstrated that repression of IL-7R α by Gfi1 was dependent on its DNA binding and transcriptional repression abilities. Lastly, zinc fingers are generally considered suitable motifs against which small molecule drugs could be designed. In case that Gfi1-ZFs repressed IL-7R α by itself, this finding might have been exploited for therapeutic purposes. In such a case it would have been possible to screen for small molecules that could specifically alter the zinc fingers domain's affinity for DNA binding¹⁰².

To sum up, we showed that the SNAG domain, the zinc fingers domain and the intermediate domain were not sufficient to repress IL-7R α by themselves. However, we also showed that both the SNAG domain and the zinc fingers domain were required by the protein, that is, they were not redundant in Gfi1's repression activity. In other words, Gfi1 protein should be intact to repress IL-7R α .

We also ectopically expressed Gfi1b and Foxp3 in 3B4.15 cells and examined their effect on IL-7R α levels after Dex stimulation. We observed that Gfi1b overexpression significantly repressed IL-7R α . The zinc fingers were highly conserved among Gfi1 and Gfi1b. Consequently they have the same consensus DNA binding sequence. It was shown that Gfi1b could also repress IL-7R α in T and B cells^{86, 87}. Thus, our result was consistent with this observation. Foxp3 overexpression also resulted in IL-7R α repression in our system. Foxp3 transcription factor is considered as the master regulator of regulatory T (Treg) cells. Loss-of-function mutations in Foxp3 result in IPEX disease which is characterized by the lack of Treg cells¹⁰³. Foxp3 expression was shown to be inversely correlated with IL-7R α . Besides, Treg cells are characterized by their lack of IL-7R α ⁸⁸. Consequently, it is possible that inappropriate expression of IL-7R α might be one of the reasons for the development of IPEX.

Because of its significance in the immune system, the regulation of IL-7R has been an important subject. This study has revealed the regulatory functions of several transcription factors on the promoter of the IL-7R α gene.

REFERENCES

1. Mazzucchelli R. & Durum S. K. Interleukin-7 receptor expression: intelligent design. *Nature Reviews Immunology*. **Vol 7**. 144-154 (2007).
2. Yu, Q., Erman, B., Park, J. H., Feigenbaum, L. & Singer, A. IL-7 receptor signals inhibit expression of transcription factors TCF-1, LEF-1, and ROR γ t: impact on thymocyte development. *J. Exp. Med.* **200**, 797–803 (2004).
3. Purohit, S. J. *et al.* Determination of lymphoid cell fate is dependent on the expression status of the IL-7 receptor. *EMBO J.* **22**, 5511–5521 (2003).
4. Jiang, Q. *et al.* Retroviral transduction of IL-7R α into IL-7R α ^{-/-} bone marrow progenitors: correction of lymphoid deficiency and induction of neutrophilia. *Gene Ther.* **12**, 1761–1768 (2005).
5. Corcoran, A. E., Riddell, A., Krooshoop, D. & Venkitaraman, A. R. Impaired immunoglobulin gene rearrangement in mice lacking the IL-7 receptor. *Nature* **391**, 904–907 (1998).
6. Brugnera, E., *et al.*, Coreceptor reversal in the thymus: signaled CD4⁺8⁺ thymocytes initially terminate CD8⁺ transcription even when differentiating into CD8⁺ T cells. *Immunity* **13**, 59-71 (2000).
7. Khaled, A. R. & Durum, S. K. Lymphocide: cytokines and the control of lymphoid homeostasis. *Nature Rev. Immunol.* **2**, 817–830 (2002).
8. Cunningham-Rundles, C. & Ponda, P. P. Molecular defects in T- and B-cell primary immunodeficiency diseases. *Nature Rev. Immunol.* **5**, 880–892 (2005).
9. Osmond, D.G., Rolink, A., and Melchers, F. Murine B lymphopoiesis: towards a unified model. *Immunol. Today* 1998, **19**: 65-68.
10. He, Y. W. & Malek, T. R. Interleukin-7 receptor α is essential for the development of $\gamma\delta$ ⁺ T cells, but not natural killer cells. *J. Exp. Med.* **184**, 289–293 (1996).
11. von Freeden-Jeffry, U., *et al.* Lymphopenia in interleukin (IL)-7 gene-deleted mice identifies IL-7 as a nonredundant cytokine. *J. Exp. Med.* **181**, 1519–1526 (1995).

12. Peschon, J. J. *et al.* Early lymphocyte expansion is severely impaired in interleukin 7 receptor-deficient mice. *J. Exp. Med.* **180**, 1955–1960 (1994).
13. Maki, K. *et al.* Interleukin 7 receptor-deficient mice lack $\gamma\delta$ T cells. *Proc. Natl Acad. Sci. USA* **93**, 7172–7177 (1996).
14. Grabstein, K. H. *et al.* Inhibition of murine B and T lymphopoiesis *in vivo* by an anti-interleukin 7 monoclonal antibody. *J. Exp. Med.* **178**, 257–264 (1993).
15. Bhatia, S. K., Tygrett, L. T., Grabstein, K. H. & Waldschmidt, T. J. The effect of *in vivo* IL-7 deprivation on T cell maturation. *J. Exp. Med.* **181**, 1399–1409 (1995).
16. Schluns, K. S., Kieper, W. C., Jameson, S. C. & Lefrancois, L. Interleukin-7 mediates the homeostasis of naive and memory CD8 T cells *in vivo*. *Nature Immunol.* **1**, 426–432 (2000).
17. Kondrack, R. M. *et al.* Interleukin 7 regulates the survival and generation of memory CD4 cells. *J. Exp. Med.* **198**, 1797–1806 (2003).
18. Puel, A., Ziegler, S. F., Buckley, R. H., & Leonard, W. J. Defective IL7R expression in T(-)B(+)NK(+) severe combined immunodeficiency. *Nature Genet.* **20**, 394-397 (1998).
19. Yeoman, H., Clark, D. R. & DeLuca, D. Development of CD4 and CD8 single positive T cells in human thymus organ culture: IL-7 promotes human T cell production by supporting immature T cells. *Dev. Comp. Immunol.* **20**, 241–263 (1996).
20. Plum, J., De, S. M., Leclercq, G., Verhasselt, B. & Vandekerckhove, B. Interleukin-7 is a critical growth factor in early human T-cell development. *Blood* **88**, 4239–4245 (1996).
21. Yao Z., *et.al.* Stat5a/b are essential for normal lymphoid development and differentiation. *PNAS* **103:4**. 1000-1005 (2006).
22. Jiang Q., *et.al.* Cell biology of IL-7, a key lymphotrophin. *Cytokine Growth Factor Rev.* **16:4**. 513-533 (2005).
23. Li, W. Q., *et.al.* IL-7 promotes T cell proliferation through destabilization of p27Kip1. *J. Exp. Med.* **203**: 573-582 (2006)
24. Khaled, A.R., *et.al.* Cytokine-driven cell cycling is mediated through Cdc25A. *J. Cell Biol.* **169**: 755–763 (2005).
25. Namen, A. E., *et.al.*, Stimulation of B-cell progenitors by cloned murine interleukin-7. *Nature* **333**. 571-573 (1998).
26. Fry, T. J. & Mackall, C. L. The many faces of IL-7: from lymphopoiesis to peripheral T cell maintenance. *J. Immunol.* **174**, 6571–6576 (2005).

27. Rich, B. E., Campos-Torres, J., Tepper, R. I., Moreadith, R. W. & Leder, P. Cutaneous lymphoproliferation and lymphomas in interleukin 7 transgenic mice. *J. Exp. Med.* **177**, 305–316 (1993).
28. Fisher, A. G., Burdet, C., Bunce, C., Merckenschlager, M. & Ceredig, R. Lymphoproliferative disorders in IL-7 transgenic mice: expansion of immature B cells which retain macrophage potential. *Int. Immunol.* **7**, 415–423 (1995).
29. Park, J. H. *et al.* Suppression of IL7R α transcription by IL-7 and other prosurvival cytokines: a novel mechanism for maximizing IL-7-dependent T cell survival. *Immunity* **21**, 289–302 (2004).
30. Munitic, I. *et al.* Dynamic regulation of IL-7 receptor expression is required for normal thymopoiesis. *Blood* **104**, 4165–4172 (2004).
31. Franchimont, D. *et al.* Positive effects of glucocorticoids on T cell function by up-regulation of IL-7 receptor α . *J. Immunol.* **168**, 2212–2218 (2002).
32. Yasuda, Y., *et al.* Interleukin-7 inhibits pre-T-cell differentiation induced by the pre-T-cell receptor signal and the effect is mimicked by hGM-CSF in hGM-CSF receptor transgenic mice. *Immunology* **106**, 212–221 (2002).
33. Palmer, M. J., Mahajan, V.S., Trajman, L., Lauffenburger, D.A. & Chen, J., Perspectives on the quantitative immunobiology of the IL-7 signaling network. *Cell Mol. Immunol.* **5 (2)**: 79-89 (2008).
34. Takaki S., *et al.*, Characterization of Lnk: An adaptor protein expressed in lymphocytes, *The Journal of Biological Chemistry* **272**, 14562-14570 (1997).
35. Maraskovsky, E. *et al.* Bcl-2 can rescue T lymphocyte development in interleukin-7 receptor-deficient mice but not in mutant rag-1^{-/-} mice. *Cell* **89**, 1011–1019 (1997).
36. Kondo, M., Akashi, K., Domen, J., Sugamura, K. & Weissman, I. L. Bcl-2 rescues T lymphopoiesis, but not B or NK cell development, in common γ chain-deficient mice. *Immunity* **7**: 155–162 (1997).
37. Khaled, A. R. *et al.* Bax deficiency partially corrects interleukin-7 receptor α deficiency. *Immunity* **17**, 561–573 (2002).
38. Candeias S., *et al.* Defective T-cell receptor gamma gene rearrangement in interleukin-7 receptor knockout mice. *Immunol Lett.* **1;57**: 9-14 (1997).
39. Yu, Q. *et al.* Cytokine signal transduction is suppressed in preselection double-positive thymocytes and restored by positive selection. *J. Exp. Med.* **203**, 165–175 (2006).
40. Jiang, Q. *et al.* Retroviral transduction of IL-7R α into IL-7R α ^{-/-} bone marrow progenitors: correction of lymphoid deficiency and induction of neutrophilia. *Gene Ther.* **12**, 1761–1768 (2005).

41. Henriques, C.M., Rino, J., Nibbs, R. J., Graham, G. J. & Barata, J. T., IL-7 induces rapid clathrin-mediated internalization and JAK3-dependent degradation of IL-7R α in T cells, *Blood* **115** (16): 3269 – 3277 (2010).
42. Munitic, I., *et al.* Dynamic regulation of IL-7 receptor expression is required for normal thymopoiesis. *Blood*. **104**: 4165–4172 (2004).
43. Tan, J. Y., *et al.* IL-7 is critical for homeostatic proliferation and survival of naive T cells. *PNAS*. **98**: 8732–8737 (2001).
44. Tanchot, C., Lemonnier, F. A., Perarnau, B., Freitas, A. A., Rocha, B., Differential requirements for survival and proliferation of CD8⁺ naive or memory T cells. *Science* **276**: 2057–2062 (1997).
45. Kaech, S. M., *et al.* Selective expression of the interleukin 7 receptor identifies effector CD8 T cells that give rise to long-lived memory cells. *Nature Immunol.* **4**, 1191–1198 (2003).
46. Surh, C. D., *et al.* Homeostasis of memory T cells. *Immunological Reviews*. **211**:1 2006. 154-163 (2006).
47. Bachmann, M. F., P. Wolint, K. Schwarz, P. Jager, A. Oxenius. 2005. Functional properties and lineage relationship of CD8⁺ T cell subsets identified by expression of IL-7 receptor α and CD62L. *J. Immunol.* **175**: 4686-4696.
48. Osborne, L. C., *et al.* Impaired CD8 T cell memory and CD4 T cell primary responses in IL-7R α mutant mice. *J. Exp. Med.* **204**: 619-631 (2007).
49. Lenz, D. C., *et al.* IL-7 regulates basal homeostatic proliferation of antiviral CD4⁺ T cell memory. *PNAS*. **101**, 9357–9362 (2004).
50. Buentke, E., *et al.* Do CD8 effector cells need IL-7R expression to become resting memory cells? *Blood*. **108**, 1949–1956 (2006).
51. Lacombe, M. H., Hardy, M. P., Rooney, J. & Labrecque, N. IL-7 receptor expression levels do not identify CD8⁺ memory T lymphocyte precursors following peptide immunization. *J. Immunol.* **175**, 4400–4407 (2005).
52. Li, J., Huston, G. & Swain, S. L. IL-7 promotes the transition of CD4 effectors to persistent memory cells. *J. Exp. Med.* **198**, 1807–1815 (2003).
53. Huster, K. M., *et al.* Selective expression of IL-7 receptor on memory T cells identifies early CD40L-dependent generation of distinct CD8⁺ memory T cell subsets. *PNAS*. **101**, 5610–5615 (2004).
54. Kieper, W. C. *et al.* Overexpression of interleukin (IL)-7 leads to IL-15-independent generation of memory phenotype CD8⁺ T cells. *J. Exp. Med.* **195**, 1533–1539 (2002).
55. Klonowski, K. D., Williams, K. J., Marzo, A. L. & Lefrancois, L. Cutting edge: IL-7-independent regulation of IL-7 receptor α expression and memory CD8 T cell development. *J. Immunol.* **177**, 4247–4251 (2006).

56. Miller, J. P. *et al.* The earliest step in B lineage differentiation from common lymphoid progenitors is critically dependent upon interleukin 7. *J. Exp. Med.* **196**, 705–711 (2002).
57. Carvalho, T. L., Mota-Santos, T., Cumano, A., Demengeot, J. & Vieira, P. Arrested B lymphopoiesis and persistence of activated B cells in adult interleukin 7^{-/-} mice. *J. Exp. Med.* **194**, 1141–1150 (2001).
58. Buckley, R. H. Molecular defects in human severe combined immunodeficiency and approaches to immune reconstitution. *Annu. Rev. Immunol.* **22**, 625–655 (2004).
59. Osmond, D.G., Rolink, A., and Melchers, F. Murine B lymphopoiesis: towards a unified model. *Immunol. Today.*, **19**: 65-68 (1998).
60. Namen, A. E. *et al.* Stimulation of B-cell progenitors by cloned murine interleukin-7. *Nature.* **333**, 571–573 (1988).
61. Hardy, R. R., Carmack, C. E., Shinton, S. A., Kemp, J. D. & Hayakawa, K. Resolution and characterization of pro-B and pre-pro-B cell stages in normal mouse bone marrow. *J. Exp. Med.* **173**, 1213–1225 (1991).
62. Corcoran, A. E., Smart, F. M., Cowling, R. J., Crompton, T., Owen, M. J., and Venkitaraman, A. R. The interleukin-7 receptor alpha chain transmits distinct signals for proliferation and differentiation during B lymphopoiesis. *EMBO J.* **15**, 1924-1932 (1996).
63. Sudo, T. *et al.* Expression and function of the interleukin 7 receptor in murine lymphocytes. *PNAS* **90**, 9125–9129 (1993).
64. Georgopoulos, K., Transcription factors required for lymphoid lineage commitment. *Curr. Opin. Immunol.* **9**: 222-227 (1997).
65. de Bruijn, M. F. & Speck., N.A., Core-binding factors in hematopoiesis and immune function. *Oncogene* **23**: 4238-4248 (2004).
66. Scott, E. W., Simon, M.C., Anastasi, J., Singh, H., Requirement of transcription factor PU.1 in the development of multiple hematopoietic lineages. *Science* **265**: 1573-1577 (1994).
67. Fisher, R. C. & Scott. E.W., Role of PU.1 in hematopoiesis. *Stem Cells* **16**: 25-37 (1998).
68. DeKoter, R. P., Lee, H. J. & Singh, H. PU.1 regulates expression of the interleukin-7 receptor in lymphoid progenitors. *Immunity* **16**, 297–309 (2002).
69. Medina, K. L. *et al.* Assembling a gene regulatory network for specification of the B cell fate. *Dev. Cell* **7**, 607–617 (2004).
70. Xue, H. H. *et al.* GA binding protein regulates interleukin 7 receptor α -chain gene expression in T cells. *Nature Immunol.* **5**, 1036–1044 (2004).

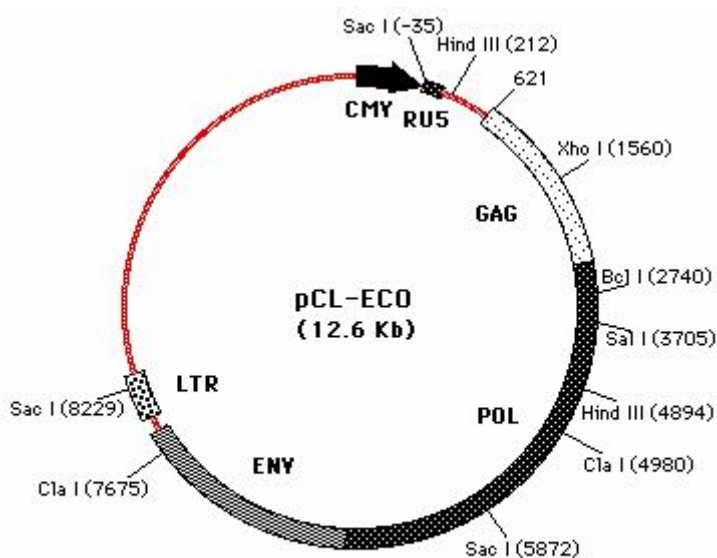
71. Egawa, T., *et.al.*, The role of the Runx transcription factors in thymocyte differentiation and in homeostasis of naive T cells. *JEM.* **204**, 81945-1957 (2007).
72. Lee, H. C., Shibata, H., Ogawa, S., Maki, K. & Ikuta, K., Transcriptional regulation of the mouse IL-7 receptor α promoter by glucocorticoid receptor. *J. Immunol.* **174**, 7800–7806 (2005).
73. Franchimont, D. *et al.* Positive effects of glucocorticoids on T cell function by up-regulation of IL-7 receptor α . *J. Immunol.* **168**, 2212–2218 (2002).
74. Galon, J. *et al.* Gene profiling reveals unknown enhancing and suppressive actions of glucocorticoids on immune cells. *FASEB J.* **16**, 61–71 (2002).
75. Miller, A.H., *et.al.*, Glucocorticoid receptors are differentially expressed in the cells and tissues of the immune system. *Cell. Immunol.* **186**, 45–54 (1998).
76. Vacchio, M. S., Papadopoulos, V., and Ashwell, J.D., Steroid production in the thymus: implications for thymocyte selection. *J. Exp. Med.* **179**, 1835–1846 (1994).
77. Purton, J. F., Boyd, R. L., Cole, T. J. & Godfrey, D. I., Intrathymic T Cell Development and Selection Proceeds Normally in the Absence of Glucocorticoid Receptor Signaling, *Immunity* **13**, 179–186 (2000).
78. McGhee, L., *et.al.*, Gfi-1 attaches to the nuclear matrix, associates with ETO (MTG8) and histone deacetylase proteins, and represses transcription using a TSA-sensitive mechanism. *Journal of Cellular Biochemistry* **89**, 1005–1018 (2003).
79. Rödel, B., *et.al.*, The zinc finger protein Gfi-1 can enhance STAT3 signaling by interacting with the STAT3 inhibitor PIAS3. *EMBO Journal* **19**, 5845–5855 (2000).
80. Möröy, T., The zinc finger transcription factor growth factor independence 1 (Gfi1). *Int. J. Biochem. Cell. Biol.* **37**: 541-546 (2005).
81. Kazanjian, A., Gross, E. A. & Grimes, H. L., The growth factor independence-1 transcription factor: New functions and new insights. *Critical Reviews in Oncology/Hematology* **59**, 85–97 (2006).
82. Rathinam, C., & Klein, C., Transcriptional Repressor Gfi1 Integrates Cytokine-Receptor Signals Controlling B-Cell Differentiation. *PLoS ONE* **2(3)**: e306. (2007).
83. Karsunky, H., Mende, I., Schmidt, T., & Möröy, T., High levels of the onco-protein Gfi-1 accelerate T-cell proliferation and inhibit activation induced T-cell death in Jurkat T-cells. *Oncogene* **21**, 1571–1579 (2002).
84. Yücel, R., Kosan, C., Heyd, F., & Möröy, T., Gfi1: green fluorescent protein knock-in mutant reveals differential expression and autoregulation of the growth factor independence 1 (Gfi1) gene during lymphocyte development. *Journal of Biological Chemistry* **279**, 40906–40917 (2004).

85. Rödel, B., Wagner, T., Zörnig, M., Niessing, J., and Möröy, T., (1998) The human homologue (GFI1B) of the chicken GFI gene maps to chromosome 9q34.13 - a locus frequently altered in hematopoietic diseases. *Genomics* **54**: 580–582 (1998).
86. Doan, L. L. *et al.* Growth factor independence-1B expression leads to defects in T cell activation, IL-7 receptor alpha expression, and T cell lineage commitment. *J. Immunol.* **170**, 2356–2366 (2003).
87. Fiolka, K., *et al.*, Gfi1 and Gfi1b act equivalently in haematopoiesis, but have distinct, non-overlapping functions in inner ear development. *EMBO reports* **7**:3, 326-333 (2006).
88. Liu W., *et al.*, CD127 expression inversely correlates with FoxP3 and suppressive function of human CD4⁺ T reg cells. *JEM.* **203**(7) 1701-1711 (2006).
89. Nunes-Cabaço, H., *et al.*, Foxp3 induction in human and murine thymus precedes the CD4⁺ CD8⁺ stage but requires early T-cell receptor expression. *Immunology and Cell Biology* **88**, 523-528 (2010).
90. Allan, S.E., *et al.*, Activation-induced FOXP3 in human T effector cells does not suppress proliferation or cytokine production. *International Immunology* **19**(4): 345-354 (2007).
91. Pleiman, C. M., *et al.* Organization of the murine and human interleukin-7 receptor genes: two mRNAs generated by differential splicing and presence of a type I-interferon-inducible promoter. *Mol. Cell. Biol.* **11**, 3052–3059 (1991).
92. Tian, B., Nowak, D. E., Jamaluddin, M., Wang, S. & Brasier, A. R. Identification of direct genomic targets downstream of the nuclear factor- κ B transcription factor mediating tumor necrosis factor signaling. *J. Biol. Chem.* **280**, 17435–17448 (2005).
93. Kinsella, T. M. & Nolan, G. P., Episomal Vectors Rapidly and Stably Produce High-Titer Recombinant Retrovirus. *Human Gene Therapy* **7**(12): 1405-1413 (1996).
94. Naviaux, R.K., Costanzi, E., Haas, M. & Verma, I., The pCL vector system: Rapid production of helper-free, high titer, recombinant retroviruses. *J. Virol.* **70**, 5701-5705 (1996).
95. Dabrowska, M. J., *et al.*, Loss of microRNA-targets in the 3'-untranslated region as a mechanism of retroviral insertional activation of Growth Factor Independence 1. *J. Virol.* **83**(16), 8051-61 (2009).
96. Varkonyi-Gasic, E., *et al.*, Protocol: a highly sensitive RT-PCR method for detection and quantification of microRNAs. *Plant Methods* **3**:12 (2007).
97. Chen, C., *et al.*, Real-time quantification of microRNAs by stem-loop RT-PCR. *Nucleic Acids Res.* **33**(20): e179 (2005).
98. Pfaffl, M.W., A new mathematical model for relative quantification in real-time RT-PCR. *Nucleic Acids Res.* **29**(9):e45 (2001).

99. Purohit, S. J., et.al., Determination of lymphoid cell fate is dependent on the expression status of the IL-7 receptor. *EMBO J.* **22(20)**: 5511–5521 (2003).
100. Grimes, H. L., et.al., The Gfi-1 Proto-Oncoprotein Contains a Novel Transcriptional Repressor Domain, SNAG, and Inhibits G1 Arrest Induced by Interleukin-2 Withdrawal. *Molecular and Cellular Biology* **16:11**, 6263-6272 (1996).
101. Rödel, B., et.al., The zinc finger protein Gfi-1 can enhance STAT3 signaling by interacting with the STAT3 inhibitor PIAS3. *EMBO J.* **19**, 5845 – 5855 (2000).
102. Jamieson, A. C., Miller, J. C. & Pabo, C. O., Drug discovery with engineered zinc-finger proteins. *Nature Reviews Drug Discovery* **2**, 361-368 (2003).
103. Wildin, R. S., & Freitas, A., IPEX and FOXP3: clinical and research perspectives. *J. Autoimmun.* **25** Suppl. 56-62 (2005).

APPENDICES

APPENDIX A – pCL-ECO MAP



Cotransfection of Phoenix cells with pCL-ECO provides high level expression of gag, pol and env proteins in a balanced stoichiometry. Pol is the reverse transcriptase and the integrase. Gag (group antigens) is a polyprotein that form the viral core, and Env is the envelope protein.

APPENDIX B – CONFIRMATION OF THE CLONING OF GFI1 TRUNCATIONS BY SEQUENCING

The LZRS vectors bearing the Gfi1 truncations were sent to sequencing. The results of the sequencing reactions, which were performed by using LZRS sequencing forward primer that binds to the 5' of the xhoI cut site, are analyzed below (Only the regions between the XhoI and NotI sites are shown). XhoI cut site is highlighted in gray, whereas NotI cut site is highlighted in gray and also italicized. The start and stop codons are both bold typed, and highlighted in green and red, respectively. The sequences which are identical to the Gfi1 coding sequence are typed in purple font color, whereas the sequences that encode for the Flag epitope are typed in blue color.

mGfi1-SNAG

CTCGAGCTCAAGCTTACCACC**ATG**CCGCGCTCATTCCCTGGTCAAGAGCAAG
AAGGCGCACAGCTATCACCAGCCGCGTTCTGGATCCATGGACTACAAAGAC
GATGACGATAAA**TAG**CGGCCGC

mGfi1-ZFs

CTCGAGGCCACC**ATG**TCCTACAAATGCATCAAATGCAGCAAGGTGTTCTCC
ACACCGCACGGGCTGGAGGTGCACGTGCGCCGGTCCCACAGCGGCACAAGA
CCTTTTCGTGCGAGATGTGCGGCAAGACCTTCGGGCACGCGGTGAGCCTG
GAGCAACACAAGGCAGTGCACCTCCAGGAACGCAGCTTTGACTGTAAGATC
TGTGGCAAGAGCTTCAAGAGGTCATCCACGCTGTCCACACATCTGCTCATT
ACTCGGACACCCGGCCCTATCCCTGTCAGTACTGTGGCAAAGATTCCACCA
GAAGTCAGATATGAAGAAACACACCTTCATCCACACAGGTGAGAAGCCCCA
CAAATGCCAGGTGTGCGGCAAAGCCTTCAGTCAGAGCTCCAACCTCATCAC
TCATAGCAGAAAGCACACAGGCTTCAAGCCCTTTGGCTGTGACCTGTGTGG
GAAGGGCTTCAGAGGAAGGTGGATCTCAGGAGGCACCGAGAGACTCAGC
ATGGACTCAAACCTCGACGGTACCGCGGGCCCGGGATCCATGGACTACAAAG
ACGATGACGATAAA**TAG**TCTAGATCATAATCAGCCATACCACATTTGTAGA
GGTTTTACTTGCTTTAAAAAACCTCCCACACCTCCCCCTGAACCTGAAACAT
AAAATGAATGCAATTCCTGCAGCCCGGGGGATCCACTAGTTCTAGAGCGGCC
CGC

mGfi1-ΔSNAG,ΔZFs

CTCGAGGCCACC**ATG**CCAGGGCCGGACTACTCCCTGCGCCTGGAGACCGTG
CCTGCGCCGGGCAGAGCAGAGGGCGGCGCTGTGAGTGCAGGCGAGTCGAA
AATGGAGCCCCGAGAGCGTTTGTCCCCGACTCTCAGCTTACCGAGGCTCCC
GACAGGGCCTCCGCGTCCCCAACAGCTGCGAAGGCAGCGTTTGTGACCCC
TGCTCCGAGTTCGAGGACTTTTGGAGGCCCCCTTCTCCCTCCGTGTCTCCAG
CGTCGGAGAAGTCACTGTGCCGCTCTCTGGACGAAGCCCAGCCCTACACGC
TGCCTTTCAAGCCCTATGCATGGAGCGGTCTTGCCGGGTCTGACCTGCGGCA
CCTGGTGCAGAGCTATCGGCAGTGCAGCGCGCTGGAGCGCAGCGCGGGCCT
GAGCCTCTTCTGCGAGCGCGGCTCGGAGCCGGGCCGCCCAGCAGCGCGCTA
CGGCCCCGAGCAGGCTGCGGGCGGAGCCGGTGCGGGACAGCCAGGGAGCT
GCGGGGTGCGCCGGGGGCGCCACCAGCGCTGCGGGCCTGGGGCTCTACGGCG
ACTTCGCGCCTGCGGCGGCCGGGCTGTACGAGCGGCCGAGCACAGCAGCAG
GCCGGCTGTACCAAGATCATGGCCACGAGCTGCACGCGGACAAGAGCGTAG
GCGTCAAGGTGGAGTCGGAGCTGCTTTGCACCCGTCTGCTGCTGGGCGGCG
GCTCCTACAAAGGATCCAT**GACTACAAAGACGATGACGATAAA****TAG**CGG
NCGC

mGfi1-ΔSNAG

CTCGAGGCCACC**ATG**CCAGGGCCGGACTACTCCCTGCGCCTGGAGACCGTG
CCTGCGCCGGGCAGAGCAGAGGGCGGCGCTGTGAGTGCAGGCGAGTCGAA
AATGGAGCCCCGAGAGCGTTTGTCCCCGACTCTCAGCTTACCGAGGCTCCC
GACAGGGCCTCCGCGTCCCCAACAGCTGCGAAGGCAGCGTTTGTGACCCC
TGCTCCGAGTTCGAGGACTTTTGGAGGCCCCCTTCTCCCTCCGTGTCTCCAG
CGTCGGAGAAGTCACTGTGCCGCTCTCTGGACGAAGCCCAGCCCTACACGC
TGCCTTTCAAGCCCTATGCATGGAGCGGTCTTGCCGGGTCTGACCTGCGGCA
CCTGGTGCAGAGCTATCGGCAGTGCAGCGCGCTGGAGCGCAGCGCGGGCCT
GAGCCTCTTCTGCGAGCGCGGCTCGGAGCCGGGCCGCCCAGCAGCGCGCTA
CGGCCCCGAGCAGGCTGCGGGCGGAGCCGGTGCGGGACAGCCAGGGAGCT
GCGGGGTGCGCCGGGGGCGCCACCAGCGCTGCGGGCCTAGGGCTCTACGGCG
ACTTCGCGCCTGCGGCGGCCGGGCTGTACGAGCGGCCGAGCACAGCAGCAG
GCCGGCTGTACCAAGATCATGGCCACGAGCTGCACGCGGACAAGAGCGTAG
GCGTCAAGGTGGAGTCGGAGCTGCTTTGCACCCGTCTGCTGCTGGGCGGCG
GCTCCTACAAATGCATCAAATGCAGCAAGGTGTTCTCCACACCCGCACGGGC
TGGAGGTGCACGTGCGCCGGTCCCACAGCGGCACAAGACACTTTGCGTGCG
AGATGTGCGGCAAGACCTTCGGGCACGCGGTGAGCCTGGAGCAACACAAG
GCAGTGCACCTCCAGGAACGCAGCTTTGACTGTAAGATCTGTGGCAAGAGC
TTCAAGAGGTCATCCACGCTGTCCACACATCTGCTCATTCACTCGGACACCC
GGCCCTATCCCTGTCAGTACT.....

mGfi1-ΔZFs

CTCGAGCTCAAGCTTACCACC**ATG**CCGCGCTCATTCCCTGGTCAAGAGCAAG
AAGGCGCACAGCTATCACCAGCCGCGTTCTCCGGGGCCGGACTACTCCCTG
CGCCTGGAGACCGTGCCTGCGCCGGGCAGAGCAGAGGGCGGGCGCTGTGAGT
GCAGGCGAGTCGAAAATGGAGCCCCGAGAGCGTTTGTCCCCCGACTCTCAG
CTTACCGAGGCTCCCGACAGGGCCTCCGCGTCCCCAACAGCTGCGAAGGC
AGCGTTTGTGACCCCTGCTCCGAGTTCGAGGACTTTTGGAGGCCCCCTTCTC
CCTCCGTGTCTCCAGCGTCGGAGAAGTCACTGTGCTGCTCTCTGGACGAAGC
CCAGCCCTACACGCTGCCTTTCAAGCCCTATGCATGGAGCGGTCTTGCCGGG
TCTGACCTGCGGCACCTGGTGCAGAGCTATCGGCAGTGCAGCGCGCTGGAG
CGCAGCGCGGGCCTGAGCCTTCTGCGAGCGCGGCTCGGAGCCGGGCCGC
CCGGCAGCGCGCTACGGCCCCGAGCAGGCTGCGGGCGGAGCCGGTGCGGG
ACAGCCAGGGAGCTGCGGGGTGCGCCGGGGGCGCCACCAGCGCTGCGGGCCT
GGGGCTCTACGGCGACTTCGCGCCTGCGGCGGCCGGGCTGTACGAGCGGCC
GAGCACAGCAGCAGGCCGGCTGTACCAAGATCATGGCCACGAGCTGCACGC
GGACAAGAGCGTAGGCGTCAAGGTGGAGTCGGAGCTGCTTTGCACCCGTCT
GCTGCTGGGCGGGCGGCTCCTACAAAGGATCCATGGACTACAAAGACGATGA
CGATAAA**TAG**CGGCCGC

APPENDIX C – AMINO ACID SEQUENCE OF THE GFI1 TRUNCATIONS

The nucleotide sequences given in Appendix B encode the following peptides. The molecular weights of these peptides are also given below. The Flag epitope tags are typed in bold.

Full length mGfi1 (with Flag tag): 441 a.a. – 47,71 kilodaltons

mGfi1-SNAG (31 a.a. – 3,66 kilodaltons)

MPRSFLVKSKKAHSYHQPRSGSMDYKDDDDK

mGfi1-ZFs (188 a.a. – 21,33 kilodaltons)

**MSYKCIKCSKVFSTPHGLEVHVRRSHSGTRPFACEMCGKTFGHAVSLEQHKAV
HSQERSFDCKICGKSFKRSSSTLSTHLLIHS DTRPYPCQYCGKRFHQKSDMKKHT
FIHTGEKPHKCQVCGKAFSQSSNLITHSRKHTGFKPFGCDLCGKGFQRKVDLRR
HRETQHGLKLDGTAGPGSMDYKDDDDK**

mGfi1- Δ SNAG, Δ ZFs (249 a.a. – 25,99 kilodaltons)

**MPGPDYSLRLETVPAPGRAEGGAVSAGESKMEPRERLSPDSQLTEAPDRASASP
NSCEGSVCDPCSEFEDFWRPPSPSVSPASEKSLCRSLDEAQPYTLPFKPYAWSGL
AGSDLRHLVQSYRQCSALERSAGLSLFCERGSEPGRPAARYGPEQAAGGAGAG
QPGSCGVAGGATSAAGLGLYGDFAPAAAGLYERPSTAAGRLYQDHGHELHAD
KSVGVKVESELLCTRLLLGGGSYKGSMDYKDDDDK**

mGfi1-ΔSNAG (422 a.a. – 45,53 kilodaltons)

MPGPDYSLRLETVPAPGRAEGGAVSAGESKMEPRERLSPDSQLTEAPDRASASP
NSCEGSVCDPCSEFEDFWRPPSPSVSPASEKSLCRSLDEAQPYTLPFKPYAWSGL
AGSDLRHLVQSYRQCSALERSAGLSLFCERGSEPGRPAARYGPEQAAGGAGAG
QPGSCGVAGGATSAAGLGLYGDFAPAAAGLYERPSTAAGRLYQDHGHELHAD
KSVGKVESELLCTRLLLGGGSYKCIKCSKVFSTPHGLEVHVRRSHSGTRHFAC
EMCGKTFGHAVSLEQHKAVHSQERSFDCKICGKSFKRSSTLSTHLLIHS DTRPYP
CQY...

mGfi1-ΔZFs (268 a.a. – 28,18 kilodaltons)

MPRSFLVKSKKAHSYHQPRSPGPDYSLRLETVPAPGRAEGGAVSAGESKMEPR
ERLSPDSQLTEAPDRASASPNSCEGSVCDPCSEFEDFWRPPSPSVSPASEKSLCCS
LDEAQPYTLPFKPYAWSGLAGSDLRHLVQSYRQCSALERSAGLSLFCERGSEPG
RPAARYGPEQAAGGAGAGQPGSCGVAGGATSAAGLGLYGDFAPAAAGLYERP
STAAGRLYQDHGHELHADKSVGKVESELLCTRLLLGGGSYKGSMD**YKDDD**
DK